PHOTOFRIN AND INDOCYANINE GREEN-MEDIATED PHOTODYNAMIC THERAPY IN CANCER TREATMENT

by

ÖZGÜNCEM BOZKULAK

BSc., in Molecular Biology and Genetics, Bogaziçi University, 2000

MSc., in Institute of Biomedical Engineering, Bogaziçi University, 2003

Submitted to the Institute of Biomedical Engineering

in partial fulfillment of the requirements

for the degree of

Doctor

of

Philosophy

Boğaziçi University

January 2010

PHOTOFRIN AND INDOCYANINE GREEN-MEDIATED PHOTODYNAMIC THERAPY IN CANCER TREATMENT

APPROVED BY:

Assoc. Prof. Murat GÜLSOY .....
(Thesis Advisor)

Assoc. Prof. Ata AKIN .....

Assoc. Prof. Burak GÜÇLÜ .....

Prof. Hale SAYBAŞILI .....

Prof. İnci ÇİLESİZ .....

DATE OF APPROVAL: 14.01.2010

ACKNOWLEDGMENTS

I thank my family for being so giving and caring over the years that goes beyond my imagination. To my dearest wife Esra for her endless support and love.

I would like to thank my supervisor Assoc Prof Murat Gülsoy and my committee members Assoc Prof Ata Akin and Assoc Prof Burak Güçlü for their friendly guidance and encouragement during the course of my thesis.

I owe my appreciation to the members of my committee Prof Hale Saybaşılı and Prof İnci Çilesiz for allocating their time for critical reviewing of this thesis.

I would like to thank Prof Charles J. Gomer for giving me the opportunity to work in his lab at Children's Hospital Los Angeles, to learn and explore. I would also like to thank Dr Angela Ferrario, Sam Wong, Natalie Rucker, and Marian Luna for their guidance and support during my studies.

I would also like to acknowledge former and current members of the Biophotonics Lab and my friends at Institute of Biomedical Engineering who made this journey fun and enjoyable.

This work was supported, in part by Boğaziçi University Research Fund under grants 07X101, 04X101, 06M102, and TUBITAK project 104M428 to Assoc Prof Murat Gülsoy.

ABSTRACT

PHOTOFRIN AND INDOCYANINE GREEN-MEDIATED PHOTODYNAMIC THERAPY IN CANCER TREATMENT

Photodynamic therapy (PDT) is a minimally invasive therapeutic approach for clinical treatment of cancer. PDT-mediated oxidative stress leads to cell death and can elicit the expression of genes associated with cell survival, such as AKT/protein kinase B. Phosphorylation and subsequent activation of AKT induces a survival response. For the first time in literature, our results from *in vitro* and *in vivo* experiments demonstrated that PDT treatments mediated by excitation of Photofrin with a 630-nm diode laser induced AKT phosphorylation. PDT-mediated AKT pathway activation may stimulate cell survival in remaining tumor tissue leading to tumor reoccurrence,therefore, inhibiting PDT-mediated AKT activation may improve treatment responsiveness. Our findings demonstrated that, minimally toxic AKT inhibitor, PI-103, effectively inhibited PDT-mediated AKT phosphorylation both *in vitro* and *in vivo*. These results have great importance in relevance to development of combinatorial therapies using PDT and PI-103 inhibitor to improve treatment responsiveness.

Indocyanine Green (ICG) exhibits maximum absorption at around 800 nm, which is an advantage for its use in treatment of deeper tumors. In this study, an 809 nm diode laser was designed and custom manufactured in our laboratory to investigate the effects of ICG-mediated PDT on human breast cancer cells. This study for the first time reported that ICG-PDT application exhibited strong and stable phototoxic effects on MDA-MB231 breast cancer cells. Collectively, these novel findings presented in this thesis study contributed largely to the knowledge of PDT in cancer treatment, which is the first reported PDT study in Turkey, and open new research areas for further investigations.

Keywords: AKT, ICG, PDT, Photofrin, 630 nm diode laser, 809 nm diode laser.

ÖZET

KANSER TEDAVİSİNDE PHOTOFRİN VE İNDOCYANİNE GREEN DOLAYLI FOTODİNAMİK TERAPİ

Fotodinamik terapi (FDT) kanserin klinik tedavisinde kullanılan, düşük yan etkili bir tedavi yöntemidir. FDT sonucunda oluşan oksidatif stres, hücrenin ölümüne ya da AKT/Protein Kinaz B gibi hücre çoğalması ile ilintili yolakları etkinleşmesine neden olabilir. AKT'nin fosforile edilmesi ve etkinleşmesi hücre çoğalmasını tetikler. 630 nm diyot laser ile uyarılan Photofrin'in kullanıldığı hücre kültürü ve hayvan modellerindeki deney sonuçlarımız literatürde ilk kez FDT'nin AKT fosforilasyonunu artırdığını göstermiştir. FDT sonrası canlı kalabilen hücrelerde etkinleşen AKT yolağının hücre çoğalmasını uyarmasının tümör tekrarlamasına neden olabileceği düşün ülmektedir. Deney sonuçlarımız ve literatürdeki verilere dayanarak FDT sonucu artan AKT etkinliğinin engellenmesinin tedavinin etkisini arttıracağını öngördük. Hücre kültürü ve hayvan modellerindeki deney sonuçlarımız, AKT yolağı engelleyici molekülü PI-103'ün FDT sonucu artan AKT fosforilasyonunu, etkili bir şekilde ve minimum toksisite ile önlediği tespit edilmiştir. Bu sonuçlar FDT ile PI-103'ün birlikte kullanımının, FDT'nin kanser tedavilerindeki etkinliğini arttırabileceğini ortaya koymuştur.

800 nm civarında maksimum emilime sahip olan, ışığa-duyarlı-ilaç, Indocyanine Green (ICG), derin tümörlerin FDT ile tedavisi için ideal bir moleküldür. Bu çalışmada ICG-FDT'nin insan meme kanseri hücre kültüründeki etkileri incelenmiştir. Laboratuvarımızda tasarlanıp, geliştirilen 809 nm diyot laser, ışık kaynağı olarak kullanılmıştır. Sonuçlarımız literaturde ilk olarak ICG-FDT uygulamasının MDA-MB231 meme kanseri hattında etkili ve kalıcıfototoksik etkisini göstermiştir. Bu tez çalışması sonuçları Türkiye'deki FDT araştırmalarının öncüsü olup, FDT ile kanser tedavisindeki bilgimizi arttırmış ve gelecek için yeni araştırma konuları ortaya koymuştur.

Anahtar Sözcükler: AKT, FDT, ICG, Photofrin, 630 nm laser, 809 nm laser.

TABLE OF CONTENTS

LIST OF FIGURES

LIST OF TABLES

LIST OF SYMBOLS

λ	Wavelength
α	Alpha subunit
β	Beta subunit
δ	Delta subunit
μ	Micro

LIST OF ABBREVIATIONS

ALA	5-aminolevulinic Acid
anti	Antibody
BD	Bowen's Disease
BSA	Bovine Serum Albumin
C	Control
CA	Canada
cm	Centimeter
CN	China
COX-2	Cyclooxygenase-2
DAB	3,3'-diaminobenzidine
DE	Germany
DMEM	Dulbecco Modification Eagle Medium
DMSO	Dimethyl sulfoxide
DN	Denmark
4EBP1	Eukaryotic Translation Initiation Factor 4E Binding Protein 1
ELISA	Enzyme Linked Immunosorbent Assay
EU	European Union
FBS	Fetal Bovine Serum
FCS	Fetal Calf Serum
FI	Finland
FR	France
g	Gram
GSK-3	Glycogen Synthase Kinase 3
H&E	Hematoxylin and Eosin
H_2O_2	Hydrogen Peroxide
Hp	Hematoporphyrin
HpD	Hematoporphyrin Derivative
hr	Hour(s)

ICG	Indocyanine Green
IE	Ireland
IL-6	Interleukin-6
IL-8	Interleukin-8
IS	Iceland
i.v.	Intravenous
J	Joule
JP	Japan
kg	Kilogram
KTP	Potassium Titanyl Phosphate
kV	Kilovolt
LED	Light Emitting Diodes
mg	Milligram
mm	Millimeter
min	Minute
MMPs	Matrix Metalloproteases
mTOR	Mammalian Target of Rapamycin
MTT	3-(4,5-dimethylthiazol)-2,5-diphenyltetrazolium bromide
NaCl	Sodium Chloride
NL	The Netherland
nm	Nanometer
NO	Norway
PBS	Phosphate Buffered Saline
PDT	Photodynamic Therapy
Phospho-AKT	Phosphorylated AKT
PH	Photofrin
PI3-K	Phosphoinositide 3-Kinase
PIP2	Phosphatidylinositol-3,4-biphosphate
PIP3	Phosphatidylinositol-3,4,5-triphosphate
PKB	Protein Kinase B
PMSF	Phenylmethylsulfonyl Fluoride

PS	Photosentisizer
^{0}PS	Non-excited Ground State Photosentisizer
^{1}PS	Excited Singlet State Photosentisizer
^{3}PS	Excited Triplet State Photosentisizer
ROS	Reactive Oxygen Species
rpS6	Ribosomal S6 Kinase 1
rpm	Rounds per Minute
RTK	Receptor Tyrosine Kinases
SCL	Skin Cell Line
SDS	Sodium Dodecyl Sulfate
Ser	Serine Aminoacid
O_2	Oxygen
$^{\cdot-}O_2$	Superoxide Anion
$^{1}O_2$	Singlet Oxygen
$^{3}O_2$	Triplet State Oxygen
$^{\cdot}OH$	Hydroxyl Radical
TBS	Tris Buffered Saline
Thr	Threonine aminoacid
TNF-α	Tumor Necrosis Factor Alpha
TTBS	Tween-Tris Buffered Saline
UK	United Kingdom
USA	United States of America
US-FDA	United States Food and Drug Administration
VEGF	Vascular Endothelial Growth Factor

1. INTRODUCTION

1.1 Motivation

Cancer has become one of the most devastating diseases worldwide. According to a World Health Organization (WHO) report published in 2008, 7.4 million people die of cancer in 2004 and 83.2 million people will die by 2015 [7]. Early diagnosis is critical for extended survival period and lower reoccurrence rates. Therefore, research has focused on understanding the molecular basis of different cancers to enable earlier diagnosis and to develop new treatment options. The best established treatment approaches include surgery, chemotherapy and radiotherapy. A relatively new and promising United States Food and Drug Administration (US-FDA) approved approach with the use of low power light sources is the Photodynamic Therapy (PDT) [8]. The main advantages of PDT over other treatment methods are; its low systemic toxicity, selective tumor cell death without damaging the surrounding healthy tissue, minimal invasiveness and inexpensive application.

Given that there is a critical need for cancer treatment that is effective, well-tolerated and that can be repeatedly used, PDT emerges as a promising alterative approach. However, previous reports suggested that PDT may induce cell survival pathways in the tumor microenvironment that may account for tumor reoccurrence. AKT/Protein kinase B is a central player in cell survival pathways that was suggested to be one of these molecules. Thus, it is conceivable that AKT activation may be induced in PDT-treated tumors. Part of this thesis was devoted to this essential need to investigate PDT-induced cell survival pathways and to test inhibitors to block this undesired activity to improve PDT responsiveness.

Another major challenge in PDT treatment is to develop new photosensitizers that can be used at wavelengths suitable to treat deep tissue tumors. The photosensitizer Indocyanine Green (ICG) has maximum absorption at around 800 nm which can

penetrate deep into the tissue. Thus, ICG-mediated PDT on breast cancer cells were tested to assess whether this method presents an alternative for deep tumor treatments in the future.

1.2 Objective

PDT is based on the induction of cell death by mediating oxidative stress and hypoxia through combined effects of light, a compound with photosensitizing properties and oxygen. Depending on its dose PDT can either kill the cells directly by necrosis or indirectly by activating apoptotic pathways. Additionally, PDT can also activate survival pathways that can reduce the PDT responsiveness causing angiogenesis and inflammation within the tumor microenvironment as an undesired effect.

One of the signaling molecules that can be activated by PDT-mediated oxidative stress is AKT/protein kinase B [9, 10, 11]. AKT is a central regulator of different cellular pathways and has to be phosphorylated to be fully active. Activated AKT molecules can stimulate cell survival in the remaining malignant cells following PDT application. This indirect effect of PDT needs to be considered to enhance PDT responsiveness in cancer treatment.

In this thesis study, the effects of two different PDT approaches had been employed. The first approach utilized light at 630 nm to activate Photofrin (PH) as a photosensitizer which is the first FDA approved drug for the treatment of different cancers with PDT. Even though the PH-PDT caused highly localized cytotoxicity, a number of reports suggested that PH-PDT can also induce cell survival by leading to tumor reoccurrence [12]. In order to increase the responsiveness of PH-PDT treatment, the source of this induction needs to be determined. Given that none of the previous studies reported the effect of PH-PDT on AKT activation, one of the objectives of this thesis study was to examine the effects of PH-PDT on the AKT pathway both *in vitro* breast cancer cell cultures and *in vivo* animal tumor models. This study opened up the interesting possibility of PH-PDT application in combination with AKT inhibitors

to increase the effectiveness of cancer treatment.

The second part of this thesis study utilized near-infrared light to activate ICG which is a photosensitizer for PDT application. Near-infrared light can penetrate deeper into the tissue than the red part of the spectrum [13]. Thus, ICG-PDT can be a good alternative for treatment of deeper tissue tumors. In this study, a laser source emitting light at 800 nm, which was developed in our laboratory, was used to investigate the photo-toxic effects of ICG *in vitro* breast cancer cell culture. The findings of this study can be used as a start point for future investigations and development of ICG-PDT applications in clinics for tumor treatment.

2. BACKGROUND

2.1 Cancer

Cancer is a genetic disease [7, 14, 15, 16, 17]. Normal cell growth is a controlled balance between growth inhibiting and promoting signals where proliferation occurs only when required. This balance is broken when increased cell numbers are required such as in wound healing and during normal tissue turnover. Differentiation of cells during this process occurs in an ordered manner and proliferation ends when no longer required. In tumor cells this process is disturbed and uncontrolled cell proliferation occurs.

Cancer usually forms as a tumor but not all tumors are cancerous. Tumors can be divided into two main groups, benign or malignant [14]. Benign tumors are rarely life threatening and grow within a well-defined capsule which limits their size and maintain the characteristics of the cell of origin. Malignant tumors invade surrounding tissues and spread to different areas of the body to generate further growth and metastases. This is partly because of the fact that tumor cells proliferate independent of growth factors as opposed to normal cells and are less adhesive than normal cells. Normal cells stop proliferating when they reach a certain density but tumor cells continue to proliferate [14, 15, 16, 17, 18].

2.2 Cancer Therapies

A detailed comparison of survival rates of cancer patients has shown that most cancers are treatable if diagnosed early. Given that cancer is one of the leading causes of death in the world, a variety of treatment options have been developed that can be used alone or in combination. Surgery is the first and most commonly used approach for removal of solid tumors. It also has an important role in diagnosing and staging of

cancer. In addition to surgery, chemotherapy [19] is another approach for treatment of both solid and metastatic tumors with anticancer drugs [20] that can destroy tumor tissue by inhibiting cellular growth and proliferation. However, these drugs can exert cytotoxic side effects by damaging rapidly dividing healthy tissue in addition to tumor cells. These undesired side effects may often result in discomfort to the patient and early termination of the treatment. Thus, development of new chemotherapy drugs with low toxicity is a main interest in treatment of cancer.

Radiation therapy [16, 18, 21] is another commonly used method for the treatment of solid tumors. This method is based on damaging cancerous tissue by using penetrating beams of high energy waves. In fact, more than 50% of all cancer patients receive radiotherapy. However, similar to chemotherapy, radiotherapy has a number of side effects such as fatigue, hair loss, blood loss, diarrhea, nausea and vomiting. In addition to these commonly used methods; angiogenesis inhibitors, bone marrow transplantation, peripheral blood stem cell transplantation and gene therapy are other alternative ways for cancer treatment [16, 17, 18].

PDT is a promising US-FDA approved approach for the treatment of solid tumors by using low power light sources and photosensitizing compounds. The main advantages of PDT over other treatment options include; localized treatment with minimal toxicity to healthy tissue, its ease of application, possible repeated administrations and relatively cost-effective. Intriguingly, results from a variety of clinical trials underlined the importance of PDT as an invaluable alternative for cancer treatment.

2.3 Photodynamic Therapy

Light has been used for treatment of a diverse array of diseases for more than thousand years [22]. It was used in ancient Egypt, India and China to treat skin diseases such as psoriasis, vitiligo and skin cancer [2, 22]. At the end of the nineteenth century Niels Finsen further developed "phototherapy" and found that red-light exposure prevented the formation and discharge of smallpox pustules [23]. Finsen also used

ultraviolet light from the sun to treat cutaneous tuberculosis. This was the beginning of the modern light therapy, and, in 1903, Finsen was awarded a Nobel Prize for his discoveries [24]. The foundations of clinical applications of PDT were established as early as the beginning of the twentieth century when Oscar Raab noted that certain wavelengths of light were lethal to the organism "paramecia" exposed to the chemical compound "acridine" [25, 26]. Herman von Tappeiner and A. Jensionek later reported that another chemical "eosin" can treat skin cancer [26]. The most explored class of chemical compounds in PDT today, the porphyrins, were investigated by Friedrich Meyer-Betz as early as 1913 [24, 25, 26]. PDT began to shape in 1960s by the studies of Richard Lipson and Baldes on the tumor accumulation of haematoporphyrin derivative (HpD) prepared by Dr. Samual Schwartz and its use in the photodetection of tumors [27, 28, 29]. HpD was further developed for laboratory and clinical investigations through the efforts of Dougherty and his colleagues in 1980s [30]. In 1987 FDA approved the first photosensitizing drug the Photofrin® (PH) [25]. Currently, there are a number of photosensitizing agents approved for the treatment of cancer and a variety of diseases [25].

Three components are required for PDT; a photosensitiser, a light source and oxygen. Cancer treatment with PDT [26, 30, 31, 32, 33, 34, 35, 36] involves the systemic administration of a photosensitizer [6, 34] followed by irradiation of targeted lesion with appropriate wavelength of light source [37, 38] (Figure 2.1). The exposure of light results in the generation of highly reactive oxygen radicals formed by the transfer of energy absorbed by photosensitizers to the molecular oxygen during the light treatment. Oxidation of biological targets such as proteins, lipids and nucleic acids by reactive oxygen species may lead to cell death by necrosis or apoptosis.

2.3.1 Photosensitizers

Photosensitizers are chemical compounds that absorb light at a specific wavelength and transfers that energy to biological molecules. In the case of PDT, this energy transfer involves the production of cytotoxic and reactive oxygen species (ROS), in-

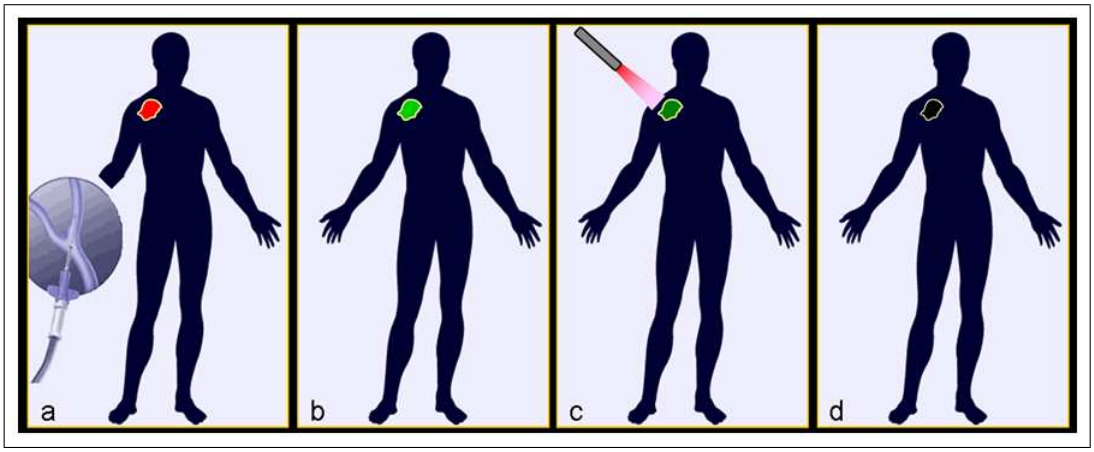

Figure 2.1 PDT procedure. PDT involves the selective uptake (a) and retention of a photosensitizer in a tumor(b), followed by irradiation with light of a particular wavelength (c), thereby initiating tumor necrosis (d) presumably through formation of singlet oxygen [1].

cluding singlet oxygen ($^1O_2$), leading to localized cell death. There is a large number of natural and synthetic molecules that can function as photosensitizers for PDT ranging from plant extracts to complex synthetic molecules. The key characteristic of any photosensitizer is its ability to preferentially accumulate in tumor tissue due to the high proliferative activity of cancer cells.

The basic mechanism by which the combination of a photosensitizer (PS), light and oxygen leading to cell death are shown in Figure 2.2. These photosensitized processes are classified as Type I and Type II depending on the nature of the primary steps [39, 40]. The non-excited ground state PS (^{0}PS) absorb visible light and shift to an electronically excited singlet state (^{1}PS*) then to the relatively long-lived excited triplet state (^{3}PS*) via intersystem crossing. The energy of the excited PS can be dissipated by thermal decay, emission of fluorescence (from ^{1}PS*) or phosphorescence (from 3PS*). In Type I reactions, the ^{3}PS* can also transfer a hydrogen atom or an electron to biomolecules (lipids, proteins, nucleic acids, etc.) or generate radicals that interact with O_2 to form ROS products such as the superoxide anion ($^{\cdot-}O_2$), the hydroxyl radical ($^{\cdot-}$OH) and hydrogen peroxide (H_2O_2). On the other hand, in Type II reactions the ^{3}PS* state can transfer energy directly to the ground-state molecular oxygen in its natural triplet state ($^3O_2$), which then yields the non-radical but highly reactive singlet oxygen [30].

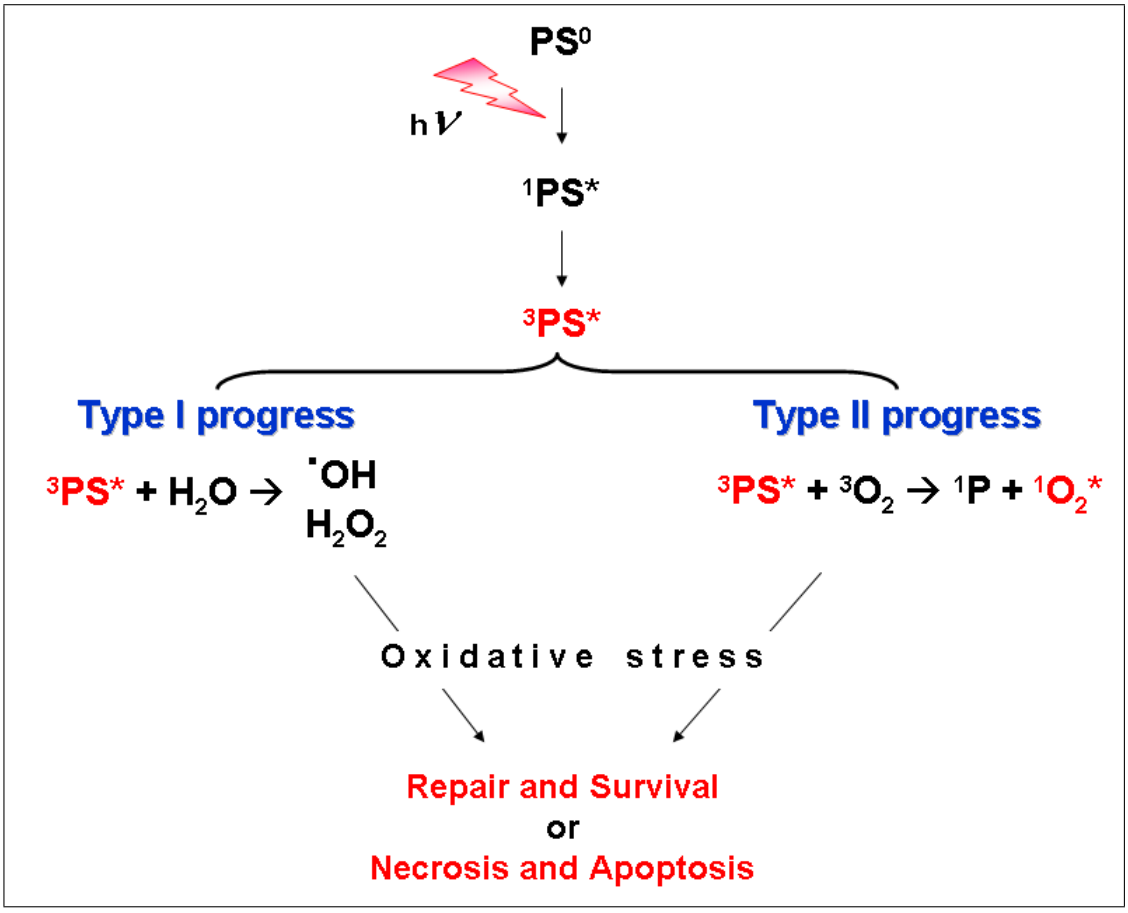

Figure 2.2 The basic pathway by which the combination of photosensitizer (PS), light and oxygen (O_2) leads to cell death or survival. Following irradiation, photosensitizers absorb light and undergo specific reactions to generate reactive oxygen species. The PS in a singlet ground state (^{0}PS) becomes activated to an excited singlet state (^{1}PS*) which is followed by intersystem crossing to an excited triplet state (^{3}PS*). Energy transfer from ^{3}PS* to biological molecules and molecular O_2 via Type I and Type II reactions generates reactive oxygen species ($^1O_2$, $^{\cdot-}O_2$, $^{\cdot-}$OH and H_2O_2) that produces different cellular responses.

Although the precise mechanisms of PDT have not yet fully understood, it is generally accepted that $^1O_2$ produced through Type II reaction is primarily responsible for cell death. The contribution of both Type I and Type II reactions to cell death depends on several factors including the PS, the subcellular localization, the substrate and the presence of O_2. Under hypoxic conditions, radicals arising from Type I photoreaction of PSs are primarily responsible for sensitization. In an oxygenated medium, $^1O_2$ largely mediates photosensitization, but the supplemental role of H_2O_2, $^{\cdot-}$OH and $^{\cdot-}O_2$ is also relevant. It is to be noted that, ROS are highly reactive and present a very short half-life. Therefore, only substrates colocalized with ROS will be affected by the PDT application. For instance, half-life $^1O_2$ is about 0.6 μs in cellular environment, 50

μs in water and 50-100μs in lipid [41, 42, 43, 44]. It has a short radius of action (about 0.1 μm) [41]. The range of cellular responses of $^1O_2$ from cytotoxicity to enhanced survival is attributed at least partly to differences in $^1O_2$ concentrations. Higher concentrations are mostly associated with cell death, whereas, lower concentrations may stimulate cellular survival pathways [45].

Photosensitizers can be categorized depending on the chemical structure. Table 2.1 outlines the photosensitizer families currently applied in clinics or under clinical investigation.

Table 2.1
Photosensitizer families [6]

Family Name	**Photosensitizers**
Porphyrin platform	HpD, HpD-based, BPD, ALA, Texaphyrins
Chlorophyll platform	Chlorins, Purpurins,Bacteriochlorins
Dyes	Phtalocyanine, Napthalocyanine

The first PSs used in experimental PDT were haematoporphyrin (Hp) and haematoporphyrin derivative (HpD) which belong to the Porphyrin family (Table 2.1). HpD is a mixture of mono-, di- and oligomers of porphyrins with photosensitizing properties [46]. Several decades ago, Lipson and colleagues reported that both Hp and HpD were localized and detected in the tumors by fluorescence and were proposed to be alternative diagnostic tools [27]. Later studies reported that HpD excited by red light eradicated mammary tumors and bladder carcinomas in mice [28, 29]. Following these preliminary findings, PDT was evaluated in clinical trails in treatment of a variety of cancers and in 1994, porfimer sodium (Photofrin®) based PDT was first approved in Canada for the treatment of bladder cancer [2].

The criteria for selection of a suitable PS for PDT application include: (i) minimal toxicity in the absence of light and cytotoxicity following photoactivation (ii) chemical purity with known molecular structure, (iii) chemical stability in biological systems, (iv) preferential accumulation in the targeted tumor tissue, (v) high quantum

yield of $^1O_2$ and (vi) high molar extinction coefficient and high absorbance, particularly in red and near infrared spectral regions (600-810 nm). This last property is related with light penetration into the tissue, which is associated with the wavelength. For instance, the penetration depth of light between $500<\lambda<600$ nm and $600<\lambda<810$ nm is about 4 mm and 8 mm, respectively [16]. Thus, for the PDT treatment of deeper tumors, light source at longer wavelengths should be applied with compatible PS.

Although some photosensitizers satisfy all or some of these criteria, currently there is only a small number of photosensitizers that have received official approval for PDT treatment of cancer [47]. These with their λ_{exc} include but are not limited to:

- Photofrin (630 nm, Axcan Pharma, Inc.)
- Levulan (predrug of protoporphyrin IX; 630 nm, DUSA Pharmaceuticals, Inc.)
- Metvix (predrug of protoporphyrin IX; 630 nm, PhotoCure ASA.)
- Foscan (652 nm, Biolitec AG)
- Laserphyrin (664 nm, Meiji Seika Kaisha, Ltd.)
- Visudyne (693 nm, Novartis Pharmaceuticals)

Several 2^{nd} generation photosensitizers (e.g. HPPH - 665 nm, SnET2 - 665 nm, Lu-Tex - 732 nm) have been investigated in many preclinical and clinical trials for various solid tumors [48, 49, 50]. The current research in PDT has been focused on the development of alternative new-generation PSs with improved physical, chemical and therapeutic properties [51].

2.3.1.1 Photofrin. Photofrin is a purified mixture of HpD and the molecular structure with absorbtion spectra are shown in Figure 2.3. It is important to note that, Photofrin can be excited by wavelengths around 630-635 nm. PH is commercially available from Axcan Pharma, Inc. and has the longest clinical history. PH was

first applied in experimental PDT in 1973; however, was finally approved in 1993 by the Canadian government for the treatment of bladder cancer [31, 32]. It was later approved by US-FDA for its applications in treatment of pre-cancerous lesions in Barrett's esophagus [8, 30, 52]. Additionally, Photofrin-PDT has been tested for cervical, stomach, skin, brain and lung cancers.

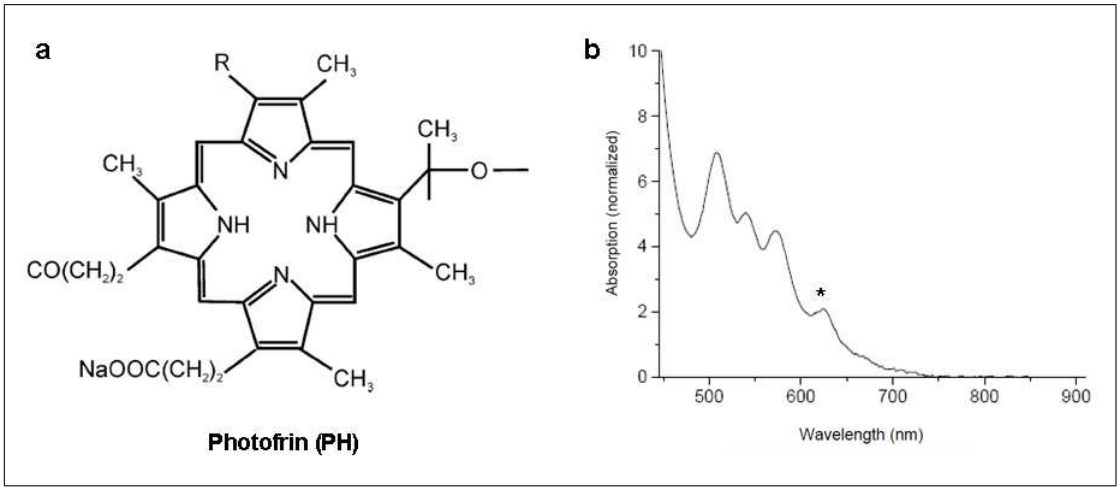

Figure 2.3 a) Molecular structure of Photofrin (PH)[2]. b) Absorption spectra of PH

2.3.1.2 Indocyanine Green. Indocyanine Green (ICG) is a water-soluble, anionic tricarbocyanine dye which exhibits strong absorption band between 600-900 nm (Figure 2.4) [3, 40, 53, 54, 55, 56, 57]. ICG has been widely applied in medical diagnosis since 1956 and was approved by the US-FDA for the measurement of cardiac output, ophthalmic angiography and capillary microscopy [55]. Human tissue is relatively transparent for near-infrared light compared to red part of the spectrum, and it can penetrate into deep tissues [13]. Therefore, searching for photosensitive agents working with near-infrared light is one of the new topics in photodynamic therapy. ICG exhibits strong maximum absorption at around 800 nm which will be an advantage for its use in PDT; light at that wavelength can be used to treat deeper tumors.

In vitro effects of ICG-PDT on cell survival have been investigated on different human cell lines. In a study where four different human skin cell lines (SCL1 and SCL2 squamous cell carcinoma, HaCaT keratinocytes, N1 fibroblasts) were used, ICG concentrations above 25 μM produced a significant photo-toxic effect when used in

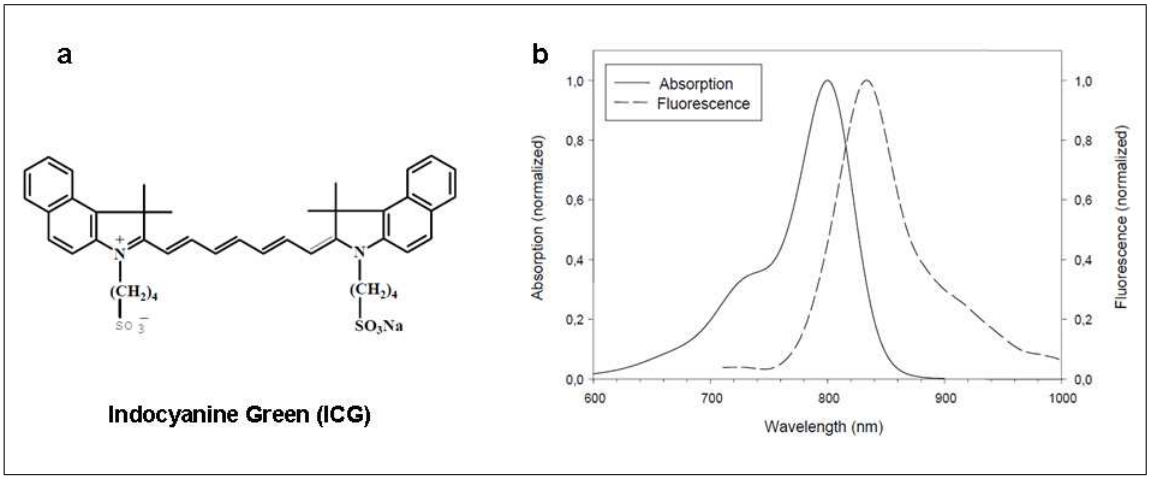

Figure 2.4 a) Molecular structure of Indocyanine Green (ICG). [2], b) Absorption spectra of ICG [3]

combination with a light (24 and 48 J/cm^2) at a wavelength of 805nm [3]. According to another study photoactivated ICG (500 μM) by a 805-nm diode laser at a power of 30 J/cm^2 can effectively destroy HT-29 human colon cancer cells [58]. Similar phototoxic effects were observed in human pancreatic ductal adenocarcinoma cell lines (MIA PaCa2, PANC-1, BxPC-3); 90% cell mortality were seen at 20 μg/ml of ICG when used together with light (0.45 W, for 5 min) at 808 nm [59]. A combined radiotherapy and ICG-PDT study was done on human prostate cell lines (PC-3 carcinoma and EPN normal) and this combination revealed an additive effect which could be more useful since they allow the reduction of ionization dose to obtain same therapeutic effect [60]. It was also found that ICG induces cell death following photoactivation in both cell lines, however due to possible more ICG uptake by PC-3 carcinoma cells, the effect of PDT is more toxic than on EPN normal prostate cells. Up till now the only ICG-PDT application on breast cancer cell lines was with MCF-7 cells [56]. It was found that cell viability is both ICG concentration and light dose dependent. In addition Crescenzi *et. al.* also checked the combinatory therapeutic effect of a chemotherapeutic drug (cisplatin) and ICG-PDT, and found that low doses of cytostatic drugs may be more effective when combined with PDT. The main mechanism of how ICG-PDT causes cell death is still unclear. It is believed to have both photo-oxidative [58, 59] and photo-thermal effects [61, 62].

2.3.2 Light Sources

PDT involves the use of a photosensitizer and light, typically visible or infrared. Since non-invasive PDT depends on targeted light delivery, it can be applied only to tumors and other lesions that can be reached by direct light or light through optical fibers. The light source and the light delivery systems have fundamental importance in PDT. There is a need for designing optimal combinations of photosensitizers, light sources and treatment parameters for all PDT applications.

Light is absorbed by the dominant chromophores; such as hemoglobin, melanin, and water in the tissue (Figure 2.5) [4] which determine how deep the light will penetrate. Each chromophore absorbs light at specific wavelength. The so-called "optical window" of living tissue is between 600-1300 nm. Thus, in order to reach the optimal depths, the photosensitizers are selected that absorb at the longest wavelength possible. However, photons above 850 nm can hardly generate triplet states with high enough energy to produce singlet oxygen.

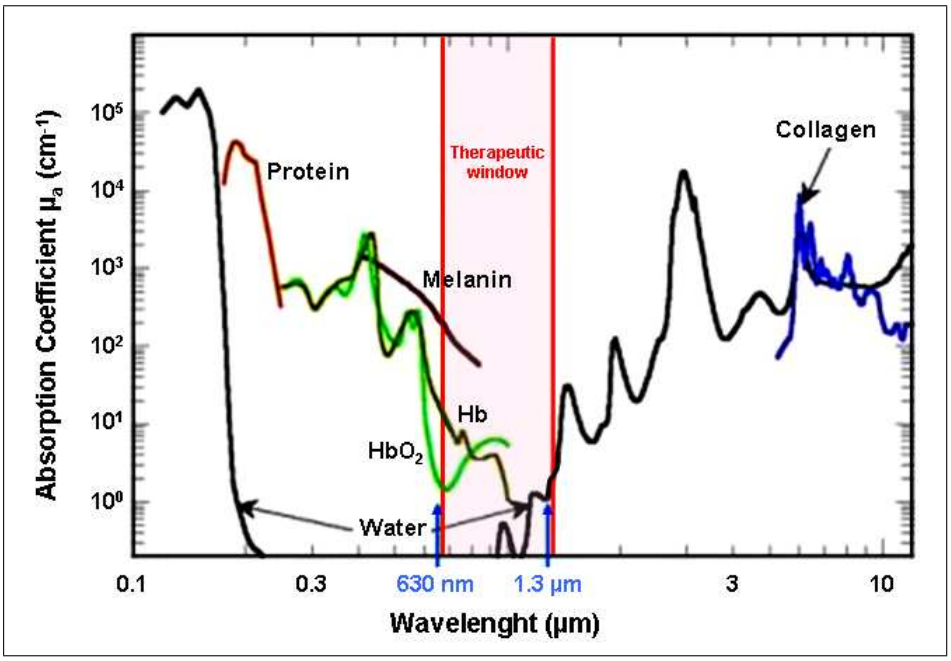

Figure 2.5 Absorption spectra for the main constituents of biological tissues [4]

The wavelength of the light should be selected depending on the depth of the lesion and the absorption band of the photosensitizer. For treatment of deep lesions,

it is desirable to apply a photosensitizer with a high absorbance at longer wavelenghts. Many of the second generation photosensitizers absorb at longer wavelengths than the traditionally used 630 nm for HpD (Photofrin) in order to treat deep tissue tumors.

The light sources must generate sufficient power and the light should be deliverable to the target tissue with high efficiency. However, increased light absorption leads to heat generation and generally, fluence rates above 150 mW/cm^2 cause hyperthermia [63]. Previous studies have reported that a low fluence rate and short exposure time are preferable in order to prevent hyperthermia [64, 65, 66]. Moreover, the fluence rate affects the direct photochemical oxygen consumption that plays a critical role in clinical PDT [67]. Typically, the power of the light ranges from 1 to 5 W with a wavelength between 630 nm and 850 nm and the irradiance up to several hundred mW/cm^2 so that the treatment can be delivered in minutes [68].

The main light sources for PDT treatment are; lasers, light emitting diodes (LEDs) and filtered lamps. One main advantage of lasers is their monochromaticity, which gives maximum efficiency of photoactivation during treatment. In early 1980s, most clinical treatments were performed with an argon-ion laser (488-514 nm). Since these lasers have the advantage of wavelength tenability, the same source could be used for different photosensitizers. However, this technology was not well-suited to the clinical environment due to its size, high electrical power usage and water-cooling requirements. Later, the argon-ion lasers were replaced by all-solid-state, frequency-doubled Nd:YAG (1064 nm) or KTP (532 nm) laser source. Although this significant advance solved some of the reliability and cooling problems, it was still cumbersome and expensive. More recently, KTP-dye systems have been largely replaced by diode lasers, which are now the standard sources for many PDT applications. Diode lasers can be very efficiently (>90 %) coupled into single optical fibers for endoscopic and interstitial light delivery. The main limitation of diode lasers in PDT application is that they produce light at a single wavelength, and thus a separate laser system is required for different photosensitizer.

LEDs became a practical technology for PDT in the past few years, especially

for irradiation of easily accessible tissue surfaces such as in dermatology. The main advantages of using LEDs over diode laser sources are their low cost, smaller size, large illumination field and ease of configuring LEDs into different irradiation geometries [34]. Initially, generation of low output power and the range of wavelengths were major limitations for LEDs. Recent improvements in LED technology enabled generation of hundreds of mW/cm2 irradiance and production of wavelengths spanning most of the visible to near infrared spectrum. Linear arrays of LEDs have been developed that can be applied endoscopically or interstitially. Similar to laser diodes, LEDs have single output wavelength; however, the cost per Watt generated is significantly less, and thus having different sources for each photosensitizer is less of a problem.

The main advantage of a number of lamp systems available for PDT is that they can be spectrally filtered to match any photosensitizer. As in the case of LEDs, flexible geometry is an advantage; however, they cannot be efficiently coupled into optical fiber bundles, so that endoscopic use is not possible.

The light sources should be determined based on the photosensitizer absorption; location, size and accessibility of the tumor; simplicity of maintenance and cost of the unit. Importantly, the clinical efficacy of PDT is dependent on the light delivery parameters including; total light dose, light exposure time, fluence rate, and mode of operation (continuous or pulsed).

2.3.3 Clinical Applications of Photodynamic Therapy

PDT is a unique treatment modality, that requires injection of a photosensitizing drug followed by a single light treatment after a certain time interval. Even though, the main disadvantage for the patient is hypersensitivity to light up to one week following treatment, this procedure is often performed on an outpatient basis and has major advantages over other cancer treatment options. In comparison, typical radiotherapy regimes include daily irradiation for a total of 6-7 weeks and chemotherapy schedules typically last for several months with severe side effects. Another treatment method;

surgery mostly requires a single procedure with general anesthesia and hospitalization for one to several weeks. Another advantage of PDT is that the treatment can be repeated in case of recurrence or a new primary tumor in the previously treated area. Such retreatment is extremely difficult for either surgery or radiotherapy, without the risk of severe normal tissue damage. Among those other treatment methods, PDT is cost-effective, have minor side effects and provide increased life expectancy [69, 70, 71].

PDT is a local, rather than systemic, treatment, therefore, suitable for solid tumors. Light applied to excite current photosensitizers can provoke tissue necrosis up to 10 mm [72]. For superficial illuminations, the indication for PDT as a primary treatment should be limited to small, accessible tumors. It can also be given in combination with debulking surgery for palliative treatment of larger tumors. An important advantage of the limited light penetration is that this protects normal healthy tissue beneath the tumor from phototoxicity. Modern fiber-optic technology facilitates delivery of light, of the desired wavelength and fluence rate, to tumors located virtually anywhere in the body. Localized illumination, together with shielding of sensitive tissues at the margin of the field, enables specific tumor treatment without destruction of critical normal tissues outside the treated area. By contrast, surgery and radiotherapy of tumors located close to critical structures can be mutilating and lead to loss of function. PDT has the advantage that, although there is severe ulceration of the illuminated area immediately after treatment, there is minimal long-term fibrosis, resulting in functional recovery without scarring. PDT spares tissue architecture, providing a matrix for regeneration of normal tissue, because it does not damage subepithelial collagen and elastin and there is preservation of noncellular supporting elements [73, 74].

Since early 1980s, PDT has been used for the treatment of a large number of diseases and cancers in clinics in USA, UK, EU, Canada, Japan and China (Table 2.2). The first indication for PDT, by using Photofrin as a photosensitizer, was in Canada for bladder cancer in 1993. This was a true milestone and set the stage for PDT to be an accepted novel treatment for cancer. Later in 1995, PDT received its first FDA approval in the US for advanced and obstructing esophageal cancer. In 2004, FDA approved Photofrin-PDT for Barrett's Esophagus. A study in Japan by

Kato *et al.* suggested HpD-PDT for the treatment of early and advanced stage non-small cell lung cancer in 1998, that was confirmed by several publications from other groups [75, 76, 77, 78]. Bronchoscopic PDT has now achieved the status of a standard protocol for early stage lung cancer in Japan. Photofrin and Foscan-PDT has been used for the treatment of head and neck cancers since early 1980s [79, 80]. Biel reported the largest series of Photofrin-PDT in head and neck cancers in 1998 [81]. Foscan-PDT was approved in Europe in 2001 for treatment of patients with advanced head and neck cancer who have exhausted other treatment options [82]. PDT has also been widely used for dermatological cancers and disease due to the ease for therapy. The first published report by Dougherty's group in 1978 pioneered the treatment of skin cancer with PDT [83]. Later in 2000, FDA approved Levulan (ALA)-PDT in treatment of a skin disease known as "actinic keratoses" [84]. It is to be noted that PDT also presents a high potential of application in ophthalmology [85, 86, 87, 88]. Visudyne (Vertiporfin)-PDT was approved in 1999 by FDA for the treatment of age-related macular degeneration (AMD) [89]. Many studies demonstrated evidence for the efficacy of PDT application in combination with various treatment approaches such as laser photocoagulation, subretinal surgery or novel anti-angiogenic drugs [90]. Furthermore, there is a considerable research interest in improving clinical applications of PDT in brain, breast, cardiovascular, gastroenterological, urological and gynecological cancers [2, 32].

It is also important to note that, current research focused on the development of next generation PSs with better efficiency. Nanotechnogical methods have been employed for development of PS-containing liposome carriers, that are coated with antibodies against tumor tissue, for targeted delivery. Another significant area of research is the combination of PDT with other treatment modalities such as chemotherapy, radiation therapy, immunotherapy and gene therapy [104].

PDT-induced cellular damage is caused by singlet oxygen species in which the dose of this reactive species determine the fate of the cell. High doses result in cell death where as low doses can stimulate proliferation of remaining tumor cells accounting for the relapse of the tumor [12]. Therefore, there is extensive interest and research

Table 2.2
List of photosensitizers and the type of cancers treated.

Type of cancer	**Photosensitizer**	**Country**	**References**
Actinic keratosis, BD	ALA (Levulan, Metvix)	USA, EU	[91]
Basal cell carcinoma	ALA (Metvix)	EU	[84, 92]
Barrett's HGD	Porfimer sodium (Photofrin)	USA, CA, EU, UK	[93]
Cervical cancer	Porfimer sodium (Photofrin)	CN, JP	[94]
Endobronchial cancer	Porfimer sodium (Photofrin)	CA, DK, FI, FR, UK, DE, IE, JP, NL, USA	[75]
Esophageal cancer	Porfimer sodium (Photofrin)	CA, DK, FI, UK, IE, JP, DE, FR, USA	[95, 96]
Gastric cancer	Porfimer sodium (Photofrin)	CN, JP	[97, 98]
Head and neck cancer	Foscan	EU, NO, IS	[99, 100]
Brain tumors	Porfimer sodium (Photofrin), ALA	DE	[101]
Bladder cancer	Porfimer sodium (Photofrin), ALA	DE, CA	[102, 103]

on understanding PDT and tumor microenvironment interactions in order to increase treatment responsiveness and minimize tumor reoccurrence following PDT. Consequently, combination therapies with PDT and multi-target inhibitors or appropriate anti-angiogenic compounds have great potential to improve cancer treatment.

2.4 Photodynamic Therapy and Tumor Microenvironment Interactions

Clinical trials have encouraging results for PDT in cancer treatment; however, recent studies showed some evidence suggesting that, besides its cytotoxic effects, PDT can stimulate survival pathways [12]. This can account for tumor recurrence, therefore, improving long-term PDT responsiveness by combination therapies are required.

Cellular components such as, mitochondria, lysosomes, and plasma membrane, are subcellular targets of PDT [105]. PDT mediates oxidative stress, localized inflammation and vascular injury within treated tumors and surrounding tissue, and each of these responses can lead to increased expression of angiogenic factors, cytokines and survival molecules [32, 33, 106]. Overexpression or activation of these molecules, including Vascular Endothelial Growth Factor (VEGF), Matrix Metalloproteases (MMPs), Cyclooxygenase-2 (COX-2), AKT/Protein Kinase B, following PDT treatment can activate pathways associated with cellular proliferation leading to tumor recurrence. In order to prevent or minimize tumor relapse, inhibitors designed to block these growth stimulating factors needs to be administered in combination with PDT [12, 107, 108, 109, 110].

There is growing evidence supporting the dependence of various components of the tumor microenvironment on the efficacy of cancer therapy [12]. The tumor microenvironment is composed of malignant cancer cells, connective tissue as well as host cells including endothelial cells and inflammatory leukocytes (macrophages and neutrophils). During angiogenesis, leukocytes and neutrophils are recruited into the tumor

tissue and stimulate VEGF and MMP-9 release to stimulate the endothelium and indirectly or directly activate tumor vascularization [111, 112, 113]. Moreover, tumor associated macrophages participate in tissue growth, tissue remodeling and angiogenesis. Furthermore, tumor microenvironment is rich in growth factors, chemokines, and proteolytic enzymes which enhance angiogenesis, tissue breakdown and tissue remodeling [114].

Cellular factors associated with PDT, such as necrosis, apoptosis and hypoxia, can stimulate survival pathways in the tumor microenvironment. For instance, PDT-induced hypoxia can lead to activation of VEGF via the Hypoxia-inducible factor 1 pathway [109]. Moreover, several studies demonstrated that, PDT can induce expression and/or activation of a number of pro-angiogenic molecules including, COX-2, prostaglandins, tumor necrosis factor alpha (TNF-α), MMPs, integrins, interleukin-6 (IL-6), and interleukin-8 (IL-8) within the tumor microenvironment [108, 109, 110, 115, 116, 117, 118, 119] (Figure 2.6).

Large body of evidence suggested that, PDT-induced activation of apoptotic and survival pathways in the tumor microenvironment may lead to increased expression of angiogenic and pro-survival factors [12]. It is conceivable that chemical inhibitors suppressing PDT-mediated angiogenesis and cell proliferation, can significantly improve treatment responsiveness. In support of this idea, preclinical investigations indicated that, combination therapies with inhibitors directed against survival factors enhance PDT responsiveness [108, 109, 110, 115, 116]. However, severe side effects in combination therapies become a major concern since increasing the number of medications can be life threatening to the patient. Therefore, current research is directed towards discovering new drugs and selecting the most effective, least cytotoxic molecular targets for improving PDT efficiency.

AKT pathway plays a central role in major cellular processes and a vast amount of literature reported this pathway in tumor development as well as in the responsiveness of tumor cells to treatment. Numerous studies have shown that oxidative stress stimulates AKT activation and promote cell survival [120, 121]. In the literature, Rose

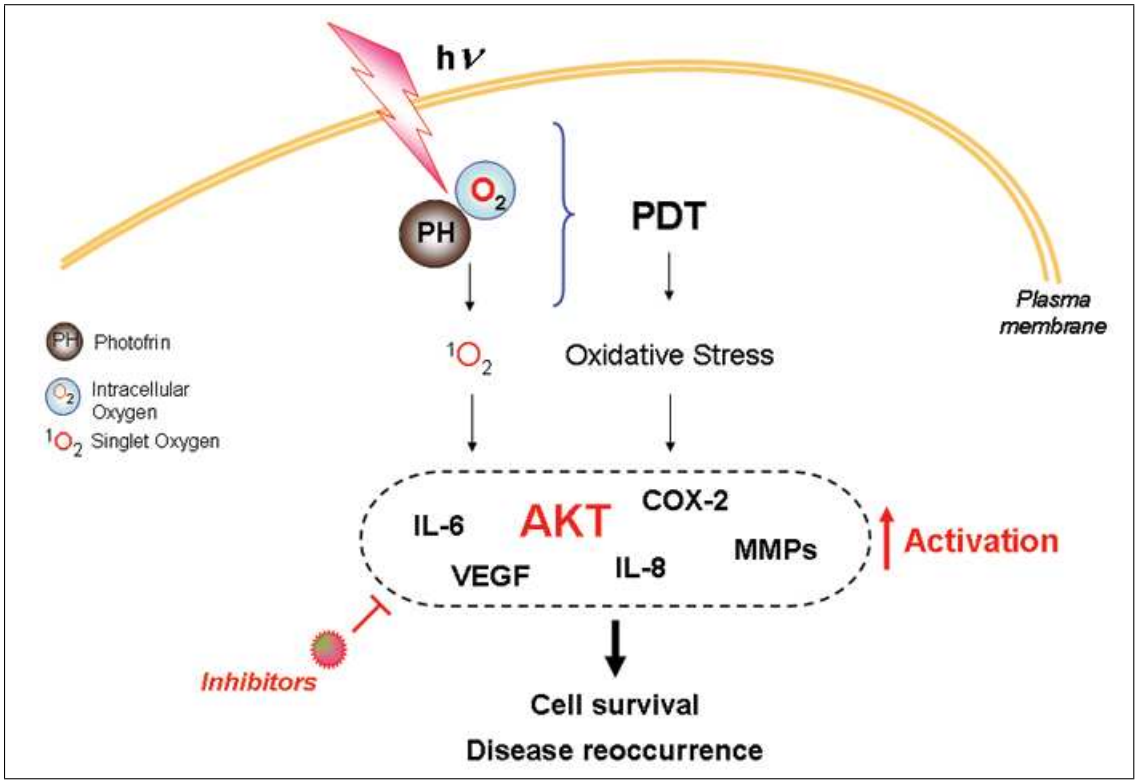

Figure 2.6 Interactions between PDT and the tumor microenvironment. PDT induces oxidative stress in the treated tumor tissue. Low levels of oxidative stress can lead to enhanced expression of a wide variety of transcription factors and cytokines directly associated with cell survival. Inhibitors of these factors is a promising way of improving PDT responsiveness.

Bengal-mediated PDT reported to induce AKT activation in mouse fibroblasts [120]. Additionally, inhibition of AKT activation resulted in enhanced cell death. Due to its critical involvement in tumorigenesis, AKT/Protein Kinase B is a candidate molecule that needs to be further investigated for its possible involvement in PDT-induced cell survival.

2.5 AKT Pathway

AKT, also known as Protein Kinase B, is a serine/threonine kinase [9, 10, 11, 122, 123, 124, 125, 126], that was identified as the human homologue for the viral oncogene v-akt which is known to be responsible for a type of leukemia in mice [127]. Three isoforms of AKT (1, 2, 3) were reported that exhibit a high degree of homology [128, 129]. (For simplicity, all three isoforms will be mentioned as "AKT" at the entirety

of this dissertation.) AKT has a characteristic kinase domain, which is involved in phosphorylation of downstream substrates resulting in either activation or inhibition of these molecules. Importantly, AKT itself has to be phosphorylated at two sites at Threonine residue 308 (Thr 308) and Serine residue at 473 (Ser 473) to be fully active.

The phosphorylation and subsequent activation of AKT is highly regulated both spatially and temporally. The following model for activation of AKT has been established (Figure 2.7): External stimuli, such as cytokines, growth factors and hormones, activate family of transmembrane Receptor Tyrosine Kinases (RTK) leading to production of phosphatidylinositol-3,4-biphosphate (PIP2) and phosphatidylinositol-3,4,5-triphosphate (PIP3) at the membrane through the activation of phosphoinositide 3-kinase (PI3-K) family members. Following PI3-K activation, AKT interacts with these phospholipids causing its translocation to the plasma membrane [130, 131] where AKT is phosphorylated at Thr 308 by a distinct protein kinase called phosphoinositide-dependent kinase 1 (PDK-1). AKT is further phosphorylated at Ser 473 by the kinase "mammalian target of rapamycin" (mTOR) in complex with the binding partner Rictor [Sarbassov D 2005]. Activated AKT then translocates to the nucleus where several of its targets reside and regulate signal transduction pathways involved in cell proliferation, apoptosis and angiogenesis [132, 133, 134, 135, 136, 137, 138, 139, 140, 141].

AKT mediates some of the biological processes attributed to PI3-K activity that are important in tumourigenesis. PI3-K activity is required in many tissues for cell survival, an observation first noted in 1995 [142] and AKT activity appears to be the predominant pathway that accounts for this [143]. Among the AKT substrates identified [144, 145] several are likely to play a role in cell survival, including Foxo transcription factors [146] glycogen synthase kinase 3 (GSK-3) [147] and mouse double minute 2 (MDM2) [148, 149, 150]. Other substrates have also been proposed, including the Bcl-2 antagonist Bad [151], IKK (the inhibitor of NFκB kinase) [152] and caspase-9 [153]. A possible mechanism that could account for the ability of AKT to increase cellular survival is through regulation of glucose metabolism by activation of GSK-3. AKT stimulates glucose uptake into the cell [154]. The importance of glucose metabolism in the ability of AKT to regulate cell survival is suggested by the fact that

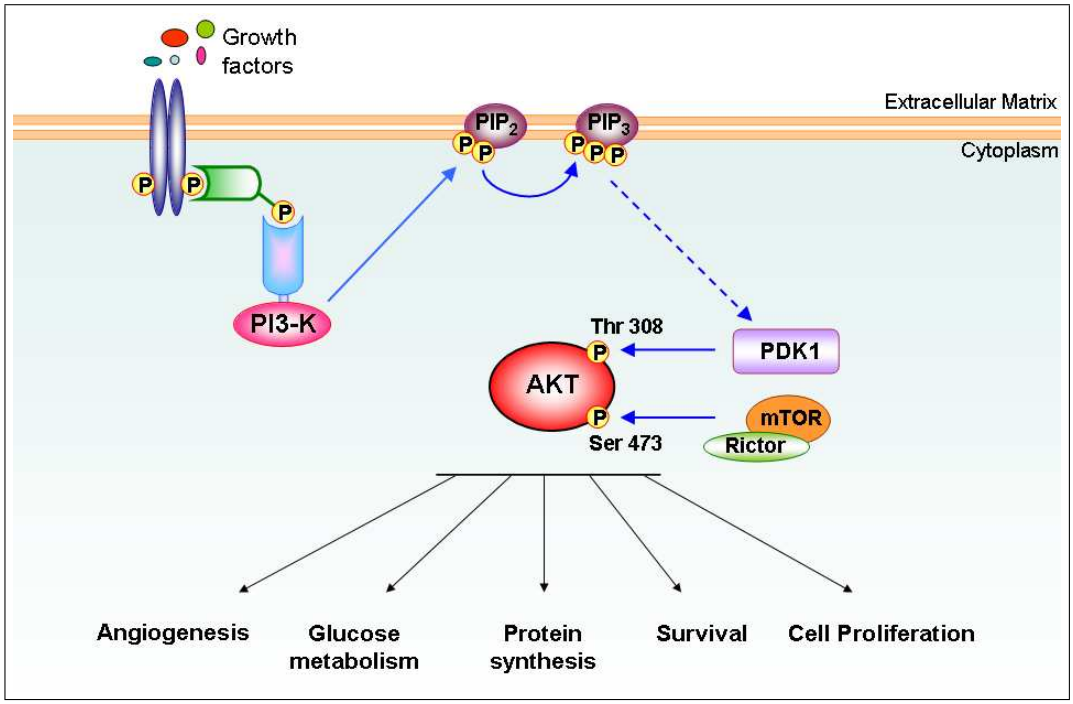

Figure 2.7 AKT Pathway. PDT induces oxidative stress in the treated tumor tissue. Activation of AKT involves growth factor binding to a receptor tyrosine kinase and activation of PI3-K, which phosphorylates membrane bound PIP2 to generate PIP3. The binding of PIP3 to AKT anchors it to the plasma membrane and allows its phosphorylation and activation by PDK1. Phosphorylation at the position Thr 308 and Ser 473 is required for the fully activation of AKT. It causes a charge-induced conformational change, allowing substrate binding and increased rate of catalysis.

activated forms of AKT are unable to inhibit apoptosis in cells that are deprived of glucose [155].

mTOR is a large protein kinase that nucleates at least two distinct multi-protein complexes; mTORC1 and mTORC2 [156]. The main difference between these two complexes is; mTORC1 contains Raptor protein as cofactor whereas mTORC2 contains Rictor as a cofactor. The mTORC1 pathway regulates protein synthesis and growth through downstream effectors, such as "eukaryotic translation initiation factor 4E binding protein 1" (4EBP1) and "ribosomal S6 kinase 1" (rpS6) (Figure 2.7) [157]. The mTORC2 complex is less understood than mTORC1 but recent work indicates that it should be considered part of the AKT pathway as it directly phosphorylates AKT on one of the two sites that are necessary for AKT activation in response to growth factor signalling [158, 159].

These findings suggest PI3-Ks, mTOR complexes and PDK1 as key players in AKT pathway and numerous studies have demonstrated deregulation of these factors in a variety of cancers. Activation of AKT has been described in breast, colon, ovarian, pancreatic, head and neck, prostate and bile duct cancers [160, 161, 162, 163, 164, 165, 166]. Importantly, activated AKT has been linked to poor prognosis in many human cancers [9]. Moreover, AKT activity has been shown to promote resistance to chemotherapy and radiotherapy [167, 168]. Thus, PI3-K, mTOR complexes, PDK-1 and AKT itself present a great potential for drug design for cancer treatment. Furthermore, an AKT pathway inhibitor promises to be useful in combination with other cancer treatments. Therefore, pharmacological inhibitors selectively targeting both PI3-K and mTOR most likely inhibit PDT-mediated AKT activation which results in effective enhancement of treatment response.

2.6 PI3-K Inhibitors

PI3-K activates an important cell survival signaling pathway, and constitutive activation is seen in ovarian, head and neck, urinary tract, cervical and small cell lung cancer [169]. Signaling through PI3-K is critical to fundamental processes in diverse cell types [169]. The eight mammalian PI3-K are divided into three classes according to their structure, regulation, and substrate specificity [160]. Among these enzymes, the three class 1A PI3-K (p110α, p110β, and p110δ) have been identified as the most critical for cell growth and survival. Class 1A PI3-K are heterodimers of a catalytic p110 lipid kinase subunit and an adaptor p85 subunit that recruits PI3-K to tyrosine phosphorylated membrane docking sites [160]. Gain of-function mutations in the *p110* gene are found in cancers of the colon, breast, and brain [170, 171]. It is increasingly clear that many of the most effective targeted cancer therapies owe their activity to unexpected synergy through inhibition of multiple targets. The requirement for inhibition of multiple targets likely reflects the complexity of signaling underlying malignant transformation and the ability of tumor cells to dynamically adapt to stress. For this reason, there is a growing consensus that inhibition of individual targets is unlikely to succeed as a therapeutic strategy in solid tumors.

Wortmannin, a furanosteroid metabolite of the fungi Penicillium funiculosum, is a specific, covalent inhibitor of PI3-Ks. Wortmannin is a more potent inhibitor than LY294002, another commonly used PI3-K inhibitor (Figure 2.8). However, Wortmannin and LY294002 have considerable side-effects due to high toxicity, therefore they are not suitable for further studies in animal models. Importantly, dual PI3-K and mTOR small molecule inhibitor PI-103 (Figure 2.8) has negligible cytotoxicity and minimal side effects besides being highly effective in AKT pathway inhibition. The activity of this compound was traced to its ability to selectively block p110α and mTOR at nanomolar concentrations. Combinatorial inhibition of p110α and mTOR was well tolerated *in vivo* and was highly effective against glioma xenografts [172]. These data suggest that combinatorial inhibition of mTOR and p110α represents a safe and effective therapy in the treatment of cancers driven by aberrant signaling through PI3-K. Signaling through PI3-K is critical to fundamental processes in diverse cell types. In part for this reason, the broad-spectrum PI3-K inhibitors Wortmannin and LY294002 are associated with significant cellular toxicity. PI3-K and mTOR inhibitor PI-103 inhibitor is active in low concentrations with minimal cytotoxicty and is a promising drug for clinical use [172, 173].

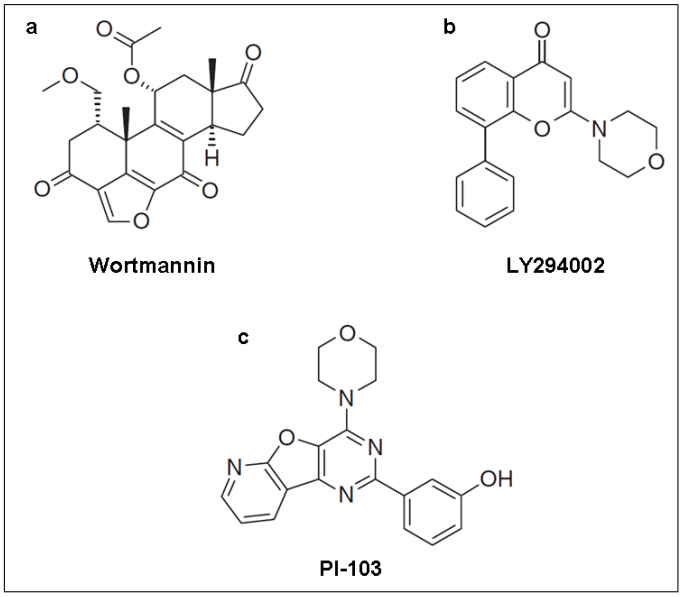

Figure 2.8 Molecular structures of PI3-K inhibitors [5]. a) Wortmannin, b) LY294002, c) PI-103

3. MATERIALS AND METHODS

3.1 Cell Culture and Mice Strains

C3H/BA murine mammary cancer cells (National Institute of Health, Bethesda, MD, USA), BT-474 human breast cancer cells (ATCC Bioproducts, Manassas VA, USA) and MDA-MB231 human breast cancer cells (gift from Prof. Mustafa B.A. Djamgoz, Imperial College, UK) were grown at 37 ^{o}C in a humidified incubator (Napco Digital, USA) under 5 % CO_2. C3H/BA and BT-474 cell lines were grown as monolayers in tissue culture flasks (75cm2; Corning, Inc., Corning, NY, USA) or tissue culture plates (100 mm, 60 mm; Corning, Inc., Corning, NY, USA in complete growth media composed of Dulbecco Modification Eagle Medium (DMEM; Mediatech, Inc., Herndon, VA, USA), 10 % Fetal Calf Serum (FCS; Omega Scientific, Inc., Tarzana, CA, USA), 0.5 % L-glutamine (Gemini Bio-Products, Woodland, CA, USA), 1 % penicillin-streptomycin (Gibco, Grand Island, NY, USA). MDA-MB231 cells were grown in tissue culture flasks in DMEM (without phenol red), supplemented with 5 % Fetal Bovine Serum (FBS; Gibco BRL-Invitrogen, Holland) 4 mM L-glutamine, 0.1 % penicillin-streptomycin. The cells were passaged in every 3 days before they become 100 % confluent. A new vial of cells frozen in liquid nitrogen were thawed in every month, and they were checked for mycoplasma every 3 months.

For *in vivo* experiments and tumor models, C3H/HeJ (The Jackson Laboratory, Bar Harbor, ME, USA) and Athymic mice (The Jackson Laboratory, Bar Harbor, ME, USA) was purchased and grown in the animal facility at Children's Hospital Los Angeles, CA, USA.

3.2 Plating Cells

C3H/BA and BT-474 cells were grown to 90 % confluency in the incubator and were only processed under tissue culture hoods (Streamline, Singapore) only with gloved hands (latex gloves; Cardinal Health, McGaw Park, IL, USA) to eliminate contamination. The growth medium inside the flask was removed with a sterile pasteur pipette (Pyrex-Corning Inc., Corning, NY, USA) connected to a controlled, continuous vacuum pump system. The cultured cells were rinsed with 6-7 ml PBS (Phosphate Buffered Saline) twice in order to completely remove the medium. Then, 10X trypsin-EDTA (Irvine Scientific, Santa Ana, CA, USA) was diluted 1:10 with PBS and 3 ml of this 1X trypsin-EDTA solution was added into each flask. Following 3-5 min incubation in the incubator, the flasks were agitated to separate the cells. 5 ml of fresh growth media was used to gently resuspend the cells in order to obtain a single cell suspension. The media containing the cells were put into a 15 ml falcon tube (Corning Labware Equipment, Inc., Corning, NY, USA). Then, 0.5 ml of cell suspension was added into 9.5 ml of isotonic solution to measure the cell count by using the cell counter (Coulter Electronics Inc., Hialeah, FL, USA).

Unless otherwise mentioned, in all *in vitro* experiments 10^6 cells were seeded per each 10 cm plates. Required amount of cells were resuspended in a new falcon tube and were spined for 5 min at 5000 rpm by using a mini centrifuge (Brinkmann Inst. Co., Westbury, NY, USA). The media was aspirated with a pasteur pipet without disturbing the cell pellet which was then resuspended in pre-warmed complete growth media to reach a volume of 10 ml for a 10 cm plate. The cells were evenly distributed throughout the plate by gentle shaking. Lastly, the plates were placed in the incubator till they were processed.

3.3 *In vitro* PDT Protocol

3.3.1 Preparing the Photosensitizer Solutions and Photosensitizer Treatments

The photosensitizer Photofrin (PH; Axcan Pharma Inc., Mont-Saint-Hilaire, Canada) was dissolved in 5 % dextrose (Baxter Healthcare Corporation, McGraw Park, IL, USA) to prepare a stock solution at a concentration of 2.5 mg/ml and was aliquoted to store at -20 ^{o}C refrigerator (Baxter Healthcare Corporation, McGraw Park, IL, USA). The aliquots were thawed only once before treatment. For the *in vitro* experiments, PH was used at a concentration of 25 μg/ml in which stock solution was diluted 1:100 with DMEM supplemented with 5 % FCS, 0.5 % L-glutamine, 1 % penicillin-streptomycin. Culture were grown for 24 hr before PH application. Following PH addition cultures were kept in dark, since PH is highly light sensitive. The cultures were incubated for 16 hr before treatment with light. In parallel, light alone or untreated controls were fed with growth media supplemented with 5 % dextrose at volumes equal to PH administration.

The photosensitizer Indocyanine Green (ICG, Pulson Medical Systems AG, Munich, Germany) was dissolved in DMEM to obtain a final concentration of 50 μM. The cell cultures were incubated in 50 μM of ICG for 24 hr in dark. During and following ICG incubations, plates were always kept in dark. The cultures were refed with fresh growth media after 24 hr. In parallel, the media of light alone or untreated control groups were replaced with fresh complete media.

3.3.2 *In vitro* Drug Treatments

Stock solutions for the PI3-K inhibitors for this study were prepared as follows: Wortmannin was purchased from Calbiochem (San Diego, CA, USA) and dissolved in dimethyl sulfoxide (DMSO) to reach a concentration of 1 mM. LY294002 was purchased from Sigma-Aldrich (St Louise, MO, USA) and dissolved in DMSO to a concentration

of 29 mM. PI-103 was purchased from Calbiochem (San Diego, CA, USA) and dissolved in DMSO to a stock concentration of 5 mg/ml. All stock solutions were aliquoted and kept at -20 ^{o}C. Immediately before the experiments, inhibitor aliquots were thawed and complete media containing Wortmannin (1 μM), LY294002 (100 μM) or PI-103 (0.25 μM) were prepared. In parallel, DMSO was added to growth media at the amounts equal to the inhibitor volumes and added to control cultures. It is important to note that, Wortmannin and LY294002 were always added to the cultures at the time of PH incubation and kept in cultures till cells were harvested. On the other hand, PI-103 was added to the cultures immediately after PDT treatment.

3.3.3 *In vitro* Light Treatments

Following 16 hr PH incubation, the PH-containing media was removed and the cells were refed with prewarmed fresh media supplemented with 10 % FBS, L-glutamine and penicillin-streptomycin for 30 min at 37 ^{o}C. At the end of incubation, cells were rinsed once with DMEM only and were exposed to broad-spectrum red light (570-650 nm, 0.35 mW/cm^2) for 1.5 min. Unless otherwise mentioned, the cells were refed with prewarmed complete growth media.

For ICG-PDT experiments, the MDA-MB231 cells incubated overnight in 50 μM ICG The next day, indicated groups were exposed to 809-nm diode laser [174] for 10 min with a power density of 60 mW/cm^2 (Figure 3.1). Each well was washed with PBS before light treatment and they were refed with 300 μl complete fresh complete media following treatment and incubated for different time points (0, 3, 6, 9, 12, 24, 48 hr).

3.3.4 Harvesting Cells

Following PH-PDT treatment, the cells were harvested in dark. The culture plates were chilled on ice, the media was aspirated and the cells were rinsed with ice-

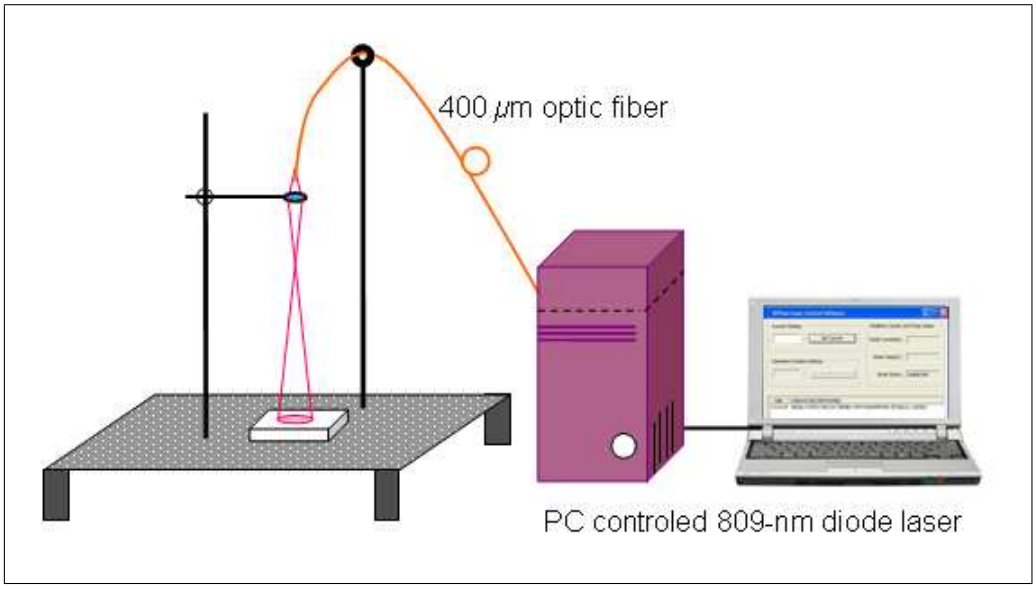

Figure 3.1 *In vitro* light treatment set-up for ICG-PDT

cold PBS. At the meantime, 10X Cell Lysis Buffer (Cell Signaling Tech., Inc., Beverly, MA, USA) was diluted to 1:10 with ultra pure water and supplemented with 1:100 Phenylmethylsulfonyl Fluoride (PMSF; Sigma-Aldrich Co. Ltd, St Louise, MO, USA) that was prepared by dissolving 17.4 mg PMSF in 1 ml 100 % ethanol (Pharmco-Aaper Subsidiaries of Commercial Alcohols, Inc., Brookfield, CT - Shelbyville, KY, USA) . The PBS was aspirated and 300 μl of ice-cold 1X cell lysis buffer was added into each 60 or 100 mm plate and the plates were sit on ice for 5 min. Then cells were collected with a cell scraper and the cell lysates were collected in pre-chilled 1.5 ml eppendorf tubes (USA Scientific, Inc., Ocala, FL, USA). The whole cell lysates were sonicated (Virsonic300, The Virtis Company Inc., Gardiner, NY, USA) on ice for 10-15 sec and centrifuged at 10.000 rpm for 10 min on a tabletop centrifuge. The cleared cell lysates were transferred into a pre-chilled clean eppendorf tubes and the samples were stored at -80^{o}C refrigerator (Thermo-Fisher Scientific, Rockford, IL, USA).

3.4 Protein Assay

In order to accurately determine the concentration of solubilized proteins in cell lysates, the protein quantification assay (Bio-Rad Laboratories, Inc., Hercules, CA,

USA) was used based on the Bradford method. This method involves the addition of an acidic dye to protein solution, and subsequent measurement at 595 nm with a spectrophotometer (Beckman Instruments Inc., Fullerton, CA, USA). First, the dye reagent concentrate was diluted 1:4 with distilled water. The 2, 4, 8 μg of a protein standard were prepared by adding 5, 10, 20 μl of bovine serum albumin (BSA, Sigma-Aldrich Co. Ltd, St Louise, MO, USA) into separate tubes of 1 ml diluted dye reagent. Then the mixture was vortexed (Baxter Healthcare Corporation, McGraw Park, IL, USA), poured into a clean 1 ml cuvettes (Sarstedt, Inc., Nurmbrecht, Germany) and the absorbance of the standards were read at 595 nm. These results were used to obtain the standard curve which would be representative of the samples to be tested. Next, the protein content of each sample was measured by adding specific amount into 1 ml diluted dye reagent and the readings were taken at 595 nm. The protein content of each sample was calculated based on where the absorbance values correspond on the standard curve.

3.5 Western Immunoblot Analysis

The changes in protein expression before and after PDT treatments were examined by Western immunoblot analysis. In this method, protein samples were mixed with 4X Sample Buffer (Bio-Rad Laboratories, Inc., Alfred Nobel Dr., Hercules, CA, USA) and size-separated on 10 % tris-glycine precast continued gels (Invitrogen Life Tech., Carlsbad, CA, USA) by using electrophoresis apparatus (Novex Experimental Tech., San Diego, CA, USA) connected to a power supply (Haakebuchler Inst. Inc., Saddle Brook, NJ, USA) generating 125 V for 2 hr. The molecular weight marker (Amersham Biosciences Corp., Piscataway, NJ, USA) was also run with the samples to be used as a control for protein size. The electrophoresis was carried out in the running buffer prepared by dissolving 3.03 tris-base (Sigma-Aldrich Co. Ltd, St Louise, MO, USA), 14.4 glycine (Sigma-Aldrich Co. Ltd, St Louise, MO, USA), and 1 g Sodium Dodecyl Sulfate (SDS; Sigma-Aldrich Co. Ltd, St Louise, MO, USA) dissolved in 1 l distilled water. Following electrophoresis, the proteins on the gel were transferred overnight onto a nitrocellulose membrane (Optitran, Schleicher & Schuell Bioscience,

Dassel, Germany) in transfer buffer at a constant 20 V generated by the transfer apparatus (Hoefer Scientific Inst., San Francisco, CA, USA). The transfer buffer was prepared by dissolving 78.82 g glycine and 19.96 g tris-base in 5.6 l distilled water and 1.4 l methanol (Sigma-Aldrich Co. Ltd, St Louise, MO, USA).

Following the transfer, membranes were blocked in 5 % non-fat milk (Nestle S.A., Verey, Switzerland) solubilized in PBS for 1 hr at room temperature by gentle agitation on the rocker platform (Bellco Biotechnology, Vineland, NJ, USA). After block, membranes were rinsed 3 times for 5 min with the fresh western wash buffer, Tween-Tris Buffered Saline (TTBS), which was prepared by dissolving 12.11 g tris-base, 9 g NaCl (Sigma-Aldrich Co. Ltd, St Louise, MO, USA) and 1 ml tween-20 (Tween-20; Bio-Rad Laboratories, Inc., Alfred Nobel Dr., Hercules, CA, USA) in 1 l of distilled water and the pH was adjusted at pH 7.5. Then, the membranes were incubated overnight at 4^oC with the primary antibodies and rinsed with TTBS 3 times for 5 min each. Depending on the experiment, the primary antibody used were as follows: anti-phospho-AKT at Ser 473 (Cell Signaling Tech., Inc., Beverly, MA, USA), anti-phospho-AKT at Thr 308 (Cell Signaling Tech., Inc., Beverly, MA, USA), anti-AKT 1/2/3 (Santa Cruz Biotech., Inc., Santa Cruz, CA, USA), anti-AKT 1/2 (Santa Cruz Biotech., Inc., Santa Cruz, CA, USA), anti-phospho-GSK-3α/β at Ser21/9 (Cell Signaling Tech., Inc., Beverly, MA, USA), anti-GSK-3α/β (Santa Cruz Biotech., Inc., Santa Cruz, CA, USA), anti-phospho-rpS6 at Ser 235/236 (Cell Signaling Tech., Inc., Beverly, MA, USA), anti- rpS6 (Cell Signaling Tech., Inc., Beverly, MA, USA) and anti-actin (MP Biomedicals, Inc., St Louis, MO, USA). Membranes were then incubated with appropriate peroxidase conjugated secondary antibodies as follows: anti-rabbit peroxidase conjugate (Sigma-Aldrich Co. Ltd, St Louise, MO, USA), anti-mouse peroxidase conjugate (Sigma-Aldrich Co. Ltd, St Louise, MO, USA) and anti-goat peroxidase conjugate (Santa Cruz Biotech., Inc., Santa Cruz, CA, USA). Anti-rabbit peroxidase conjugates were used for phospho-AKTs, AKT, phospho-GSK-3, phospho-rpS6, rpS6 primary antibodies. On the other hand, anti-mouse peroxidase conjugates were used for GSK-3 and actin. The membranes were rinsed with TTBS 3 times for 5min and the resulting immuno-complexes were visualized by incubation the membranes with enhanced chemiluminescence western blotting reagent (ECL-TM; GE Healthcare, Buckinghamshire, UK) and detecting

chemiluminescence by autoradiography. The exposed films (Chemiluminescence Film; Kodak Biomax Industrie, Cedex, France) were processed by the medical film processor (Konica-Minolta Medical and Graphic Inc., Tokyo, Japan). Protein loading was controlled by comparing the intensity of the protein band representing actin protein in each sample.

3.6 ELISA

Quantitative analysis of AKT activation was performed by FACE Cell-Based AKT ELISA Kit (Active Motif, Carlsbad, CA, USA). Briefly, 2.5x10^4 BT-474 cells were seeded in the 96-well plate and incubated for 24 hr in complete growth media. Then, cell cultures were incubated with PH (25 μM) for 16 h at 37 ^{o}C and exposed to 570-650 nm light for 1.5 min (315 J/m^2). After treatment, the cells were refed with complete growth media for 1 hr and were fixed with formaldehyde. Samples were treated according to the manufacturers' instructions for AKT ELISA kit. The readings were taken at crystal violet light. The data were normalized for protein concentrations.

3.7 MTT Cell Viability Assay

3.7.1 MTT Assay for PH-PDT Experiments

10^4 BT-474 and C3H/BA cells in 100 μl complete growth media were seeded for each well of 96-well plate (TPP, Switzerland) and incubated at 37 ^{o}C for 24 hr. The following day, the cell cultures were refed with fresh 5 % FBS complete media supplemented with 25 μg/ml of PH for 16 hr. Following photosensitizer treatments, the cultures were fed with complete growth media for 30 min, quickly rinsed with serum free medium and exposed to 570-650 nm light for 1, 1.5 and 2 min. At time points indicated for each experiment, cell viability was measured with 3-(4,5-dimethylthiazol)-2,5-diphenyltetrazolium bromide (MTT; ATCC Bioproducts, Manassas VA, USA) assay

according to the manufacturer's protocol. Following 24 hr of PDT application, 10 μl of MTT reagent was added to each well and incubated for 2 to 4 hr at 37oC until the purple precipitate was visible. Then the plates were washed with 100 μl of detergent reagent at room temperature in dark for 2 hr. Finally, the absorbance was measured at 570 nm by using with Microplate Reader (MR600; Dynatech Products, USA). 8 wells were used for each group and the mean was determined from these wells and standard error was calculated.

3.7.2 MTT Assay for ICG-PDT Experiments

1.5x10^4 MDA-MB231 cells were seeded in 96-well plates and incubated overnight in 100 μl complete growth media. ICG and ICG-PDT groups were incubated in 50 μM of ICG (dissolved in medium) for 24 hr. In parallel, the media of Control and Light groups were replaced with fresh complete media. The next day, indicated groups were rinsed with PBS and exposed to 809-nm diode laser for 10 min. Cells were refed with 300 μl complete fresh complete media following treatment and incubated for different time points (0, 3, 6, 9, 12, 24 and 48 hr). Cell viability after each treatment was determined by MTT (Roche-Diagnostics GmbH, Mannheim, Germany) assay according to manufacturers' specifications. The wells were refed with media supplemented with 0.5 mg/ml MTT reagent and incubated for 4 h at 37 ^{o}C. For the time 0 group, the cells were directly exposed to MTT right after treatment. To terminate the reaction, 100 μl solubilization medium was added to each well and incubated overnight. The next day the optical density of the wells were measured at 595 nm with a microplate reader (Model 680; Bio-Rad Laboratories, Hercules, USA).

3.8 Apoptotic Cell Death Detection Assay

10^6 cells suspended in 10 ml 10 % FBS growth media were plated in 100 mm plates. Following 24 hr incubation at 37 ^{o}C, the media was replaced with 5 % FBS medium containing 25 μg/ml PH and incubated for 16 hr. The cells were refed with

fresh media for 30 min, rinsed with serum free media and treated with 570-650 nm for 1.5 min and refed with 1.5 ml of 10 % FBS complete growth medium. Following 6 hr incubation, the cells were lifted from the plate and transferred into a 1.5 ml eppendorf tube. 100 μl of cell suspension was used for cell death determination and the rest of the suspension was lysed and processed for protein assay and western blot analysis. This 100 μl of PH-PDT treated cell suspension was mixed with 200 μl of 10 % FBS complete media and spined at 1200 rpm for 10 min. Then the supernatant was discarded and cell pellet was resuspended in 200 μl of cell lysis buffer supplied with the apoptotic cell death detection kit (Cell Death Detection ELISA-Plus; Roche Diagnostics GmbH, Mannheim, Germany) and incubated at room temperature for 30 min. After a second spin at 1200 rpm for 10 min, the supernatant was recovered and equal protein amounts of each sample was prepared by diluting with lysis buffer. 20 μl of equilibrated samples were mixed with 80 μl of reaction buffer and transferred into the streptavidin-coated microplate supplied with the apoptosis kit. Microplate was covered with foil in order to protect from light and gently shaken for 2 hr at room temperature. The solution was removed and each well was rinsed 3 times with 200 μl incubation buffer. Then 100 μl of developing buffer was added to each well and the microplate was gently shaken until the color development for photometric analysis at 405 nm.

3.9 Colony Assay

$3x10^2$ or $3x10^3$ cells were plated in triplicates in 60 mm plates in 6 ml complete growth media and incubated at 37 ^{o}C for 24 hr. The indicated groups were treated with PH (25 μg/ml) for 16 hr and were refed with fresh complete media for 30 min. The cultures were then quickly rinsed with serum free media and treated with broad spectrum of light and refed with complete media with or without the 0.25 μM of PI-103 inhibitor. Then cell cultures were incubated for 11 days to observe colony formation. After the colonies reached a certain size, the cells were rinsed with PBS and fixed with 70 % alcohol and the plates were left open to for alcohol to evaporate. After the plates were completely dry, they were stained with methylene blue working solution. First, Methylene blue stock solution was prepared by dissolving 10 g methylene blue

(Sigma-Aldrich Co. Ltd, St Louise, MO, USA) in 1 l of 95 % ethanol. Then, 30 ml of stock was mixed with 100 ml of 0.01 % potassium hydroxide (Sigma-Aldrich Co. Ltd, St Louise, MO, USA) and the plates were treated with this solution for at least 30 min. Once the colonies on each plate was visible with blue color, the dishes were gently rinsed with running tab water and they were let to dry. Colonies having more than 30 cells were counted under light.

3.10 *In vivo* Treatment Protocol

Mouse breast cancer (BA) and human breast cancer (BT-474) cells were grown as a monolayer in complete growth media. Primary BA tumors were generated by subcutaneous trochar injection of $1x10^6$ cells in 50 μl media into the hind flank of 8 to 10 week-old female C3H/HeJ mice (Figure 3.2a). Once tumor lesions reach around 5 mm in diameter, these tumors were surgically removed, diced into 1 mm^3 pieces and injected (Implant Needles; Popper and Sons, Inc., New Hyde Park, NY, USA) into the hind flank of new 8 to 10 week-old female C3H/HeJ mice (Figure 3.2b) to create secondary tumors. On the other hand, BT-474 tumors were generated by injecting $8x10^6$ cells within 100 μl matrigel matrix (BD Biosciences, San Jose, CA) to the hind flank of 10 to 12 week-old female athymic mice. *In vivo* tumor treatments of lesions measuring 6-7 mm in largest diameter involved an i.v. injection of PH (5 mg/kg) for 24 hr followed by tumor irradiation using a non-thermal argon-pumped 630 nm diode laser (Diomed Inc., Andover, MA, USA)(Figure 3.2c). Light was delivered via a 800 μm quartz fiber microlens. The light delivery was split (Fiber splitter; Laser Technologies Inc., Buellton, CA, USA) into three fibers to enable treatment of three mice at a time (Figure 3.3). The light output at treatment site was measured with a power meter (Coherent, Palo Alto, CA, USA). A light dose rate of 75 mW/cm^2 and the total light dose 100 J/cm^2 was used to treat tumors.

It is important to note that, mice were kept in dark for the rest of the experiment following PH administration. Since PH is dissolved in dextrose, control groups were given 5 % dextrose at volumes equal to PH administration. Moreover, 630 nm diode

laser was equilibrated by 664 nm Diode Laser (Miravant Systems Inc., Santa Barbara, CA, USA) before use. For PI-103 applications *in vivo*, mice were injected twice with 50 mg/kg of PI-103 solubilized in DMSO. The first injection was the time of PDT treatment and the second injection was 20 min following the first injection. Control animals received equal volumes of DMSO.

Following treatments, mice were sacrificed with overdose of CO_2 and each tumor was surgically removed and divided in to two. One half of the tumor was stored in formalin for further immunohistochemistry application and the other half was ground (Virtishear Company, Gardiner, NY, USA) and homogenized in cell lysis buffer for western blot analysis.

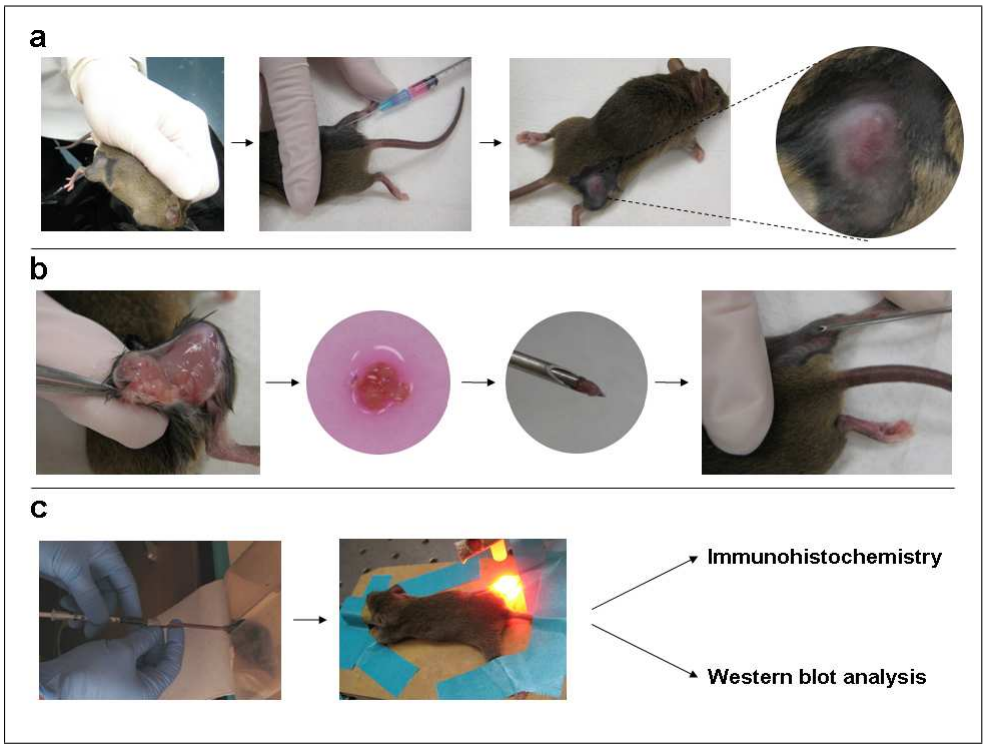

Figure 3.2 *In vivo* PDT treatment procedure.Right flank of 15 weeks old C3H/HeJ female mice was shaved, and animals were anaesthetized with isoflurane. a) 2-3 animals were injected with C3H/BA cells (10^6/tumor in 50 μl DMEM) into shaved flank of animal and they were kept 2-3 weeks for the primary tumor to grow. When the tumor became visible under the skin, animals were sacrificed with overdose CO_2 . b) Tumors were surgically removed, cut into small pieces (1 mm^3) and trocar injected into shaved flanks of experimental animals. Animals were housed in cages (4±1 animals per cage) in temperature controlled vivarium, food and water were available ad libitum. c) When tumors reached to a certain size (6-7 mm) animals were injected with PH (5 mg/kg) intravenously and kept in dark for 24 hr. Tumor area was illuminated with light at 630 nm. After certain time point animals were sacrificed with overdose CO_2, tumors were removed, and cut into two; one half was fixed with paraformaldehyde for immunohistochemistry and the other was homogenized for western blot analysis.

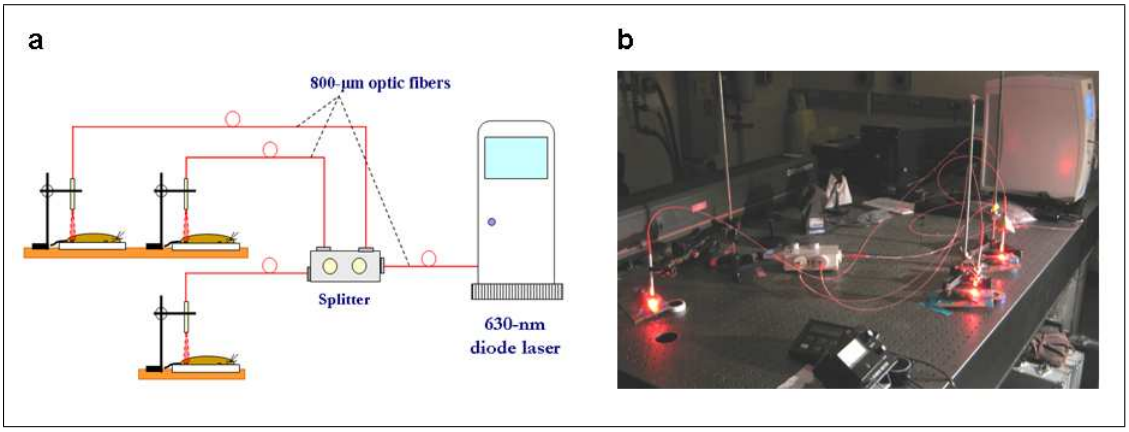

Figure 3.3 *In vivo* light treatment during PDT. Three animals were treated at a time. Optical fiber coming out of 630 nm diode laser was split in three 800 μm optic fibers. Animals were taped so that the tumor under the light stays at a fixed position and the optic fibers were positioned such a way that the light covers all the tumor area. Each tumor area was illuminated with 630 nm diode laser at a dose rate of 75 mW/cm^2 and the total light dose 100 J/cm^2. Before every treatment, light output at tumor site was measured with a powermeter.

3.11 Immunohistochemistry

Immunohistochemistry was done on paraffin-embedded 5 μm tissue sections mounted on poly-L-lysine-coated slides (Corning Labware Equipment, Inc., Corning, NY, USA). For de-paraffinization, slides were baked at 60 ^{o}C for 1 hr by using an incubator shaker (New Brunswick Scientific Co., Inc., Edison, NJ, USA), washed 3 times with xylene for 5 min each, rinsed with 2 times with 100 % and 95 % ethanol for 10 min each and washed in 2 times in water for 5 min. After antigen retrieval (BioGenex, Ran Raman, CA, USA) in a microwave oven for 15 min, slides were maintained at a sub-boiling temperature for 15 min and cooled on bench. Then, slides were washed 3 times with water for 5 min each and incubated in 3 % Hydrogen Peroxide (H_2O_2; Sigma-Aldrich Co. Ltd, St Louise, MO, USA) for 10 min. Next, sections were washed in 1X TTBS for 5 min and blocked with 5 % goat serum for 1 hr at room temperature. Then, slides were incubated with avidin and biotin supplied in Avidin/Biotin Blocking Kit (Vector Laboratories, Inc., Burlingane, CA, USA) for 15 min each and the sections were incubated with the immunohistochemistry-specific antibodies for phospho-AKT at Ser 473 position (Cell Signaling Tech., Inc., Beverly, MA, USA) or phospho-AKT blocking peptide (Cell Signaling Tech., Inc., Beverly, MA, USA) to check the specific binding of the phospho-AKT antibody overnight at 4 ^{o}C. The following day, biotinylated-goat

anti-rabbit IgG (Vector Laboratories, Inc., Burlingane, CA, USA) was applied on the sections for 30 min at room temperature. Then, sections were rinsed with TTBS for 5 min and incubated with Vectastain ABC Kit (Vector Laboratories, Inc., Burlingane, CA, USA) for 30 min at room temperature followed by detection of immunoreactivity using 3,3'-diaminobenzidine (DAB) Peroxidase Substrate Kit (Vector Laboratories, Inc., Burlingane, CA, USA). Finally, sections were lightly counter stained with hematoxylin solution (Sigma-Aldrich Co. Ltd, St Louise, MO, USA) and mounted with mounting medium (Fluka Biochemika-Sigma-Aldrich Co. Ltd, St Louise, MO, USA). The slides were analyzed and the representative pictures were taken by CCD camera attached microscope (Olympus, Tokyo, Japan).

3.12 Statistical Analysis

Statistical analysis was performed using a two-tailed paired Student's t-test to determine statistical differences for groups as indicated.

4. RESULTS AND DISCUSSION

4.1 Multiple Components of PH-PDT can Phosphorylate AKT

Therapeutic PDT applications in cancer therapy is encouraging but long term PDT responsiveness needed to be improved to decrease tumor recurrence [30]. Preclinical investigations show that PDT can induce expression and/or activation of pro-angiogenic molecules including VEGF, COX-2, prostaglandins, TNF-α, MMPs, integrins, IL-6 and IL-8 within the tumor microenvironment [108, 109, 110, 115, 116, 117, 118]. Overexpression of these molecules is often associated with a survival phenotype and recent studies show that targeted therapy directed at these molecules can enhance the therapeutic effectiveness of PDT [12].

AKT/Protein Kinase B is a signaling molecule that plays a key role in integrating cellular responses to growth factors and extracellular signals [160]. The AKT pathway plays a major role in tumor development as well as in the responsiveness of tumor cells to treatment [175]. Phosphorylation of AKT activates this molecule and can provide cells with a survival signal that protects them from apoptotic stimuli. Numerous studies have shown that oxidative stress stimulates AKT phosphorylation and proteins activated by phosphorylated AKT promote cell survival [120, 121].

In this study, it was examined whether PH-PDT phosphorylates AKT in mouse and human breast cancer cell lines cultured *in vitro* and grown as solid tumors in mice. It was found that PH-mediated PDT induced strong AKT phosphorylation and that inhibition of this activation after PDT increases the treatment responsiveness [176]. However, it was also observed that PH alone, without any light exposure, induced measurable levels of AKT phosphorylation in cancer cells exposed to the photosensitizer in culture and that 630 nm light alone induced AKT phosphorylation in transplanted tumors growing in mice [176]. These results indicate that individual components of the PDT and not just PDT can play a role in activating the AKT pathway. These findings

suggest that targeting AKT pathway may improve PDT responsiveness and warrants further investigations.

4.1.1 Oxidative Stress Induced by H_2O_2 Stimulates AKT Phosphorylation via PI3-K Pathway

AKT is a target of PI3-K and oxidative stress generating reactive oxygen species, such as H_2O_2, as well as hypoxia can phosphorylate and activate AKT pathway and lead to increased cell survival [120, 121, 177, 178]. To confirm these previous findings in our cell culture system, C3H/BA and BT-474 breast cancer cell lines were exposed to H_2O_2 and the level of total AKT and phosphorylated AKT at Ser 473 (phospho-AKT) was measured in a time course experiment. Protein samples from cell cultures were collected at different time points following incubation with H_2O_2 and analyzed by western blot using AKT and phospho-AKT specific antibodies as well as Actin antibodies as a loading control. These experiments demonstrated that, H_2O_2-induced AKT phosphorylation was detectable as early as 15 minutes upon exposure which persisted at least for 3 hr in both cell lines (Figure 4.1). In the same experimental set-up, the PI3-K inhibitor Wortmannin was used to test whether H_2O_2-induced AKT phosphorylation was dependent on PI3-K activity. Addition of Wortmannin to H_2O_2-treated C3H/BA or BT-474 cells effectively blocked AKT phosphorylation without altering total AKT protein levels. Consistent with previous findings [120, 178], our results indicate that H_2O_2-induced AKT phosphorylation was sensitive to PI3-K inhibitor Wortmannin in C3H/BA and BT-474 cells.

4.1.2 Photofrin-PDT Induces AKT Phosphorylation *in vitro*

A variety of cytotoxic and survival responses are observed following PDT. A previous study reported that, oxidative stress associated with Rose Bengal-mediated PDT activated AKT in mouse fibroblasts [120]. To determine whether Photofrin (PH)-mediated PDT initiates a similar response as determined for H_2O_2, BT-474 cells were

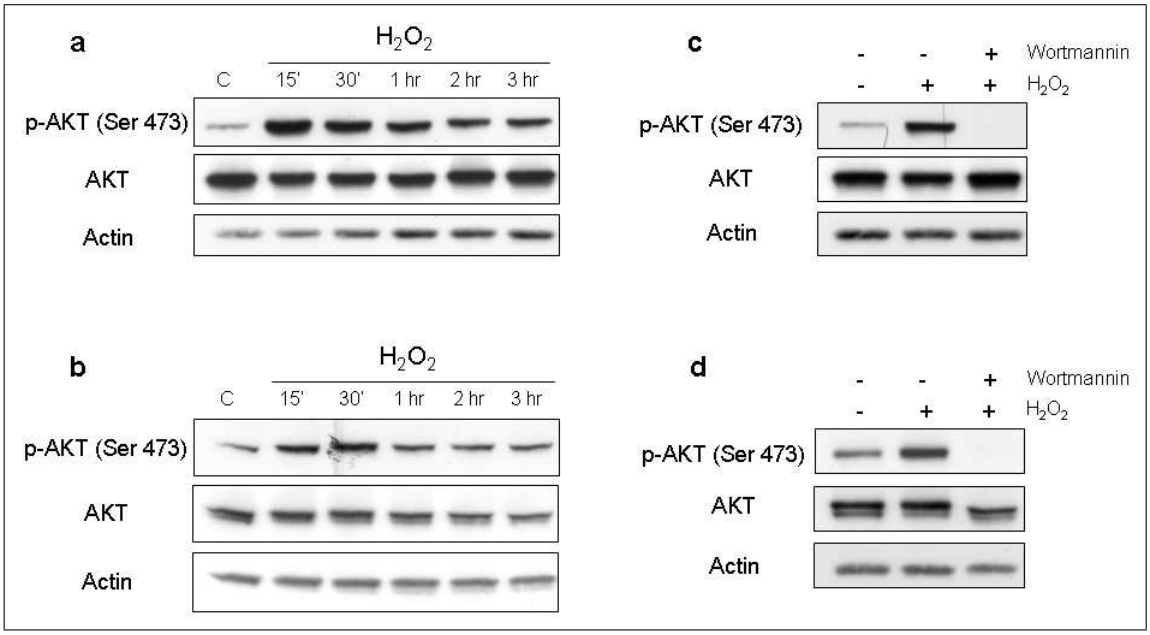

Figure 4.1 H_2O_2 induces PI3-K-dependent AKT phosphorylation in both C3H/BA (a, c) and BT-474 (b, d) cells. Cells were plated for 24 hr prior to exposure to H_2O_2 (500 μM) in PBS for 10 min, which is followed by incubation with complete media (a, b). Cell lysates were collected at indicated time points and were subjected to western blot analysis using phospho-AKT (Ser 473), total AKT and actin antibodies. PI3-K inhibitor Wortmannin blocks AKT phosphorylation in both C3H/BA (c) and BT-474 (d) cells. H_2O_2-treated cells were incubated with complete media supplemented with Wortmannin (100 nM) for 30 min (c, d). At the end of incubation, cell lysates were collected and analyzed as described above. "C" stands for control.

tested for PH-mediated PDT treatment. To start with, the optimum light dose for PDT treatments were determined by using MTT cell viability assay. For this, BT-474 and C3H/BA cell lines were incubated with PH and exposed to 210, 315 and 420 J/m^2 of broad-spectrum red light (570-650 nm). The MTT analysis following treatment showed that, doses of 315 and 420 J/m^2 lead to a statistically significant decrease in cell viability over control for both cell types used (Figure 4.2). In order to keep the treatment time short at an effective dose with relatively less side effects, 315 J/m^2 was chosen to be the optimal dose for the rest of the PDT applications in this study.

Next, BT-474 cells were tested for PH-mediated PDT treatment to investigate its effects on AKT phosphorylation. For this, BT-474 cells were incubated with PH and treated with red light. The effects of PH-PDT on AKT phosphorylation were then determined by either western blot analysis (Figure 4.3) or ELISA assay (Figure 4.4). In western blot analysis, AKT phosphorylation was detected 2 hr following PDT

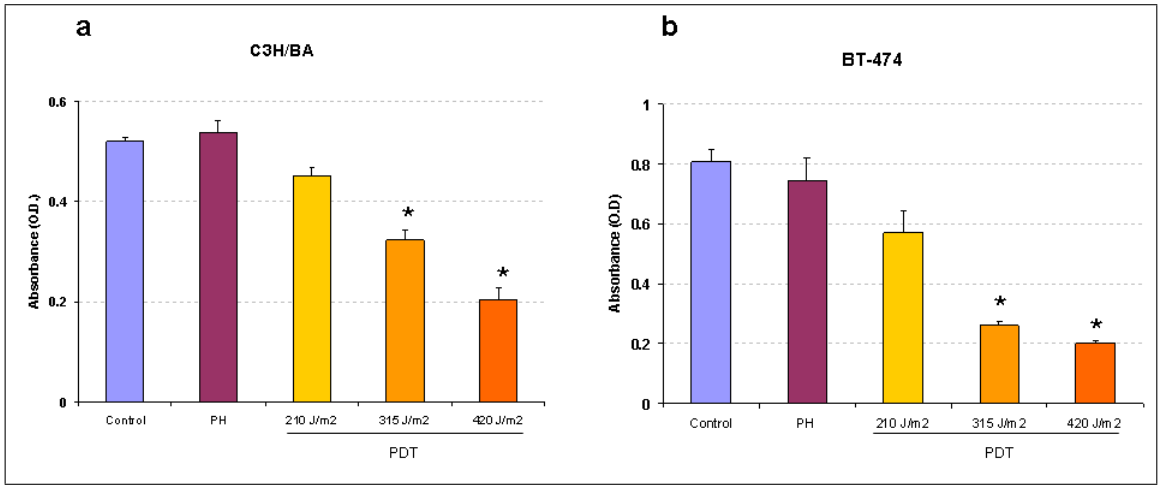

Figure 4.2 The cytotoxic effects of PDT is directly related to the light dose. Cells were then photosensitized with PH (25 μg/ml) for 16 hr in dark and exposed to light at 570-650 nm for 1, 1.5 and 2 min (210, 315 and 420 J/m^2, respectively). After treatment, cells were refed with complete media and incubated for 24 hr in dark. Cell viability was measured by MTT assay according to manufacturer's specifications (details in Materials and Methods Section). Results are expressed as the mean $\pm$ SE of three separate experiments done in a group of 8 wells for each condition. * The decrease in cell viability in PDT treated samples were statistically significant ($p < 0.01$)

.

treatment (Figure 4.3). Even though the signal for phospho-AKT persisted for 24 hr post-treatment, the levels decreased by time. Although, the phospho-AKT levels detected were highest in PDT group, PH alone sample harvested 2 hr post-incubation showed a slight increase in phospho-AKT levels compared to control (C) (Figure 4.3). Importantly, the level of total AKT protein detected remained the same in all groups at different time points. In order to confirm our results quantitatively, a cell-based ELISA kit was used to measure levels of phospho-AKT in PDT treated BT-474 cells. Since the phospho-AKT levels detected by western blot analysis were highest 2 hr after treatment, ELISA assay was performed 2 hr following PH-PDT as described in Materials and Methods section of this thesis (Section 3.6). Our results showed a significant increase in phospho-AKT in samples detected for PDT treated cells compared to both control and PH alone (Figure 4.4). Taken together, our results indicated that PH-PDT treatment significantly increased AKT phosphorylation which persisted for at least 24 hr suggesting a long-term response to PDT treatment.

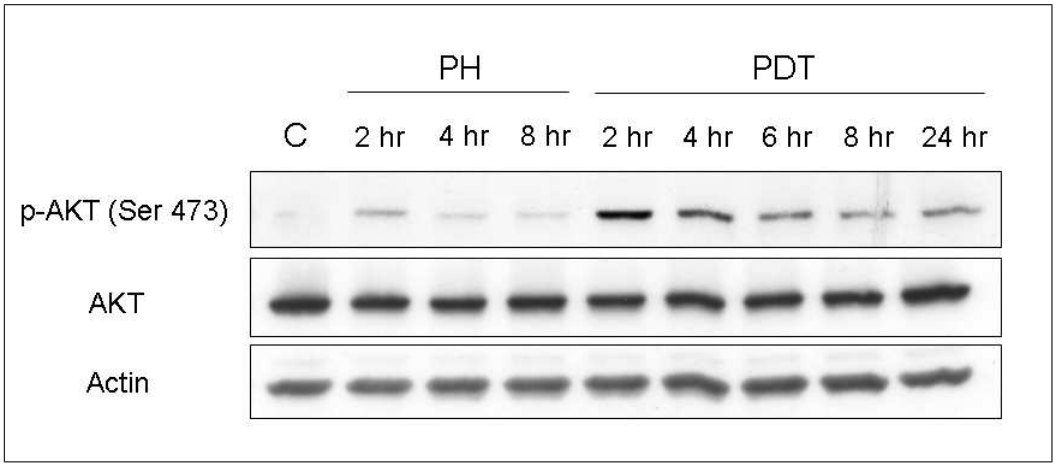

Figure 4.3 PH-PDT induces AKT phosphorylation in a time dependent manner. BT-474 cells were incubated overnight in complete media. Cells were then photosensitized with PH (25 μg/ml) for 16 h in dark. Cells were fed with complete media for 30 min before treatment with light (570-650 nm) for 1.5 min (315 J/m^2). After treatment, cells were fed with complete media and were lysed at indicated time points. Cell lysates were subjected to western blot analysis with AKT, phospho-AKT (Ser 473) and actin antibodies.

4.1.3 PH-PDT Induces AKT Phosphorylation *in vivo*

In the previous section, PH-PDT treatment was shown to induce AKT phosphorylation *in vitro*. To examine the *in vivo* relevance of this finding, solid tumors generated in mice were treated with PH-PDT and the induction of AKT phosphorylation was detected with immunohistochemical analysis. For this experiment, BT-474 cells were injected subcutaneously to athymic mice to create solid tumors. When the tumors reached a certain size, the tumor area was treated with red light following injection of PH or vehicle control. Immunohistochemical analysis of PH-PDT treated, PH alone or control tumor sections were performed for hematoxylin and eosin (H&E), phospho-AKT antibodies with or without blocking peptide (Figure 4.5). The H&E stained sections from different tumors showed similar morphology and cell distribution. PDT-treated samples had stronger hematoxylin staining compared to controls and cells lack nuclei suggesting the presence of red blood cells. This observation may be a consequence of hemorrhage in the tissue triggered by PDT treatment. As expected, tumor sections stained for phospho-AKT antibody showed a strong staining in PDT treated samples compared to PH alone and control (Figure 4.5). However, the phospho-AKT stained samples of PH alone treatment was only slightly stronger than

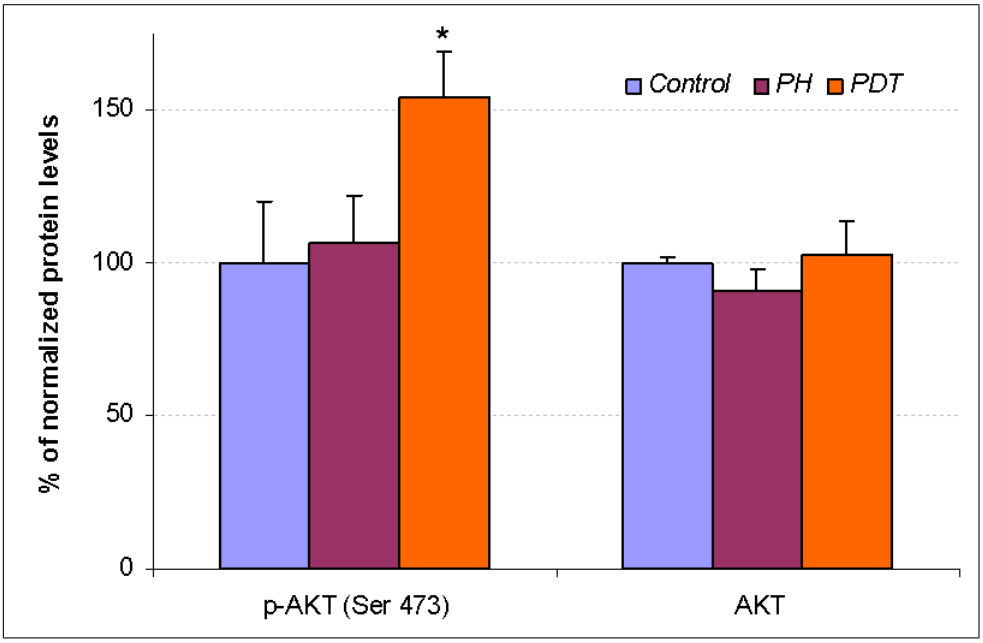

Figure 4.4 Photofrin (PH)-mediated PDT induces AKT phosphorylation. BT-474 cells were plated in the 96-well plates for 24 hr. Cell cultures were treated with PH (25 μg/ml) or carrier dextrose solution and incubated for 16 hr in dark. Then a group of PH-treated cells were exposed to broad-spectrum red light (570-650 nm, 0.35 mW/cm^2) for 1.5 min (315 J/m^2). All cells were fixed with formaldehyde 2 hr after treatment and transferred to ELISA plates (FACE Cell-based AKT kit) to detect total AKT and phospho-AKT (Ser 473) levels with specific antibodies. The colorimetric readings were taken at 450 nm. The data is corrected for crystal violet readings and presented as percentage normalized to controls. *The increase in phospho-AKT in PDT group was statistically significant ($p<0.05$) above control and PH-treated samples.

control samples. Importantly, the samples that were stained for phospho-AKT antibody in the presence of its blocking peptide did not show any positive staining in all groups (Figure 4.5). This result suggests that the phospho-AKT antibody specifically recognize the phospho-AKT protein in these tissue sections. The results of this *in vivo* study is in accordance with our previous cell culture analysis (Section 4.1.2) suggesting that PH-PDT stimulates AKT phosphorylation.

4.1.4 PH-PDT and PH Alone Induce AKT Phosphorylation via PI3-K Pathway

In the first set of experiments, our results indicate that PH-PDT induced AKT phosphorylation in human breast cancer cells *in vitro* and *in vivo* animal tumor models. To test whether PDT-induced AKT phosphorylation is dependent on PI3-K pathway,

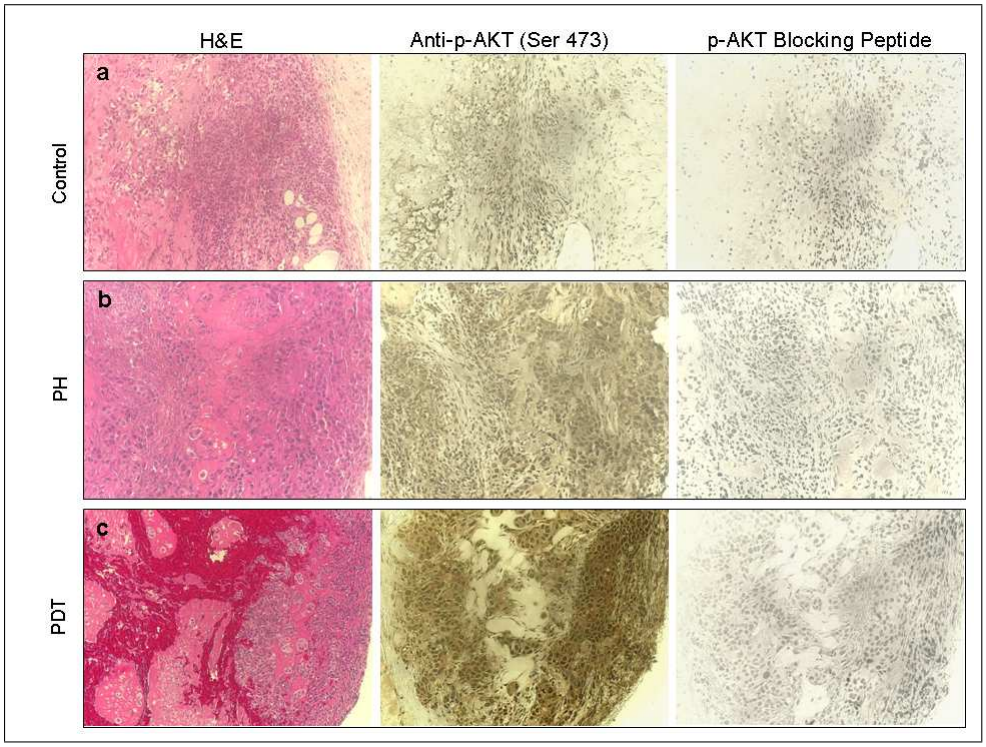

Figure 4.5 PH-PDT induced AKT phosphorylation in tumors created in mice. Tumors were created by injecting BT-474 cells within matrigel to the hind flank of athymic mice. When the tumors reached 6-7 mm in largest diameter, PH (5 mg/kg) was injected intravenously to each mouse 24 hr before treatment with 630-nm diode laser at a total light dose of 100 J/cm^2 with a dose rate of 75 mW/cm^2. Mice were sacrificed with overdose of CO_2 for 1 hr after PDT treatment. The tumors were removed surgically and and prepared for immunohistochemistry analysis. Paraffin embedded 5 μm tissue sections were stained with H&E (Hematoxylin and Eosin) (left), phospho-AKT (Ser 473) specific antibody (middle) and phospho-AKT (Ser 473) blocking peptide (right). a, no treatment. b, PH only without light treatment. c, PDT treatment. Magnification, x 20.

murine and human breast cancer cells were utilized in PH-PDT experiments in the absence and presence of PI3-K inhibitors. Figure 4.6 shows the protein expression profiles for phospho-AKT, total AKT and actin in murine C3H/BA mammary carcinoma cells and human BT-474 breast cancer cells. AKT phosphorylation was examined at 2 and 6 hr after PDT or after PH incubation. Two inhibitors of PI3-K, Wortmannin and LY294002, attenuated AKT-induced phosphorylation indicating that PDT and PH were acting through the PI3-K signaling pathway. These *in vitro* experiments demonstrated that treatment of murine and human breast cancer cells with PH-mediated PDT induced phosphorylation of AKT via PI3-K pathway. Additionally, PH in the absence of light also induced AKT phosphorylation and this result agrees with recent studies demonstrating that both the heme molecule and an extended porphyrin, Motexafin gadolinium, induce AKT phosphorylation [179, 180].

To test whether exposure of the murine and human breast cancer cells to red light in the absence of exogenous photosensitizer (PH), the same experimental set-up was used to monitor AKT phosphorylation. Exposure of these cell lines to red light in the absence of PH did not induce AKT phosphorylation above control levels (Figure 4.7), indicating that red light does not have additive effects on PDT-induced AKT phosphorylation *in vitro*.

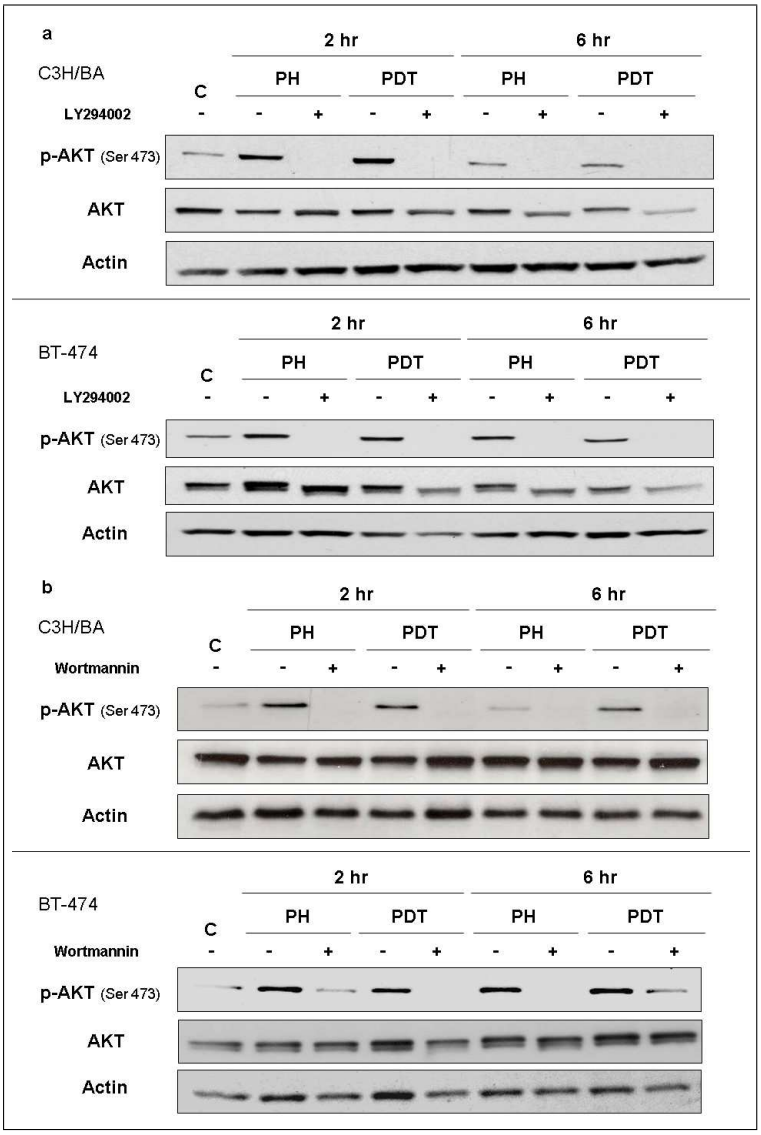

Figure 4.6 Photofrin-mediated PDT and PH alone induce AKT phosphorylation in murine and human breast cancer cells. Murine BA and human BT cells were incubated with PH (25 μg/ml) along with or without LY294002 (100 μM) (a) or Wortmannin (1 μM) (b) for 16 hr in the dark and then exposed to 315 J/m^2 of broad-spectrum red light. Cells were then incubated in the dark for an additional 2 or 6 hr in the presence or absence of LY294002 (100 μM) (a) or Wortmannin (1 μM) (b). Cell lysates from control, PH alone and PH-PDT cultures were collected and assayed for phospho-AKT, total AKT and Actin.

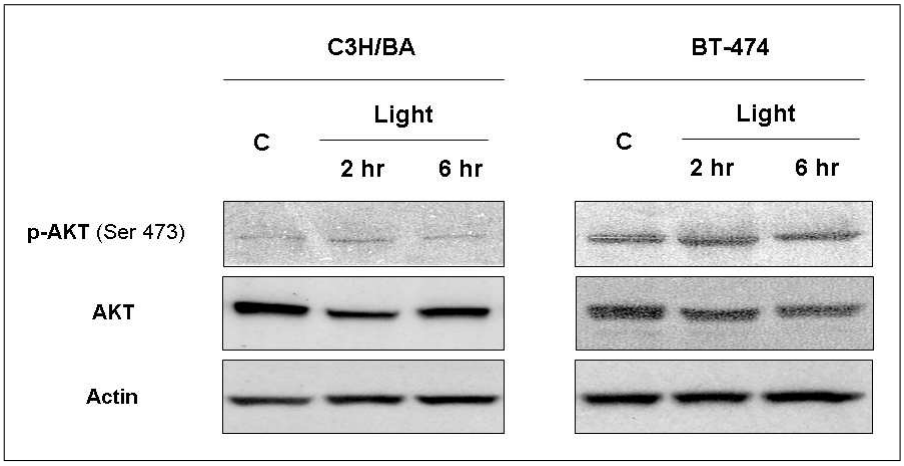

Figure 4.7 Exposure of murine or human breast cancer cells to 315 J/m^2 red light alone does not increase AKT phosphorylation at that dose of light. Murine BA and human BT cells were incubated in the dark for 16 hr, exposed to red light (315 J/m^2) and then incubated in the dark for an additional 2 or 6 hr. Cell lysates from control and light-treated cultures were collected and assayed for phospho-AKT, total AKT and Actin.

4.1.5 PI3-K Inhibitors Increase Apoptosis in PDT-treated Breast Cancer Cells

A major function of activated AKT is to promote cell survival and to block apoptosis. Phosphorylation of the pro-apoptotic effector molecules such as BAD and Caspase-9, by activated AKT decreases their ability to induce apoptosis [175]. Next it was determined whether inhibition of AKT-phosphorylation by PI3-K inhibitors, Wortmannin and LY294002, induces apoptosis *in vitro*. For this purpose, C3H/BA and BT-474 cells were treated with light alone, PH alone, PH in combination with light or left untreated and the levels of apoptosis was determined by Apoptosis Detection ELISA Kit. Our results showed that cells treated with Wortmannin or LY294002 induced increased levels of apoptosis in PH-PDT treated cells (Figure 4.8) while as shows in Figure 4.6, these inhibitors block AKT phosphorylation. The observed apoptosis involves direct toxicity by the inhibitors and could include a role for phospho-AKT. These results showed a role for PI3-K inhibitors in modulating cellular apoptosis following PH-mediated PDT. Additional experiments are needed to confirm a direct effect of AKT in modulating PDT response. Our results agree with a previous study showing AKT phosphorylation following exposure of mouse fibroblasts to singlet oxygen generated by rose bengal-mediated photosensitization [120]. This study also reported

that inhibition of AKT activation using Wortmannin and LY294002 resulted in increased cellular apoptosis. Continued examination of methods to selectively attenuate AKT phosphorylation may prove useful in improving PDT responsiveness by enhancing treatment-related apoptosis.

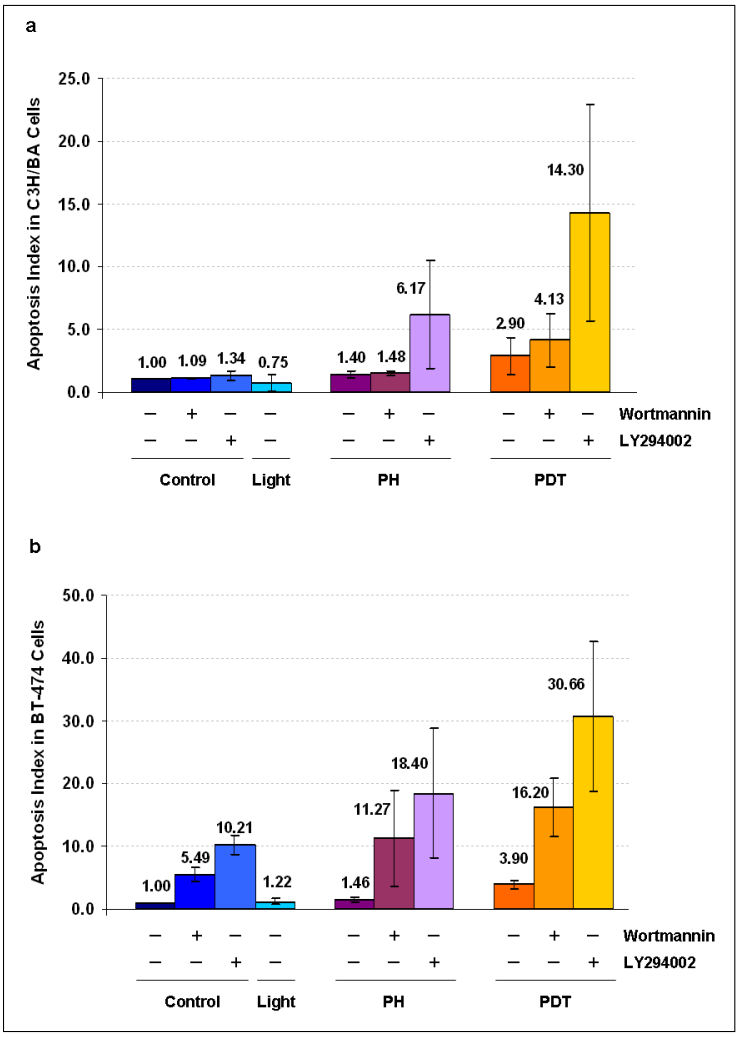

Figure 4.8 PI3-K inhibitors increase apoptosis in PDT-treated murine C3H/BA and human BT-474 breast cancer cells. a) C3H/BA cells and b) BT-474 cells were treated with PH-mediated PDT in the presence or absence of Wortmannin or LY294002 as described in Fig. 4.6. Apoptosis was measured as an enrichment factor 6 hr following treatment using the Cell Death Apoptosis Detection ELISA Plus kit. Results are expressed as the mean ± SE of three separate experiments.

4.1.6 Photofrin-mediated PDT and Light Alone Induce AKT Phosphorylation *in vivo* Tumor Models

The *in vivo* effects of PH-mediated PDT on AKT phosphorylation was examined by using tumors generated from the same cell lines described above for *in vitro* experiments (Section 4.1.5). Western immunoblot analysis and the corresponding densitometry readings were evaluated for murine C3H/BA tumors exposed to PDT, light alone, or untreated controls (Figure 4.9). Both PDT and light exposure induced phosphorylated AKT levels above background. Moreover, the level of phospho-AKT was highest at 0.5 hr post PDT treatment and decreased by time. Figure 4.10 shows western immunoblots and densitometric readings for murine C3H/BA tumors exposed to PH alone, light alone or untreated controls. In this experiment, phospho-AKT levels in tumors receiving PH alone or light alone was not significantly increased compared to controls. Interestingly, the intracellular levels of PH are higher for the *in vitro* experiments (Figure 4.6) and this may be why AKT phosphorylation was observed following PH alone in cells but not in tumors.

Similarly, the levels of AKT phosphorylation following PH-PDT treatment was determined for human BT-474 tumors by western immunoblot analysis. The results demonstrated that AKT phosphorylation was significantly increased only following PH-mediated PDT for BT-474 tumors (Figure 4.11) similar to the results obtained for C3H/BA tumors (Figure 4.9 and 4.10). These findings suggested that, PH-PDT induces a significant increase in AKT phosphorylation *in vivo*. Interestingly, PH alone did not induce AKT phosphorylation *in vivo*, in contrast to *in vitro* findings. Additionally, administration of the photosensitizer PH without subsequent light exposure did not result in increased AKT phosphorylation while exposure of tumors to light alone resulted in a small but not significant increase in AKT phosphorylation over control levels. Collectively, these results demonstrate that individual components of the PDT process, photosensitizer alone and light alone, as well as the complete PDT procedure can activate the AKT signaling pathway.

Improvements in PDT responsiveness may be achieved by employing combined

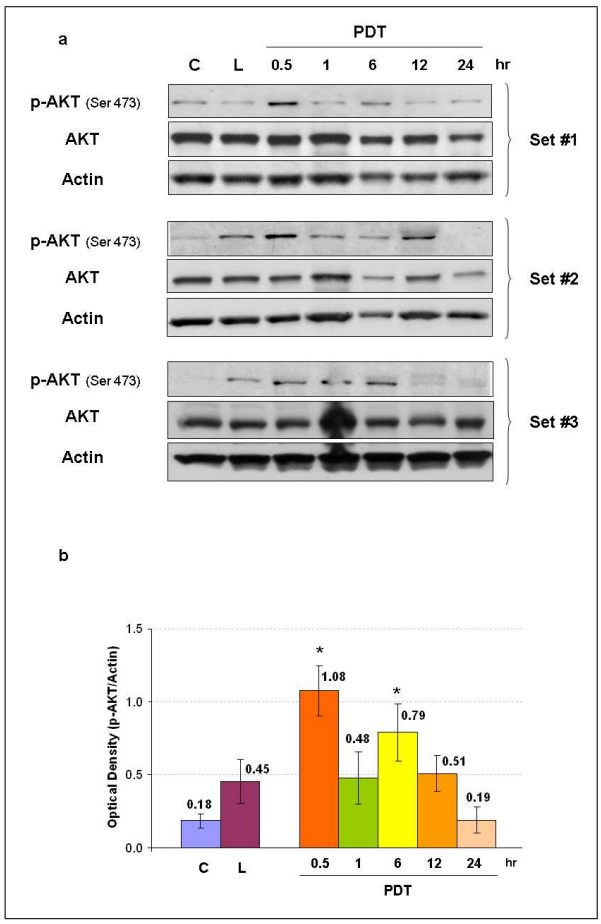

Figure 4.9 Photofrin-mediated PDT and light alone induce AKT phosphorylation in murine BA breast cancer tumors. C3H/HeJ female mice with subcutaneously transplanted BA tumors were injected with PH (5 mg/kg) and then 24 hr later the tumors were exposed to a 100 J/cm^2 dose of 630 nm light. Additional tumor-bearing mice not injected with PH were also exposed to light alone. Tumor lysates were collected at various time intervals (0.5-24 hr) after treatment and assayed for phospho-AKT, total AKT and Actin. (a) Western immunoblot analysis for three separate experiments and (b) densitometric readings obtained from the immunoblots. *The increases in phospho-AKT above control were statistically significant ($p<0.05$) at 0.5 and 6 hr after PDT (n = 3).

modalities targeting malignant cells and survival pathways. Inhibition of PDT-induced AKT activation with the use of appropriate, non toxic inhibitors may enhance the PDT response. In the second part of this study, a new PI3-K inhibitor was tested in an attempt to improve PDT responsiveness.

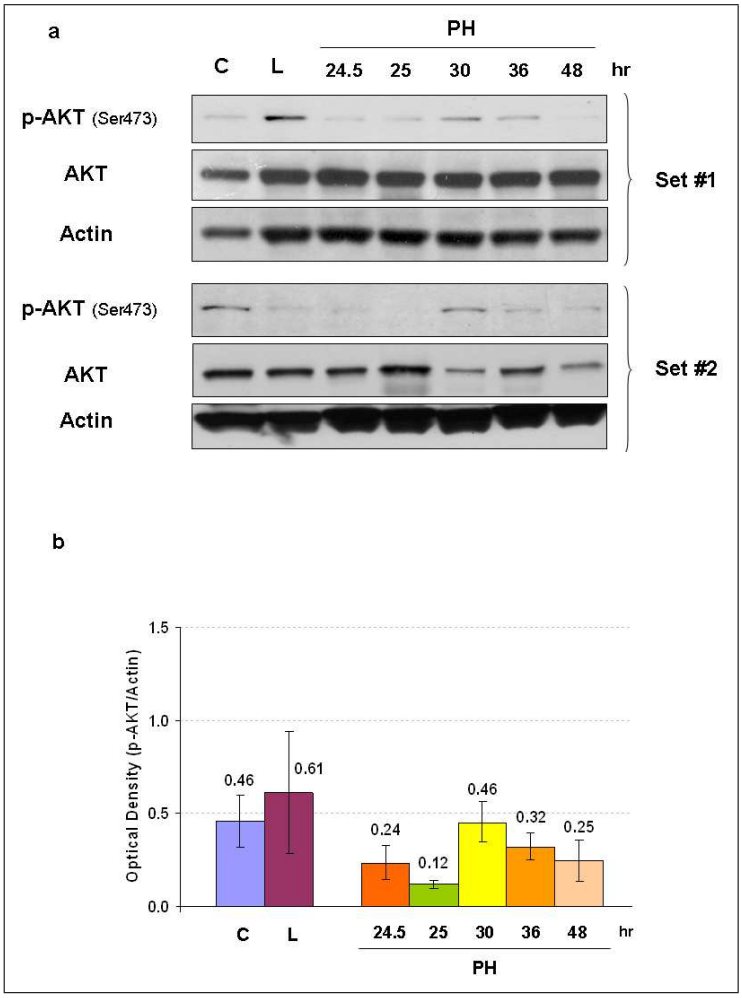

Figure 4.10 Photofrin alone does not induce AKT phosphorylation in murine BA breast cancer tumors. C3H/HeJ mice with subcutaneously transplanted BA tumors were injected with PH (5 mg/kg) and then kept in the dark until assayed for protein expression. Tumor lysates were collected at various time intervals (24.5-48 hr) after PH injection and assayed for phospho-AKT, total AKT and Actin. (a) Western immunoblot analysis for two separate experiments and (b) densitometric readings obtained from the immunoblots.

4.2 Inhibition of PDT-mediated AKT Activation can Enhance Treatment Responsiveness

Clinical applications of PDT in cancer treatment are encouraging; however, improvement of long-term PDT responsiveness is needed to decrease tumor recurrences. In the first part of this thesis study it was shown that multiple components of PH-PDT can induce AKT activation [176]. The aim of the following section of this study is to evaluate PDT responsiveness in combination with an effective AKT inhibitor, PI-103, both *in vitro* and *in vivo* experiments. PI-103 is a non-toxic, dual PI3-K /mTOR

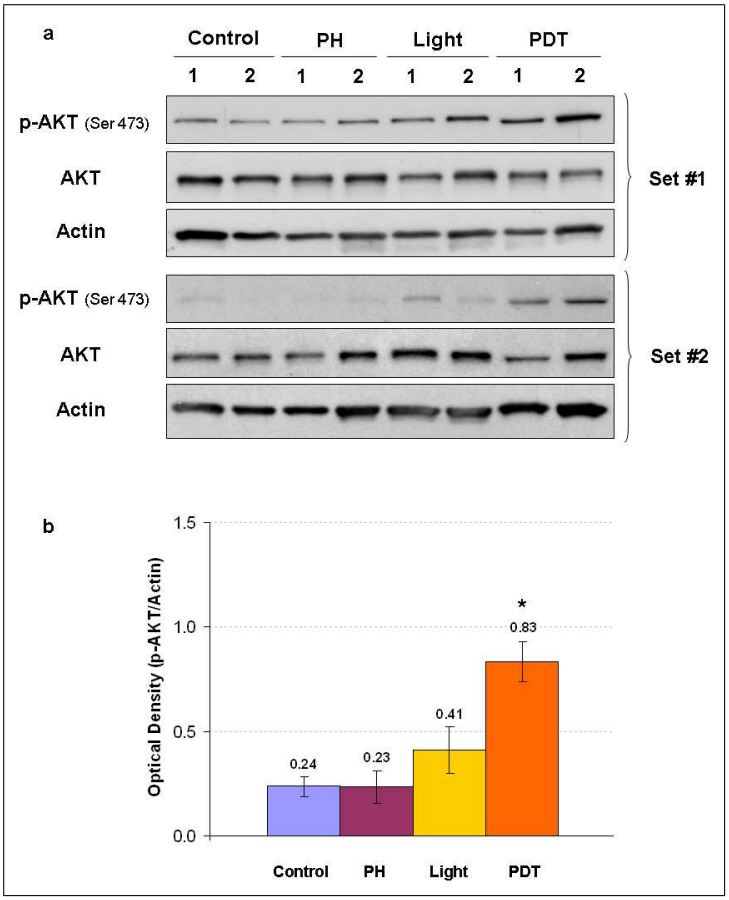

Figure 4.11 PH-mediated PDT and light alone induce AKT phosphorylation in human BT breast cancer tumors. Athymic mice with subcutaneously transplanted BT tumors were injected with PH (5 mg/kg) and then 24 hr later the tumors were exposed to a 100 J/cm^2 dose of 630 nm light. Additional mice were exposed to light alone or kept in the dark following PH administration. Tumor lysates were collected 1 hr after treatment and assayed for phospho-AKT, total AKT and actin. (a) Western immunoblot analysis for two separate experiments and (b) densitometric readings obtained from the immunoblots. *The increase in phospho-AKT above control was statistically significant ($p<0.05$) for PDT (n = 4).

inhibitor that was shown to effectively inhibit AKT phosphorylation in different mouse tumor models [172].

4.2.1 PI3-K Inhibitor PI-103 Effectively Inhibits PDT-mediated AKT Activation *in vitro*

In order to confirm that PI-103 effectively inhibits AKT phosphorylation in the C3H/BA mouse mammary carcinoma cell cultures, these cells were exposed to PH alone, PH treatment followed by light exposure (PH-PDT) or were left untreated in

the absence or presence of PI-103. The cell lysates were collected and the levels of phospho-AKT at the position of both Ser 473 and Thr 308 as well as total AKT and actin were evaluated by western immunoblot analysis. As shown in Figure 4.12, PI-103 at the concentration of 0.1 μM significantly decreased AKT phosphorylation at both sites and importantly, phospho-AKT was completely diminished in cells treated with 1 μM or above concentration of PI-103 inhibitor. Moreover, DMSO was used as a carrier for PI-103 and it was added to cultures that did not receive PI-103 and showed no inhibitory effect. These results clearly demonstrate that PI-103 effectively inhibit PDT-mediated AKT phosphorylation at both Ser 473 and Thr 308 without affecting the total AKT expression in our culture system (Figure 4.12).

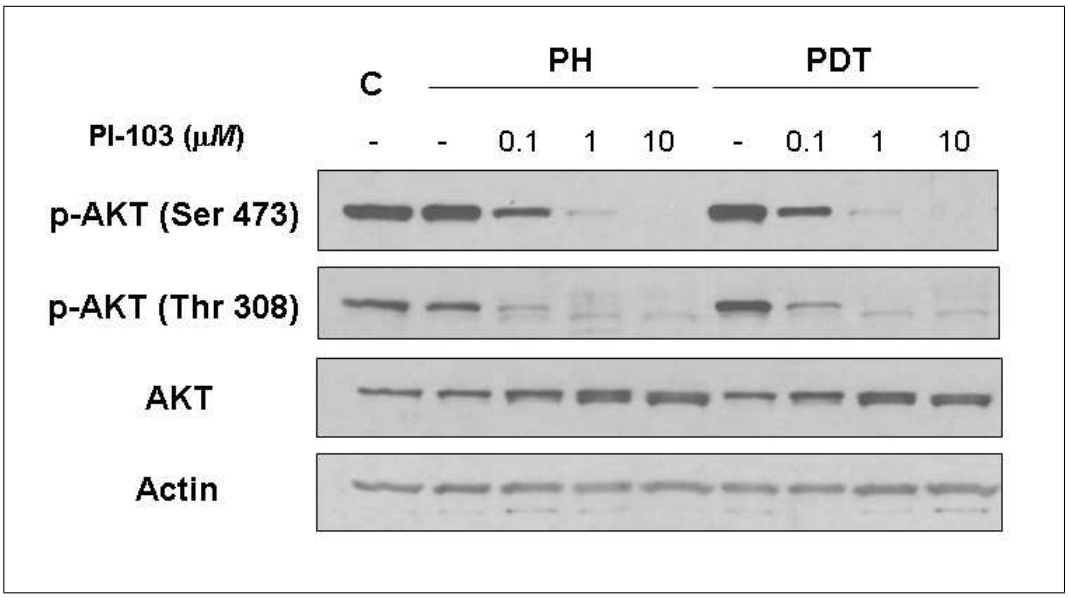

Figure 4.12 PI-103 inhibits AKT phosphorylation at both Ser 473 and Thr 308. C3H/BA cells were grown for 24 hr in complete media and than incubated with PH (25 μg/ml) in dark for 16 hr that was followed by exposure to broad-spectrum red light (315 J/m^2) as indicated. After treatments, cell cultures were refed with fresh media in the absence or presence of PI-103 at 0.1, 1, 10 μM concentrations. Following 2 hr incubation, cell lysates were collected and analysed by western immunoblot analysis for protein levels of phospho-AKT at the position of both Ser 473 and Thr 308, total AKT and actin.

4.2.2 PI-103 Inhibits PDT-mediated AKT Phosphorylation in a Concentration Dependent Manner

In order to determine the minimum and most effective PI-103 concentration with least side effects, the PH-PDT treated C3H/BA cell cultures were incubated at

different PI-103 concentrations and cell lysates were analyzed 2 hr (Figure 4.13a) and 24 hr (Figure 4.13b) post-treatment. The Figure 4.13 clearly shows that PDT-enhanced phospho-AKT levels gradually decreases as the PI-103 concentration increase, where, concentrations between 0.2 and 0.3 μM is sufficient for complete inhibition of AKT phosphorylation (Figure 4.13a). Importantly, this dose dependent decrease in AKT phosphorylation was also observed 24 hr post-PDT treatment suggesting that, the effects of PI-103 in AKT inhibition is stable in our cell culture system (Figure 4.13b).

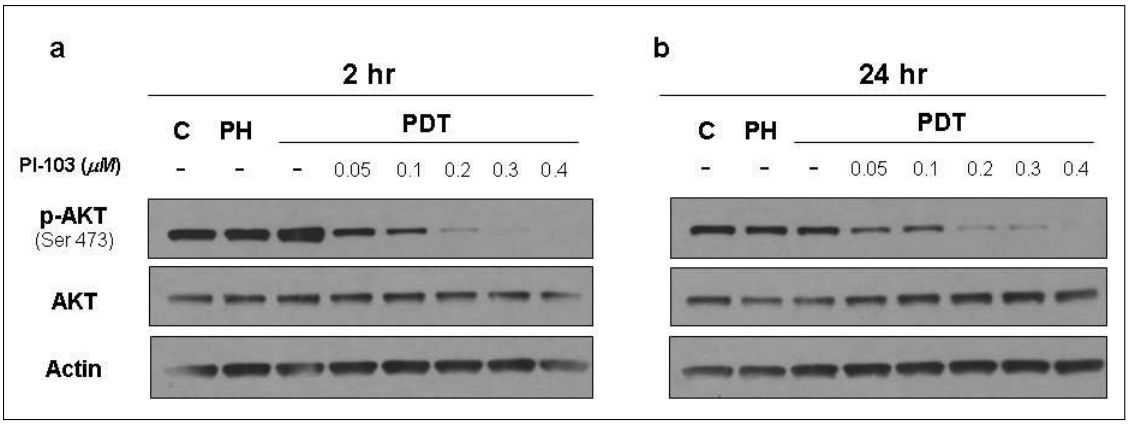

Figure 4.13 PI-103 inhibits PDT-mediated AKT phosphorylation in a concentration dependent manner. (a, b) C3H/BA cells were plated for 24 hr in complete media and then treated with PH (25 μg/ml) for 16 h followed by light (315 J/m^2) exposure as indicated. After treatments, cell cultures were refed with fresh media in the absence or presence of PI-103 at various concentration from 0.05 to 0.4 μM for 2 hr (a) or 24 hr (b). Following treatment, cell lysates were collected and analyzed by western immunoblot analysis for protein levels of phospho-AKT at the position of Ser 473, total AKT and actin.

After determining the optimum PI-103 concentration as 0.25 μM for *in vitro* experiments, next, the earliest effective time point for PI-103 treatment was determined. For this experiment, the effect of PI-103 was evaluated in a time course where cell lysates were collected starting from 15 min to 1 hr (Figure 4.14). Our western blot analysis results showed that PI-103 completely inhibited PDT-mediated AKT phosphorylation at both Ser 473 and Thr 308 within 15 min. Taken together, these findings clearly demonstrated that concentrations of PI-103 as low as 0.25 μM effectively inhibited PDT-mediated AKT phosphorylation and this effect was rapid (within 15 min) but importantly stable at least for 24 hr.

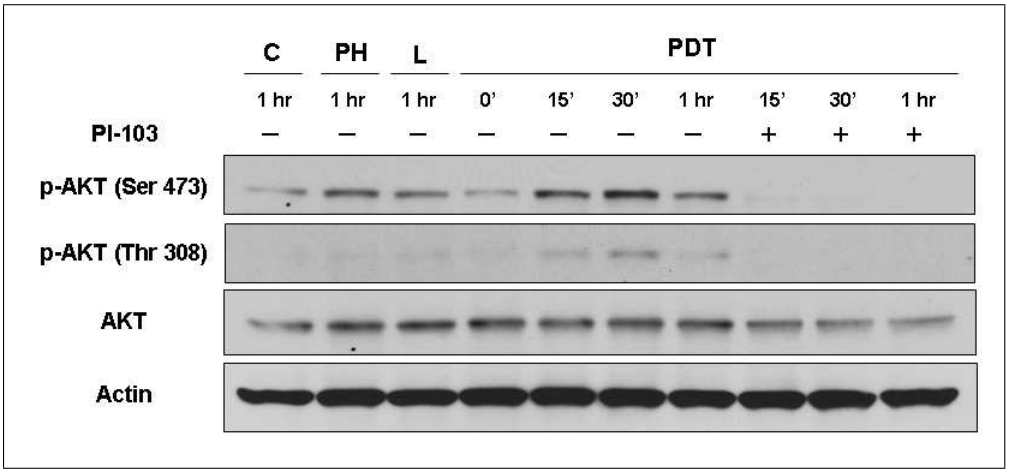

Figure 4.14 PI-103 inhibits PDT-mediated AKT phosphorylation within 15 min. C3H/BA cells were plated for 24 hr in complete media and then treated with PH (25 μg/ml) for 16 hr followed by light (315 J/m^2) exposure as indicated. After treatments, cell cultures were refed with fresh media in the absence or presence of PI-103 at the concentration of 0.25 μM. Cell lysates were collected 15 min, 30 min or 1 h following treatment and analyzed by western immunoblot analysis for protein levels of phospho-AKT at the position of both Ser 473 and Thr 308, total AKT and actin.

4.2.3 PI-103 Effectively Decreased the Formation and Size of Colonies in Combination with PDT

To determine the toxicity of PI-103 on C3H/BA cells; PH-PDT-treated, PH alone or control cells were grown in dark in the presence or absence of various PI-103 concentrations for 11 days. The number of colonies formed at the end of this period was examined by methylene blue staining. In parallel, the level of PDT-mediated AKT phosphorylation under these conditions were analyzed by western blot. As found in the previous section, 0.25 μM of PI-103 effectively inhibited PDT-mediated AKT phosphorylation at both Ser and Thr sites (Figure 4.15a). Moreover, the number and size of colonies formed in 11 day old cultures were gradually decreased in PH alone or PDT-treated cells incubated in the presence of increasing amounts of PI-103 (Figure 4.15b). Quantification of the number of colonies indicated that cultures grown in 0.25 μM or higher concentrations of PI-103 has a significant toxic effect on the colony formation (Figure 4.15c). Together, our results in colony formation assay showed that PI-103 treatment in combination with PH-PDT treatment has significant cytotoxic effects and grants further analysis *in vitro* and *in vivo* experiments.

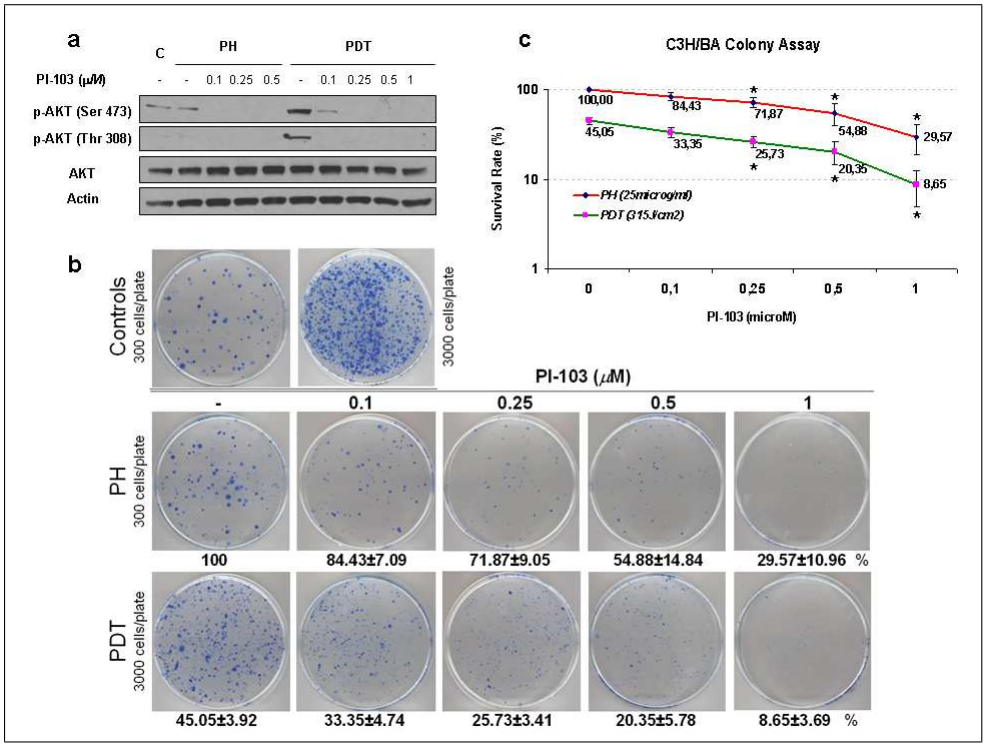

Figure 4.15 PDT-induced AKT phosphorylation and colony formation was dose dependently blocked by PI-103. Murine C3H/BA cells were plated for 24 hr in complete media and incubated with PH for 16 hr in dark and exposed to broad-spectrum red light (315 J/m^2). Then, cell cultures were incubated in dark for an additional 2 hr in the presence or absence of PI-103 at concentrations ranging from 0.1 to 1 μM. (a) Cell lysates from control, PH alone and PDT cultures were collected and assayed for protein levels of phospho-AKT, total AKT, and actin by western blot analysis. (b) Following culturing as explained above, PH-PDT-treated (3000 cells seeded), PH alone (300 cells seeded) or control cells (300 and 3000 cells seeded) were grown in dark in the presence or absence of PI-103 for 11 days. To determine colony formation, the cultures were stained with methylene blue and plates were scanned for image analysis. The remaining colonies having 30 cells or more are counted and illustrated as a graph for survival rate in different concentrations of PI-103 (c). The PH alone control was normalized to untreated controls without PI-103 and set to 100 %. * The decrease in survival was statistically significant ($p<0.05$) compared to cultures grown in the absence of PI-103. The experiment was carried out in triplicates where n = 3.

4.2.4 PI-103 Increased Apoptosis in PH-PDT Treated Murine Breast Cancer Cells

In order to further investigate the cytotoxic effects of PI-103 on PDT-treated C3H/BA cells, it was examined whether PI-103 treatment caused apoptosis. For this analysis, the apoptosis-induced DNA damage was quantitatively determined by colorimetric ELISA analysis 6 hr post-PDT. Our results demonstrated that, PI-103 at a concentration of 0.25 μM induced a significant increase in apoptosis in only PDT-treated C3H/BA cells compared to controls (Figure 4.16). This finding implied that PI-103

significantly increased the PDT treatment response *in vitro*, whereas, the previously examined PI3-K inhibitors, Wortmannin and LY294002, were unable to significantly increase apoptosis in PDT-treated cultures (Figure 4.8). Collectively, PI-103 emerges as a promising and effective inhibitor of AKT phosphorylation that should be further investigated for experimental and clinical application in combination with PDT treatment.

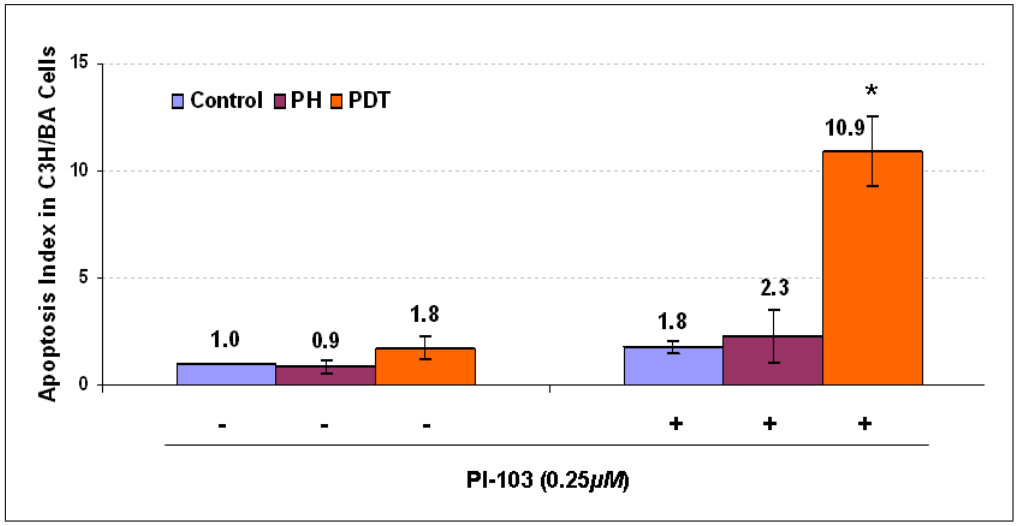

Figure 4.16 PI-103 increased apoptosis in PDT-treated murine C3H/BA breast cancer cells. Murine C3H/BA cells were plated for 24 hr in complete media and incubated with PH for 16 hr in dark and exposed to broad-spectrum red light (315 J/m^2). Then, cell cultures were incubated in dark for an additional 6 hr in the presence or absence of PI-103 at a concentration of 0.25 μM. Apoptosis was measured by using the Cell Death Apoptosis Detection ELISA Plus kit according to manufacturer's protocols. Results are expressed as the mean $\pm$ SE of three separate experiments. *The change in apoptosis was statistically significant ($p<0.05$).

4.2.5 PI-103 Effectively Inhibits Phosphorylation of Downstream Targets of AKT

It is well-documented that, AKT activation increases cell survival. A possible mechanism that could account for this is that, AKT directly regulates glucose metabolism by activation of Glycogen synthase kinase 3 (GSK-3) [144, 145, 147]. Another possible AKT-regulated pathway is through mTOR, which is a large protein kinase that regulates protein synthesis and growth through downstream effectors, such as "ribosomal S6 kinase 1" (rpS6) (Figure 2.7) [157]. AKT phosphorylation leads to direct phosphorylation of GSK-3 and indirectly stimulates rpS6 phosphorylation that

results in activation of AKT pathway.

To this point, the effects of PI-103 on PDT-mediated AKT phosphorylation have been investigated. Next, it was examined whether PI-103-mediated inhibition of AKT phosphorylation leads to deactivation of AKT pathway. For this experiment, the phosphorylation of GSK-3 and rpS6 was analyzed in PDT-stimulated C3H/BA cancer cells in the presence of various concentrations of PI-103. The phosphorylated and total protein levels of AKT, GSK-3 and rpS6 as well as actin were analyzed by western blots (Figure 4.17). As previously shown, PDT-mediated phosphorylation of AKT at Ser 473 was completely diminished by PI-103 at concentrations above 0.2 μM where total AKT protein levels were remained unchanged. Importantly, this inhibition in AKT phosphorylation correlated with a complete block of rpS6 phosphorylation and a significant decrease in GSK-3 phosphorylation in samples treated with PI-103 was dose dependent. Surprisingly, total rpS6 protein levels were decreased in PI-103 treated samples suggestive of downregulation of rpS6 protein expression which was an intriguing observation for further investigation. Taken together, these results clearly demonstrated that PI-103 inhibited phosphorylation of AKT and its downstream targets GSK-3 and rpS6, and led to subsequent inactivation of AKT pathway.

4.2.6 PI-103 Inhibits PDT-mediated AKT Phosphorylation in Animal Tumor Models

The previous analysis firmly established an inhibitory role for PI-103 on PDT-mediated AKT phosphorylation and activation *in vitro*. In order to determine the *in vivo* relevance of this finding, C3H mice with subcutaneously transplanted breast adenocarcinoma tumors were treated with PDT in combination with PI-103 and assayed for protein levels of phospho-AKT by western blot analysis (Figure 4.18). First, it was reevaluated whether PH alone, light exposure alone or PDT induces AKT phosphorylation in animal tumors. The quantitative densitometric analysis of phospho-AKT protein levels in tumors treated with PH alone or light alone was slightly but insignificantly increased compared to the levels detected for untreated control tumors (Figure

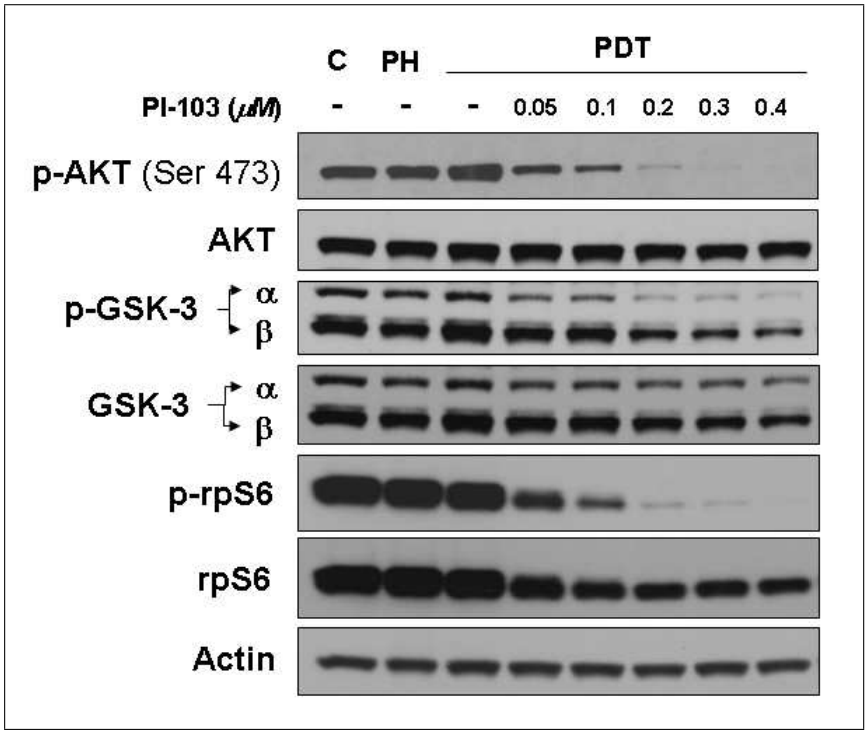

Figure 4.17 PI-103 inhibits phosphorylation of downstream targets of AKT. Murine C3H/BA cells were plated for 24 hr in complete media and incubated with PH for 16 hr in dark and exposed to broad-spectrum red light (315 J/m^2). Then, cell cultures were incubated in dark for an additional 2 hr in the presence or absence of PI-103 at the concentrations of 0.05, 0.1, 0.2, 0.3 and 0.4 μM and cell lysates were collected and assayed for phospho-AKT, total AKT, phospho-GSK-3α/β, GSK-3α/β, phospho-rpS6, rpS6 and Actin.

4.18a). Even though some animals in each group showed detectably higher levels compared to counterparts, the statistical analysis did not show any significant change. These differences can be explained by animal to animal experimental variation. On the other hand, tumors treated with PDT showed significantly higher levels of phospho-AKT compared to controls. Importantly, the result of this experiment was consistent with the previous analysis (Section 4.1.6) [176] and showed that single components of PDT may induce low levels of AKT phosphorylation *in vivo*; however, only PDT treatment led to significant enhancement compared to control.

Next, the inhibitory effects of PI-103 on PDT-mediated AKT phosphorylation was evaluated *in vivo*. The animal tumors were created and treated as explained above with an additional PI-103 treatment after PDT. Consistent with results obtained from cell cultures (Figure 4.12), PI-103 treated tumors showed a near complete reduction in AKT phosphorylation induced by PDT (Figure 4.18b). This presented a novel

finding since the application of PI-103 or any other AKT inhibitor was not reported to be successful in combination therapies with PDT *in vivo*. Given that, effective doses of PI-103 did not cause any detectable levels of toxicity in murine tumor models, the application of PI-103 in combination with PDT in clinical research grants further investigations and an intriguing possibility to enhance treatment response.

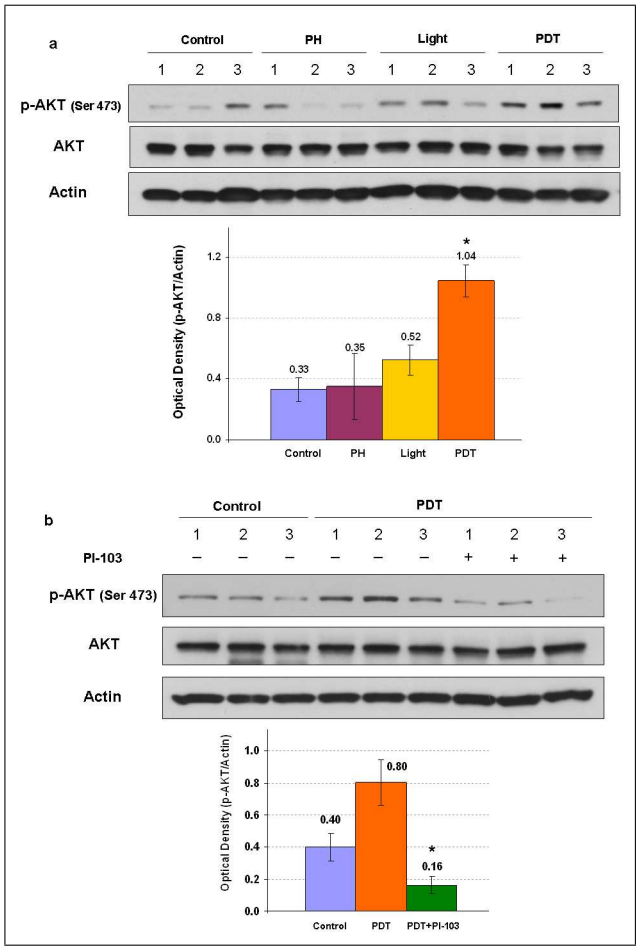

Figure 4.18 PI-103 inhibits PDT-induced AKT phosphorylation in murine BA tumors. (a) C3H/BA mice with subcutaneously transplanted tumors were injected intravenously with PH (5 mg/kg) and kept in dark for 24 hr. Then, the tumors were exposed to 100 J/cm^2 dose of 630 nm light. Additional mice were exposed to light alone or kept in the dark following PH administration. Mice were sacrificed 40 min following PDT treatment and tumor lysates were collected and assayed for phospho-AKT, total AKT and actin protein levels by western blot analysis. *The increase in phospho-AKT levels for PDT treatment was statistically significant over PH alone, light alone and untreated controls ($p<0.05$, n = 3). (b) Tumors were generated and treated in mice as above and PDT was followed by two injections of PI-103 (50 mg/kg) in 20 min interval. Control mice were injected with DMSO vehicle. Mice were sacrificed 20 min following the second PI-103 injection. Tumor lysates were collected and assayed as above. *The phospho-AKT levels in tumors treated with PI-103 in combination with PDT was statistically lower than PDT-treated or control mice ($p<0.05$, n=3).

4.3 Photo-toxic Effects of 809-nm Diode Laser and Indocyanine Green on MDA-MB231 Breast Cancer Cells

This part of the thesis is devoted for the results of experiments which employed a different photosensitizer Indocyanine Green (ICG) for PDT application on breast cancer cells. Breast cancer is the most common cause of cancer mortality in women [181]. For our analysis, an aggressive type of human breast cancer cell line, MDA-MB231, was used for ICG-mediated PDT treatment for the first time in the literature [182]. For these analysis, cultures incubated with ICG were treated with a computer controlled 809 nm diode laser that was designed and manufactured in our laboratory [174]. The laser system was set to deliver the light output via optic fibers to a lens system in order to illuminate specific wells of the culture plate with a constant energy density.

ICG is a non-toxic, water-soluble and bio-compatible molecule that has photosensitizing ability for PDT applications. Since ICG exhibits strong maximum absorption at around 805 nm, that represents an advantage for its use in PDT. Importantly, light at that wavelength can be used to treat deeper tumors which is a major limitation for clinical applications of PDT. Therefore, ICG-PDT is an ideal candidate for therapy for patients with solid breast cancer. In this study we investigated the inhibitory growth effects of ICG-PDT on MDA-MB231 human breast cancer cells in a time course experiment.

4.3.1 ICG-PDT Exhibits Strong Photo-toxic Effects on Breast Cancer Cells

To determine the effects of ICG-PDT on the viability of MDA-MB231 human breast cancer cells, MTT cell survival assay was employed. To start with, the immediate cytotoxic effects was measured after treatment (t = 0). Even though ICG or light treatments on their own did not result in any significant cytotoxicity, the ICG-PDT treatment lead to a significant decrease in cell viability compared to untreated cultures

(Figure 4.19). It is surprising to observe this five fold decrease in ICG-PDT samples over controls immediately after treatment. This result indicates that ICG-PDT effectively causes cell death in MDA-MB231 cells within minutes after treatment.

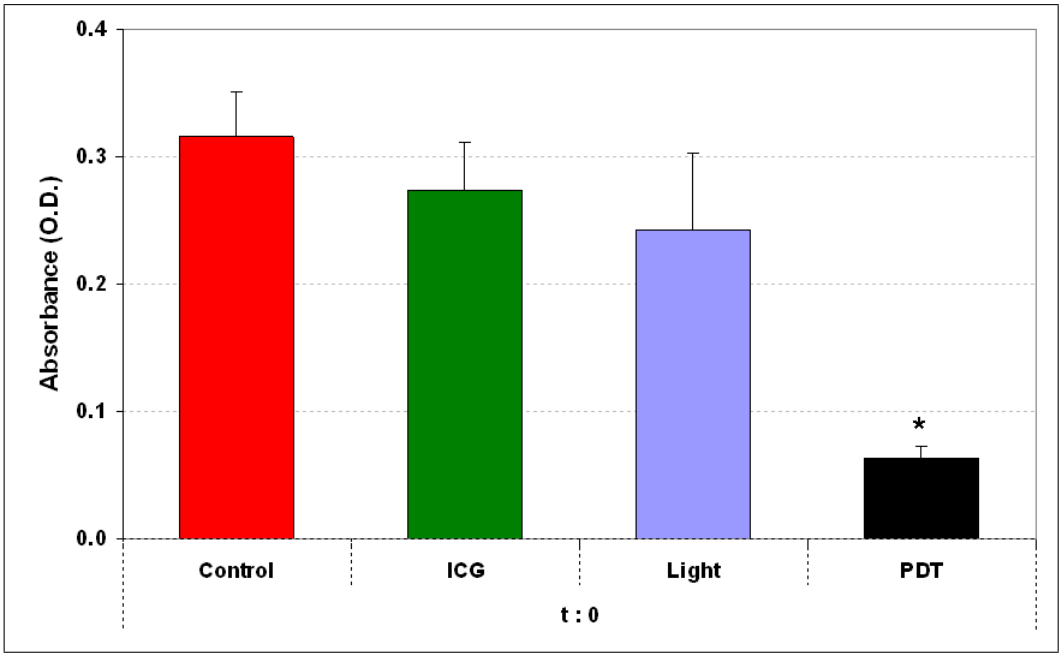

Figure 4.19 ICG-PDT exhibits significant cytotoxicity in human MDA-MB231 breast cancer cells within minutes. MDA-MB231 breast cancer cells grown in 96-well plates for 16 hr were divided into ICG-PDT, ICG alone, Light alone and untreated control groups. Indicated groups were refed with complete media supplemented with 50 μM ICG for 24 hr in dark. Light and ICG-PDT samples were exposed to light at 809 nm with a total energy density of 24 J/cm^2. Immediately after treatment the viability of cells in each well was measured by MTT analysis (Details in Materials and Methods). *The decrease in cell viability in ICG-PDT group is significant ($p<0.01$, n = 16) over controls.

4.3.2 The Growth Inhibitory Effect of ICG-PDT is Stable

Next, the cytotoxic effects of ICG-PDT was analyzed at different time points and stability of this effect was measured by MTT assay. To check the ICG-PDT responsiveness on MDA-MB231 cell line, cultures following 3, 6, 9, 12, 24 and 48 hr after PDT treatment were analyzed in a time course experiment (Figure 4.20). The results of this experiment showed that, at all time points cell cultures that received ICG-PDT treatment had significantly decreased cell viability compared to other groups that received ICG alone, light alone or kept untreated (Figure 4.20a). Importantly, this high photo-toxic effect of ICG-PDT was stable at least for 48 hr.

In order to quantitatively examine relative cell viability after PDT treatment, the absorbance values measured at each time point for ICG-PDT treated cultures with respect to control were plotted as per cent value (Figure 4.20b). This analysis indicated that the photo-toxic effects of ICG-PDT gradually increased by time. The samples collected at 3 hr after ICG-PDT treatment showed that only 26 % of the population remained alive. Importantly, 48 hr after ICG-PDT treatment, relative cell viability of MDA-MB231 breast cancer cells with respect to control decreased to 4.6 %. This is a significant finding in that, even though the cell numbers doubled in 48 hr as observed by the absorbance readings increasing from 0.3 (at t = 0) to 0.6 (at t = 48 hr), the ICG-PDT values continued to decrease. This analysis showed that, the ICG-mediated PDT treatment have long-lasting cytotoxic effects on MDA-MB231 breast cancer cells. These findings are in accordance with previous reports showing that, cancer cell lines incubated with ICG followed by laser irradiation in the range of NIR lead to cell death by photo-oxidation [56, 3, 58, 59, 60]. The findings of this study grants further experimental and clinical investigation of ICG-PDT applications in breast cancer treatment.

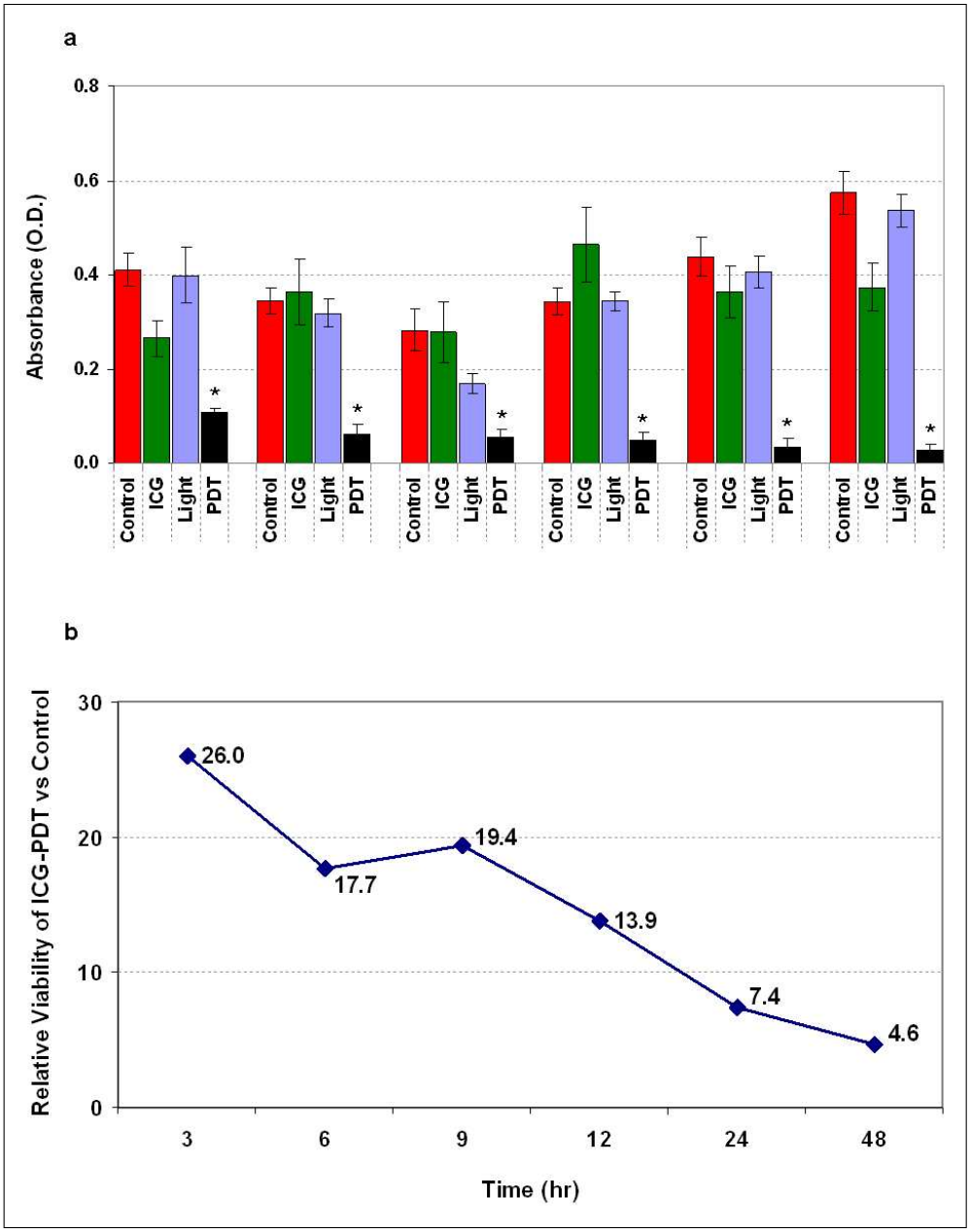

Figure 4.20 ICG-mediated PDT treatments severely and stably decreased cell viability in human MDA-MB231 breast cancer cells. (a) MDA-MB231 breast cancer cells grown in 96-well plates for 16hr were divided into ICG-PDT, ICG alone, Light alone and untreated control groups. Indicated groups were refed with complete media supplemented with 50 μM ICG for 24 hr in dark. Light and ICG-PDT samples were exposed to light at 809 nm with a total energy density of 24 J/cm^2. Following 3, 6, 9, 12, 24 and 48 hr after treatment, the viability of cells in each well was measured by MTT analysis (Details in Materials and Methods). * The decrease in cell viability in ICG-PDT groups are significant ($p<0.01$, n=16) over controls. (b) Quantitative analysis of relative cell viability of ICG-PDT over controls at different time points after treatment.

5. CONCLUSION

5.1 Combination Cancer Therapies Employing AKT Pathway Inhibitors with PH-PDT may Enhance Treatment Response

PDT is a well-established, minimally invasive, non-toxic approach for clinical cancer treatment. Additionally, PDT treatment has relatively less side-effects, short patient recovery period and is easier to apply compared to other therapy methods, such as surgery, chemotherapy and radiotherapy. PDT has three major components; a photosensitizer, light at a certain wavelength and oxygen. According to the location, size and the tissue origin of the tumor, an appropriate photosensitizer and compatible light source are determined for PDT procedure. Among all approved photosensitizers, Photofrin stands as the first and the most commonly used photosensitizing drug for PDT applications in clinical cancer treatment. Even though there is a high success rate in death of tumor cells by PDT, there is also a risk of tumor relapse following treatment. It is well-accepted that, the remaining tumor cells that survived besides treatment are the main cause of tumor reoccurrence. The molecular analysis of the remaining tumor cells indicated a possible role for PDT-mediated oxidative stress to enhance cell survival [12]. Discovering the molecular components of this PDT-induced cellular survival is one of the major challenges for improving PDT response to prevent tumor reoccurrence.

A variety of cytotoxic and survival responses are observed following PDT [30]. Oxidative stress is effective at initiating numerous molecular responses including the activation of AKT [107, 120]. AKT is a target of PI3-K and this pathway plays a critical role not only in tumor development but also in the tumors response to cancer treatment. A major function of phosphorylated and activated AKT is to promote cell survival and to block apoptosis [175]. AKT increases cell survival in a PI3-K-dependent manner and efforts to target or deregulate AKT are being pursued as means of enhancing conventional chemotherapy and radiation therapy [175].

This thesis study addressed important issues to develop better approaches to enhance PDT response in cancer treatment. The results of these study showed that PH-mediated PDT induces AKT phosphorylation in murine and human breast cancer cells and tumors [176]. These results are expected as previous reports have clearly shown that reactive oxygen species, including singlet oxygen, can phosphorylate and activate AKT [120, 121]. The possible mechanism of PDT-induced AKT activation is illustrated in Figure 5.1. In addition, it was also demonstrated that blockage of AKT phosphorylation using PI3-K inhibitors can increase apoptosis in PDT-treated cells and this also agrees with previous work [120]. The observations of AKT phosphorylation following incubation of breast cancer cells with PH in the absence of light and following treatment of experimental breast cancer tumors with light alone suggest that individual components of PDT can activate signaling pathways. It is currently unclear exactly why PH alone or light alone can induce AKT phosphorylation. A variety of chromophores, including porphyrin-based molecules, are found within cells and these molecules may interact with light to elicit the photochemical generation of oxidative stress. The *in vivo* light dose was higher than the *in vitro* light dose and this could contribute to the observed increase in AKT phosphorylation in tumors treated with light alone but not in cell cultures. In conclusion, individual components of the PDT procedure were able to induce AKT phosphorylation in cancer cells and in animal tumor models.

The findings from our *in vitro* experiments with AKT pathway inhibitors; Wortmannin, LY294002 and PI-103, showed that these inhibitors attenuated PDT-induced phosphorylation. However, Wortmannin and LY294002 have considerable side-effects due to high toxicity, therefore they are not suitable for further studies in animal models. Importantly, dual PI3-K and mTOR inhibitor PI-103 (Figure 5.1) has negligible cytotoxicity and minimal side effects besides being highly effective in AKT pathway inhibition. Our further analysis in animal models clearly showed that PI-103 inhibited PDT-mediated AKT phosphorylation in tumors without any detectable side-effects. In this regard, our findings suggest PI-103 as a promising candidate improve PDT treatment. In order to enhance clinical response of PDT treatment, PI-103 may be co-administered with PDT to inhibit AKT activation, thus prevent tumor relapse. In fact, specific inhibition of AKT pathway is a good therapeutic strategy for cancer. Many

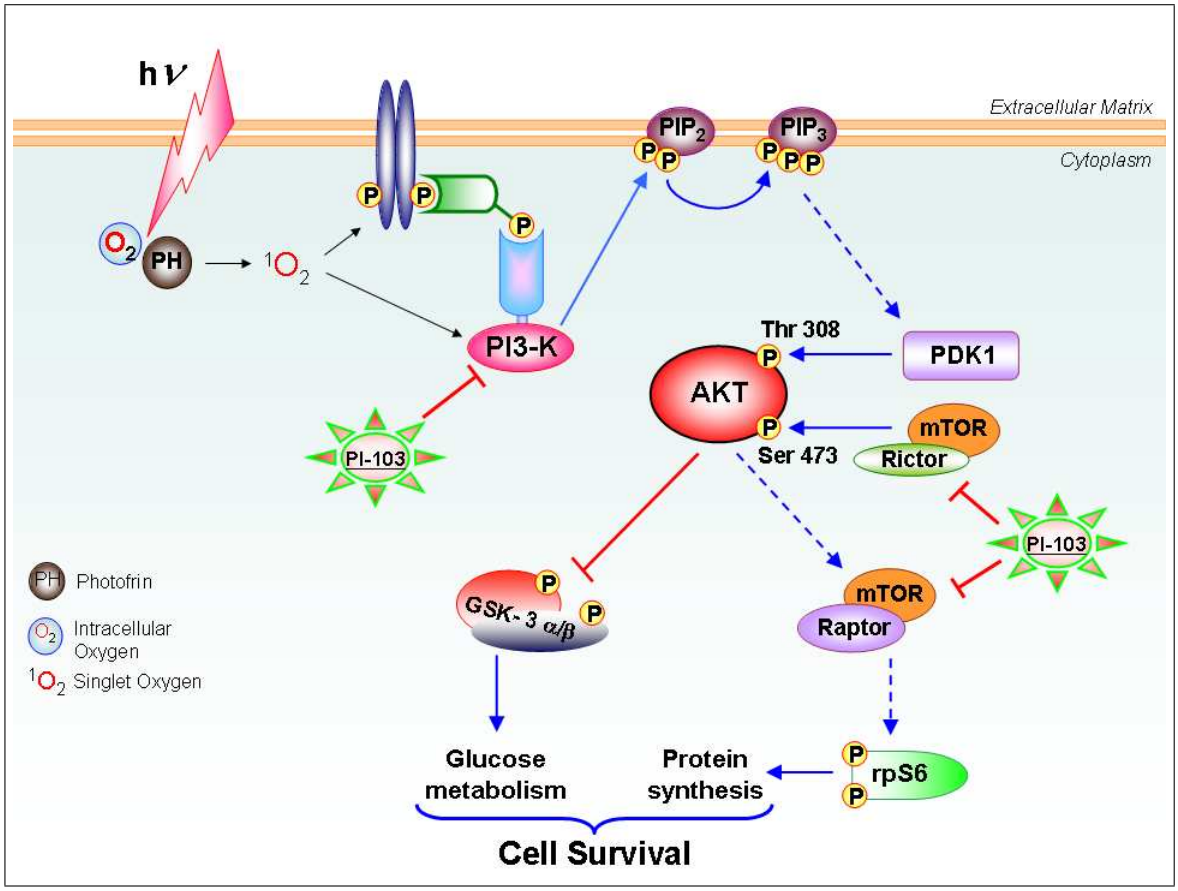

Figure 5.1 Schematic presentation of pathways leading to PDT-mediated AKT activation

of the new targeted agents have been specifically designed to act on AKT related targets. In fact, PDT responsiveness can be increased with combinatorial approaches with multitarget inhibitors or appropriate anti-angiogenic compounds [108, 109, 110, 116]. Our findings strongly support the possibility that PDT treatment in combination with AKT inhibitors have clinical relevance in cancer treatment in humans. Our results grants further *in vivo* and clinical studies to investigate this possibility.

5.2 ICG-PDT is a Promising Alternative for Treatment of Deep-tissue Tumors

Our discussion in the previous section focused on improving PDT response to prevent tumor reoccurrence by combination therapies. Another major challenge in PDT treatment is to develop new photosensitizers that are suitable to be used at wavelengths to treat deep tissue tumors. The photosensitizer ICG has maximum absorption at around 800 nm which can penetrate relatively deep into the tissue. Our studies focused on the initial *in vitro* examination of ICG-PDT on breast cancer cells to test the possibility that whether this method presents an alternative for treatments deeply localized tumors in future.

ICG-PDT has been reported to be effective in inducing cell death in a variety of cancer cell lines. Even though, it has not been approved for clinical treatment of cancer, it represents a promising candidate. The molecular basis of ICG-PDT mediated cell death is unclear; However, it has been proposed to have both photothermal [61, 62, 183] and photochemical [58, 59] effects. In our studies, highly metastatic breast cancer cells, which have never been reported in ICG-PDT experiments, were employed. Additionally, a computer controlled 809 nm diode laser which was designed and manufactured by our group was used to photoactivate ICG [174]. Our results showed that ICG when used in combination with near-infrared light showed an effective phototoxic effect on human breast cancer cells [182]. Importantly, this cytotoxic effects mediated by ICG-PDT was rapid and stable. In order to examine the *in vivo* relevance of this finding, future work should focus on testing the *in vivo* effects of ICG-PDT on animal tumor models. Additionally, it is important to investigate the molecular basis of ICG-PDT mediated cell death in tumors to develop strategies to overcome possible side-effects as observed for PH-PDT. Our findings represent a promising start for the ICG-PDT applications on the treatment of breast cancer in clinics.

REFERENCES

1. Bozkulak, O., "Kanser Tedavisinde Fotodinamik Tedavi," *Bilim ve Teknik*, Vol. 42, no. 498, pp. 62–65, 2009.

2. Allison, R. R., H. C. Mota, and C. H. Sibata, "Clinical PDT in north America: An historical review," *Photodiagnosis Photodyn Ther*, Vol. 1, pp. 263–277, 2004.

3. Abels, C., S. Fickweiler, P. Weiderer, W. Bäumler, F. Hofstadter, M. Landthaler, and R. M. Szeimies, "Indocyanine green (ICG) and laser irradiation induce photooxidation," *Arch Dermatol Res*, Vol. 292, pp. 404–411, 2000.

4. Koenig, K., "Multiphoton microscopy in life sciences," *J Microsc*, Vol. 2, pp. 83–104, 2000.

5. Knight, Z. A., and K. M. Shokat, "Chemically targeting the PI3-K family," *Biochem Soc Trans*, Vol. 35, pp. 245–249, 2007.

6. Allison, R. R., G. H. Downie, R. Cuenca, X. Hu, C. Childs, and C. Sibata, "Photosentisizers in clinical PDT", journal =,"

7. Theakston, F., *World Health Statistics 2008*, France: WHO Press, 2008.

8. "FDA approves Photofrin for treatment of pre-cancerous lesions in Barrett's Esophagus," *http://www.fda.gov/bbs/topics/ANSWERS/2003/ANS01246.html*.

9. Osaki, M., M. Oshimura, and H. Ito, "PI3K-Akt pathway: Its function and alterations in human cancer," *Apoptosis*, Vol. 9, pp. 667–676, 2004.

10. Vara, J. A. F., E. Casado, J. de Castro, P. Cejas, C. Belda-Iniesta, and M. González-Barón, "PI3K/Akt signaling pathway and cancer," *Cancer Treat Rev*, Vol. 30, pp. 193–204, 2004.

11. Franke, T. F., C. P. Hornik, L. Segev, G. A. Shostak, and C. Sugimoto, "PI3K/Akt and apoptosis: size matters," *Oncogene*, Vol. 22, pp. 8983–8998, 2003.

12. Gomer, C. J., A. Ferrario, M. Luna, N. Rucker, and S. Wong, "Photodynamic therapy: combined modality approaches targeting the tumor microenvironment," *Laser Surg Med*, Vol. 38, no. 5, pp. 516–521, 2006.

13. Bashkatov, A. N., E. A. Genina, V. I. Kochubey, and V. Tuchin, "Optical properties of human skin, subcutaneous and mucous tissues in the wavelength range from 400 to 2000 nm," *J Phys D: Appl Phys*, Vol. 38, pp. 2543–2555, 2005.

14. Alberts, B., D. Bray, J. Lewis, M. Raff, K. Roberts, and J. D. Watson, *Molecular biology of the cell*, New York: Garland, 3rd ed., 1994.

15. Macdonald, F., C. Ford, and A. Casson, *Molecular biology of cancer*, New York: BIOS Scientific, 2nd ed., 2004.

16. Pecorino, L., *Molecular biology of cancer: mechanisms, targets, and therapeutics*, Oxford: Oxford University Press, 2005.

17. "American cancer society," *http://www.cancer.org/docroot/home/index.asp*.

18. Panno, J., *Cancer: The role of genes, lifestyle, and environment*, New York: NY Facts On File Inc., 2005.

19. Institute, N. C., *Chemotherapy and you. A guide to self-help during cancer treatment*, USA: National Institutes of Health, 2007.

20. "Chemotherapy drugs," *http://www.chemocare.com/bio/*.

21. Institute, N. C., *Radiation Therapy and you. A guide to self-help during cancer treatment*, USA: National Institutes of Health, 2007.

22. Ackroyd, R., C. Kelty, N. Brown, and M. Reed, "The history of photodetection and photodynamic therapy," *Photochem Photobiol*, Vol. 74, no. 5, pp. 656–669, 2001.

23. Finsen, N. R., "Remarks on the red-light treatment of small-pox," *Br Med J*, Vol. 1, no. 2214, pp. 1297–1298, 1994.

24. Dennis, E. J., G. J. Dolmans, D. Fukumura, and R. K. Jain, "Photodynamic therapy for cancer," *Nat Rev Cancer*, Vol. 3, pp. 380–387, 2003.

25. Kufe, D. W., R. E. Pollock, R. R. Weichselbaum, R. C. Bast, and T. S. Gansler, *Cancer Medicine*, USA: BC Decker Inc., 6th ed., 2003.

26. Kessel, D., "Photodynamic therapy: from the beginning," *Photodiagnosis Photodyn Ther*, Vol. 1, pp. 3–5, 2004.

27. Lipson, R. L., E. J. Baldes, and A. M. Olsen, "Further evaluation of the use of hematoporphyrin derivative as a new aid for the endoscopic detection of malignant disease," *Dis Chest*, Vol. 64, pp. 676–679, 1964.

28. Lipson, R. L., E. J. Baldes, and M. J. Gray, "Hematoporphyrin derivative for detection and management of cancer," *Cancer*, Vol. 20, no. 12, pp. 2255–2257, 1967.

29. Gray, M. J., L. R. Lipson, J. V. Maeck, L. Parker, and D. Romeyn, "Use of hematoporphyrin derivative in detection and management of cervical cancer," *Am J Obstet Gynecol*, Vol. 99, no. 6, pp. 776–771, 1967.

30. Dougherty, T. J., C. J. Gomer, B. W. Henderson, G. Jori, D. Kessel, M. Korbelik, J. Moan, and Q. Peng, "Photodynamic therapy," *J Natl Cancer Inst*, Vol. 90, no. 12, pp. 889–905, 1998.

31. Prasad, P., *Introduction to Biophotonics*, Canada: John Wiley and Sons Inc., 2003.

32. Huang, Z., "A review of progress in clinical photodynamic therapy," *Technol Cancer Res Treat*, Vol. 4, no. 3, pp. 283–293, 2005.

33. Patrice, T., *Comprehensive Series in Photochemistry and Photobiology*, Cambridge, UK: The Royal Society of Chemistry, 2003.

34. Brown, S. B., E. A. Brown, and I. Walker, "The present and future role of photodynamic therapy in cancer treatment," *Lancet Oncol*, Vol. 5, pp. 497–508, 2004.

35. Robertson, C. A., D. H. Evans, and H. Abrahamse, "Photodynamic therapy (PDT): A short review on cellular mechanism and cancer research applications for PDT," *J Photochem Photobiol B*, Vol. 96, no. 1, pp. 1–8, 2009.

36. Huang, Z., H. Xu, A. D. Meyers, A. T. Musani, L. Wang, R. Tagg, A. B. Barqawi, and Y. K. Chen, "Photodynamic therapy for treatment of solid tumors- potential and technical chalanges," *Technol Cancer Res Treat*, Vol. 7, no. 4, pp. 309–320, 2008.

37. Moser, J., *Photodynamic tumor therapy : 2nd and 3rd generation photosensitizers*, Amsterdam, The Netherlands: Harwood Academic Publishers, 1998.

38. Brancaleon, L., and H. Moseley, "Laser and non-laser light sources for photodynamic therapy," *Lasers Med Sci*, Vol. 17, pp. 173–186, 2002.

39. Mang, T. S., "Lasers and light sources for PDT: past, present and future," *Photodiagnosis Photodyn Ther*, Vol. 1, pp. 43–48, 2004.

40. Bonnett, R., *Chemical Aspects of Photodynamic Therapy*, Singapore: Gordon and Breach Science Publishers, 2000.

41. Fuchs, J., and J. Thiele, "The role of oxygen in cutaneous photodynamic therapy," *Free Radic Biol Med*, Vol. 24, no. 5, pp. 835–847, 1998.

42. Klotz, L. O., K. D. Kroncke, and H. Sies, "Singlet oxygen-induced signaling effects in mammalian cells," *Photochem Photobiol Sci*, Vol. 2, pp. 88–94, 2003.

43. Schieke, S. M., C. V. Montfort, D. P. Buchczyk, A. Timmer, S. Grether-Beck, J. Krutmann, N. J. Holbrook, and L. O. Klotz, "Singlet oxygen-induced attenuation of growth factor signaling: Possible role of ceramides," *Free Radic Res*, Vol. 38, no. 7, pp. 729–737, 2004.

44. Castano, A. P., T. N. Demidova, and M. R. Hamblin, "Mechanisms in photodynamic therapy: part one-photosentisizers, photochemistry, and cellular localization," *Photodiagnosis Photodyn Ther*, Vol. 1, pp. 279–293, 2004.

45. Martindale, J. L., and N. J. Holbrook, "Cellular response to oxidative stress: signaling for suicide and survival," *J Cell Physiol*, Vol. 192, pp. 1–15, 2002.

46. Kessel, D., C. K. Chang, and B. Musselman, "Chemical, biologic and biophysical studies on hematoporphyrin derivative," *Adv Exp Med Biol*, Vol. 193, pp. 213–227, 1985.

47. Pervaiz, S., and M. Olivo, "Art and science of photodynamic therapy," *Clin Exp Pharmacol Physiol*, Vol. 33, pp. 551–556, 2006.

48. Loewen, G. M., R. Pandey, D. Bellnier, B. Henderson, and T. Dougherty, "Endobronchial photodynamic therapy for lung cancer," *Lasers Surg Med*, Vol. 38, pp. 364–370, 2006.

49. Jankun, J., L. Lilge, A. Douplik, R. W. Keck, M. Pestka, M. Szkudlarek, P. J. Stevens, R. J. Lee, and S. H. Selman, "Optical characteristics of the canine prostate at 665 nm sensitized with tin etiopurpurin dichloride: need for real-time monitoring of photodynamic therapy," *J Urol*, Vol. 172, no. 2, pp. 739–743, 2004.

50. Du, K. L., R. Mick, T. M. Busch, T. C. Zhu, J. C. Finlay, G. Yu, A. G. Yodh, S. B. Malkowicz, D. Smith, R. Whittington, D. Stripp, and S. M. Hahn, "Preliminary results of interstitial motexafin lutetium-mediated PDT for prostate cancer," *Lasers Surg Med*, Vol. 38, no. 5, pp. 427–434, 2006.

51. Wainwrigh, M., "Photodynamic therapy: the development of new photosensitisers," *Anticancer Agents Med Chem*, Vol. 8, no. 3, pp. 280–291, 2008.

52. Pharma, A., "Photofrin," *http://www.photofrin.com*.

53. Nahimisa, T., "Indocyanine green test and its development," *Tokai J Exp Clin Med*, Vol. 7, pp. 419–423, 1982.

54. Kim, G., S. W. Huang, K. C. Day, M. O'Donnell, R. R. Agayan, M. A. Day, R. Kopelman, and S. Ashkenazi, "Indocyanine-green-embedded PEBBLEs as a contrast agent for photoacoustic imaging," *J Biomed Opt*, Vol. 12, no. 4, p. 044020, 2007.

55. Fickweiler, S., R. M. Szeimies, W. Bäumler, P. Steinbachb, S. Karrer, A. E. Goetzc, C. Abels, and F. Hofstadter, "Indocyanine green: intracellular uptake and phototherapeutic effects in vitro," *J Photochem Photobiol B*, Vol. 38, pp. 178–183, 1997.

56. Crescenzi, E., L. Varriale, M. Iovino, A. Chiaviello, B. M. Veneziani, and G. Palumbo, "Photodynamic therapy with indocyanine green complements and enhances low-dose cisplatin cytotoxicity in MCF-7 breast cancer cells," *Mol Cancer Ther*, Vol. 3, no. 5, pp. 537–544, 2004.

57. Chen, W. R., M. Korbelik, K. E. Battels, H. Liu, J. Sun, and R. E. Nordquist, "Enhancement of laser cancer treatment by a chitosan-derived immunoadjuvant," *Photochem Photobiol*, Vol. 81, no. 1, pp. 190–195, 2005.

58. Baumler, W., C. Abels, S. Karrer, T. Weiss, H. Messmann, and M. L. R. M. Szeimies, "Photo-oxidative killing of human colonic cancer cells using indocyanine green and infrared light," *Br J Cancer*, Vol. 80, no. 3/4, pp. 360–363, 1999.

59. Tseng, W. W., R. E. Saxton, A. Deganutti, and C. D. Liu, "Infrared laser activation of indocyanine green inhibits growth in human pancreatic cancer," *Pancreas*, Vol. 27, no. 3, pp. e42–45, 2003.

60. Colasanti, A., M. Kisslinger, M. Quarto, and P. Riccio, "Combined effects of radiotherapy and photodynamic therapy on an in vitro human prostate model," *Acta Biochem Pol*, Vol. 51, no. 4, pp. 1039–1046, 2004.

61. Bailey, C. A., T. M. Cowan, V. G. Liu, E. C. Lemley, and W. R. Chen, "Optimization of selective hyperthermia," *J Biomed Opt*, Vol. 9, no. 3, pp. 648–654, 2004.

62. Liu, V. G., T. M. Cowan, S. W. Jeong, S. L. Jacques, E. C. Lemley, and W. R. Chen, "Selective photothermal interaction using an 805-nm diode laser and indocyanine green in gel phantom and chicken breast tissue," *Lasers Med Sci*, Vol. 17, no. 4, pp. 272–279, 2002.

63. Svaasand, L. O., "Photodynamic and photohyperthermic response of malignant tumors," *Med Phys*, Vol. 12, pp. 455–461, 1985.

64. Sitnik, T. M., J. A. Hampton, and B. W. Henderson, "Reduction of tumour oxygenation during and after photodynamic therapy in vivo: effects of fluence rate," *Br J Cancer*, Vol. 77, pp. 1386–1394, 1998.

65. Busch, T. M., E. P. Wileyto, M. J. Emanuele, F. D. Piero, L. Marconato, E. Glatstein, and C. J. Koch, "Photodynamic therapy creates fluence rate-dependent gradients in the intratumoral spatial distribution of oxygen," *Cancer Res*, Vol. 62, pp. 7273–7279, 2002.

66. Henderson, B. W., T. M. Busch, and J. W. Snyder, "Fluence rate as a modulator of PDT mechanisms," *Lasers Surg Med*, Vol. 38, pp. 489–493, 2006.

67. Henderson, B. W., T. M. Busch, L. A. Vaughan, N. P. Frawley, D. Babich, T. A. Sosa, J. D. Zollo, A. S. Dee, M. T. Cooper, D. A. Bellnier, W. R. Greco, and A. R. Oseroff, "Photofrin photodynamic therapy can significantly deplete or preserve oxygenation in human basal cell carcinomas during treatment, depending on fluence rate," *Cancer Res*, Vol. 60, pp. 525–529, 2000.

68. Wilson, B. C., and M. S. Patterson, "The physics, biophysics and technology of photodynamic therapy," *Phys Med Biol*, Vol. 53, no. 9, pp. 61–109, 2008.

69. Hopper, C., C. Niziol, and M. Sidhu, "The cost-effectiveness of Foscan mediated photodynamic therapy (Foscan-PDT) compared with extensive palliative surgery and palliative chemotherapy for patients with advanced head and neck cancer in the UK," *Oral Oncol*, Vol. 40, pp. 372–382, 2004.

70. Kübler, A., C. Niziol, M. Sidhu, A. Dünne, and J. A. Werner, "Analysis of cost effectiveness of photodynamic therapy with Foscan (Foscan-PDT) in comparison with palliative chemotherapy in patients with advanced head-neck tumors in Germany," *Laryngorhinootologie*, Vol. 84, no. 10, pp. 725–732, 2005.

71. Hur, C., N. S. Nishioka, and G. S. Gazelle, "Cost-effectiveness of photodynamic therapy for treatment of Barrett's Esophagus with high grade dysplasia," *Dig Dis Sci*, Vol. 48, pp. 1273–1283, 2003.

72. Ris, H. B., H. J. Altermatt, R. Inderbitzi, R. Hess, B. Nachbur, J. C. Stewart, Q. Wang, C. K. Lim, R. Bonnett, M. C. Berenbaum, and U. Althaus, "Photodynamic therapy with chlorins for diffuse malignant mesothelioma: initial clinical results," *Br J Cancer*, Vol. 64, no. 6, pp. 1116–1120, 1991.

73. Grant, W. E., P. M. Speight, C. Hopper, and S. G. Bown, "Photodynamic therapy: an effective, but non-selective treatment for superficial cancers of the oral cavity," *Int J Cancer*, Vol. 71, no. 6, pp. 937–942, 1997.

74. Verrico, A. K., A. K. Haylett, and J. V. Moore, "In vivo expression of the collagenrelated heat shock protein HSP47, following hyperthermia or photodynamic therapy," *Lasers Med Sci*, Vol. 16, pp. 192–198, 2001.

75. Kato, H., "Photodynamic therapy for lung cancer-a review of 19 years' experience," *J Photochem Photobiol B*, Vol. 42, pp. 96–99, 1998.

76. Kato, H., M. Harada, S. Ichinose, J. Usuda, T. Tsuchida, and T. Okunaka, "Photodynamic therapy (PDT) of lung cancer: Experience of the tokyo medical university," *Photodiag Photodyn Ther*, Vol. 1, pp. 49–55, 2004.

77. Mathur, P. N., E. Edell, T. Sutedja, and J. Vergnon, "Treatment of early stage non-small cell lung cancer," *Chest*, Vol. 123, pp. 176–180, 2003.

78. McCaughan, J. S., T. E. Williams, and B. H. Bethel, "Photodynamic therapy of endobronchial tumors," *Lasers Surg Med*, Vol. 6, pp. 336–345, 1986.

79. Keller, G. S., D. R. Doiron, and G. U. Fisher, "Photodynamic therapy in otolaryngology–head and neck surgery," *Arch Otolaryngol*, Vol. 111, no. 11, pp. 758–761, 1985.

80. Schuller, D. E., J. S. McCaughan, and R. P. Rock, "Photodynamic therapy in head and neck cancer," *Arch Otolaryngol*, Vol. 111, no. 6, pp. 351–355, 1985.

81. Biel, M. A., "Photodynamic therapy and the treatment of head and neck neoplasia," *Laryngoscope*, Vol. 108, pp. 1259–1268, 1998.

82. Lou, P. J., L. Jones, and C. Hooper, "Clinical outcomes of photodynamic therapy for head-and-neck cancer," *Technol Cancer Res Treat*, Vol. 2, pp. 311–317, 2003.

83. Dougherty, T. J., J. E. Kaufman, A. Goldfarb, K. R. Weishaupt, D. Boyle, and A. Mittleman, "Photoradiation therapy for the treatment of malignant tumors," *Cancer Res*, Vol. 38, no. 8, pp. 2628–2635, 1978.

84. Taub, A. F., "Photodynamic therapy in dermatology: history and horizons," *J Drugs Dermatol*, Vol. 3, no. 1 Suppl, pp. S8–S25, 2004.

85. Michels, S., and U. Schmidt-Erfurth, "Photodynamic therapy with verteporfin: a new treatment in ophthalmology," *Semin Ophthalmol*, Vol. 16, no. 4, pp. 201–206, 2001.

86. Mennel, S., I. Barbazetto, C. H. Meyer, S. Peter, and M. Stur, "Ocular photodynamic therapy–standard applications and new indications (Part 1)," *Ophthalmologica*, Vol. 221, no. 4, pp. 216–226, 2007.

87. Mennel, S., I. Barbazetto, C. H. Meyer, S. Peter, and M. Stur, "Ocular photodynamic therapy-standard applications and new indications (Part 2)," *Ophthalmologica*, Vol. 221, no. 5, pp. 282–291, 2007.

88. Cook, H. L., P. J. Patel, and A. Tufail, "Age-related macular degeneration: diagnosis and management," *Br Med Bull*, Vol. 85, pp. 127–149, 2008.

89. Houle, J. M., and H. A. Strong, "Duration of skin photosensitivity and incidence of photosensitivity reactions after administration of verteporfin," *Retina*, Vol. 22, no. 6, pp. 691–697, 2002.

90. Mennel, S., N. Hausmann, C. H. Meyer, and S. Peter, "Photodynamic therapy for exudative hamartoma in tuberous sclerosis," *Arch Ophthalmol*, Vol. 124, no. 4, pp. 597–599, 2006.

91. Salim, A., J. A. Leman, J. H. McColl, R. Chapman, and C. A. Morton, "Randomized comparison of photodynamic therapy with topical 5-fluorouracil in Bowen's Disease," *Br J Dermatol*, Vol. 148, no. 3, pp. 539–543, 2003.

92. Ibbotson, S., H. Moseley, L. Brancaleon, M. Padgett, M. O'Dwyer, J. Woods, A. Lesar, C. Goodman, and J. Ferguson, "Photodynamic therapy in dermatology: Dundee clinical and research experience," *Photodiagnosis Photodyn Ther*, Vol. 1, no. 3, pp. 211–223, 2004.

93. Overholt, B. F., M. Panjehpour, and D. L. Halberg, "Photodynamic therapy for barrett's esophagus with dysplasia and/or early stage carcinoma: long-term results," *Gastrointest Endosc*, Vol. 58, pp. 183–188, 2003.

94. Yamaguchi, S., H. Tsuda, M. Takemori, S. Nakata, S. Nishimura, N. Kawamura, K. Hanioka, T. Inoue, and R. Nishimura, "Photodynamic therapy for cervical intraepithelial neoplasia," *Oncology*, Vol. 69, no. 2, pp. 110–116, 2005.

95. Moghissi, K., K. Dixon, J. A. Thorpe, M. Stringer, and P. J. Moore, "The role of photodynamic therapy (PDT) in inoperable oesophageal cancer," *Eur J Cardiothorac Surg*, Vol. 17, no. 2, pp. 95–100, 2000.

96. Sibille, A., R. Lambert, J. C. Souquet, G. Sabben, and F. Descos, "Long-term survival after photodynamic therapy for esophageal cancer," *Gastroenterology*, Vol. 108, no. 2, pp. 337–344, 1995.

97. Wang, J. B., and L. X. Liu, "Use of photodynamic therapy in malignant lesions of stomach, bile duct, pancreas, colon and rectum," *Hepatogastroenterology*, Vol. 54, no. 75, pp. 718–724, 2007.

98. Wiedmann, M. W., , and K. Caca, "General principles of photodynamic therapy (PDT) and gastrointestinal applications," *Curr Pharm Biotechnol*, Vol. 5, no. 4, pp. 397–408, 2004.

99. Betz, C. S., W. Rauschning, E. P. Stranadko, M. V. Riabov, V. Albrecht, N. E. Nifantiev, and C. Hopper, "Optimization of treatment parameters for Foscan-PDT of basal cell carcinomas," *Lasers Surg Med*, Vol. 40, no. 5, pp. 300–311, 2008.

100. Biel, M., "Advances in photodynamic therapy for the treatment of head and neck cancers," *Lasers Surg Med*, Vol. 38, no. 5, pp. 349–355, 2006.

101. Eljamel, M. S., C. Goodman, and H. Moseley, "ALA and Photofrin fluorescence-guided resection and repetitive PDT in glioblastoma multiforme: a single centre Phase III randomised controlled trial," *Lasers Med Sci*, Vol. 23, no. 4, pp. 361–367, 2008.

102. Nseyo, U. O., J. DeHaven, T. J. Dougherty, W. R. Potter, D. L. Merrill, S. L. Lundahl, and D. L. Lamm, "Photodynamic therapy (PDT) in the treatment of patients with resistant superficial bladder cancer: a long-term experience," *J Clin Laser Med Surg*, Vol. 16, no. 1, pp. 61–68, 1998.

103. Denzinger, S., and M. Burger, "Photodynamic diagnostics of bladder tumors," *Curr Urol Rep*, Vol. 9, no. 2, pp. 101–105, 2008.

104. Zuluaga, M. F., and N. Lange, "Combination of photodynamic therapy with anti-cancer agents," *Curr Med Chem*, Vol. 15, no. 17, pp. 1655–1673, 2008.

105. Castano, A. P., T. N. Demidova, and M. R. Hamblin, "Mechanisms in photodynamic therapy: Part two-cellular signaling, cell metabolism and modes of cell death," *Photodiag Photodyn Ther*, Vol. 2, pp. 1–23, 2005.

106. Fingar, V. H., T. J. Wieman, S. A. Wiehle, and P. B. Cerrito, "The role of microvascular damage in photodynamic therapy: The effect of treatment on vessel constriction, permeability, and leukocyte adhesion," *Cancer Res*, Vol. 52, pp. 4914–4921, 1992.

107. Almeida, R. D., B. J. Manadas, A. P. Carvalho, and C. B. Duarte, "Intracellular Signaling Mechanisms in Photdynamic Therapy," *BioChim Biophys Acta*, Vol. 1704, pp. 59–86, 2004.

108. Ferrario, A., C. F. Chantrain, K. F. von Tiehl, S. Buckley, N. Rucker, D. R. Shalinsky, H. Shimada, Y. A. DeClerck, and C. J. Gomer, "The matrix metalloproteinase inhibitor prinomastat enhances photodynamic therapy responsiveness in a mouse tumor model," *Cancer Res*, Vol. 64, pp. 2328–2332, 2004.

109. Ferrario, A., K. F. von Tiehl, N. Rucker, M. A. Schwarz, P. S. Gill, and C. J. Gomer, "Anti-angiogenic treatment enhances photodynamic therapy responsiveness in a mouse mammary carcinoma," *Cancer Res*, Vol. 60, pp. 4066–4069, 2000.

110. Ferrario, A., K. F. von Tiehl, S. Wong, M. Luna, and C. J. Gomer, "Cyclooxygenase-2 inhibitor treatment enhances photodynamic therapy-mediated tumor response," *Cancer Res*, Vol. 62, pp. 3956–3961, 2002.

111. Albini, A., F. Tosetti, R. Benelli, and D. M. Noonan, "Tumor inflammatory angiogenesis and its chemoprevention," *Cancer Res*, Vol. 65, pp. 10637–10641, 2005.

112. Karin, M., "Cancer research in flames; tracking inflammation's role in promoting malignancy could lead to better treatments," *Scientist*, Vol. 19, pp. 24–25, 2005.

113. Benelli, R., M. Morini, F. Carrozzino, N. Ferrari, S. Minghelli, L. Santi, M. Cassatella, D. M. Noonan, and A. Albini, "Neutrophils as a key cellular target for angiostatin: Implications for regulation of angiogenesis and inflammation," *FASEB J*, Vol. 16, pp. 267–269, 2002.

114. Coussens, L. M., and Z. W. Z, "Inflammation and cancer," *Nature*, Vol. 420, pp. 860–867, 2002.

115. Ferrario, A., A. M. Fisher, N. Rucker, and C. J. Gomer, "Celecoxib and NS-398 enhance photodynamic therapy by increasing in-vitro apoptosis and decreasing in-vivo inflammatory and angiogenic factors," *Cancer Res*, Vol. 65, pp. 9473–9479, 2005.

116. Ferrario, A., and C. J. Gomer, "Avastin enhances photodynamic therapy treatment of Kaposi's Sarcoma in a mouse tumor model," *J Environ Path Tox Oncol*, Vol. 25, pp. 251–259, 2006.

117. Gollink, S. O., S. S. Evans, H. Baumann, B. Owczarczak, P. Maier, L. Vaughan, W. C. Wang, E. Unger, and B. W. Henderson, "Role of cytokines in photodynamic therapy-induced local and systemic inflammation," *Br J Cancer*, Vol. 88, pp. 1772–1779, 2003.

118. Makowski, M., T. Grzela, J. Niderla, M. Azarczyk, P. Mroz, M. Kopee, M. Legat, K. Strusinska, K. Koziak, D. Nowis, P. Mrowka, M. Wasik, M. Jakobisiak, and J. Golab, "Inhibition of cyclooxygenase-2 indirectly potentiates antitumor effects of photodynamic therapy in mice," *Clin Cancer Res*, Vol. 9, pp. 5417–5422, 2003.

119. Akita, Y., K. Kozaki, A. Nakagawa, T. Saito, S. Ito, Y. Tamada, S. Fujiwara, N. Nishikawa, K. Uchida, K. Yoshikawa, T. Noguchi, O. Miyaishi, K. Shimozato, S. Saga, and Y. Matsumoto, "Cyclooxygenase-2 is a possible target of treatment approach in conjunction with photodynamic therapy for various disorders in skin and oral cavity," *Br J Dermatol*, Vol. 151, pp. 472–480, 2004.

120. Zhuang, S., and I. E. Kochevar, "Singlet oxygen-induced activation of Akt/protein kinase B is independent of growth factor receptors," *Photochem Photobiol*, Vol. 78, pp. 361–371, 2003.

121. Yang, P., J. J. Peairs, R. Tano, and G. J. Jaffe, "Oxidantmediated Akt activation in human RPE cells," *Invest. Ophthalmol. Vis. Sci.*, Vol. 47, pp. 4598–4606, 2006.

122. Nicholson, K. M., and N. G. Anderson, "The protein kinase B/Akt signaling pathway in human malignancy," *Cell Signal*, Vol. 14, pp. 381–395, 2002.

123. Giancotti, V., "Breast cancer markers," *Cancer Lett*, Vol. 243, no. 2, pp. 145–159, 2006.

124. Samuels, Y., and K. Ericson, "Oncogenic PI3K and its role in cancer," *Curr Opin Oncol*, Vol. 18, pp. 77–82, 2006.

125. Hennessy, B. T., D. L. Smith, P. T. Ram, Y. Lu, and G. B. Mills, "Exploiting the PI3K/AKT pathway for cancer drug discovery," *Nature Reviews Drug Discovery*, Vol. 4, pp. 988–1004, 2005.

126. Bianco, R., D. Melisi, F. Ciardiello, and G. Tortora, "Key cancer cell signal transduction pathways as therapeutic targets," *Eur J Cancer*, Vol. 42, pp. 290–294, 2006.

127. Staal, S. P., "Molecular cloning of the akt oncogene and its human homologues AKT1 and AKT2: amplification of AKT1 in a primary human gastric adenocarcinoma," *Proc Natl Acad Sci USA*, Vol. 84, no. 14, pp. 5034–5037, 1987.

128. James, S. R., C. P. Downes, R. Gigg, S. J. Grove, A. B. Holmes, and D. R. Alessi, "Specific binding of the Akt-1 protein kinase to phosphatidylinositol 3,4,5-trisphosphate without subsequent activation," *Biochem J*, Vol. 315, no. 3, pp. 709–713, 1996.

129. Stephens, L., K. Anderson, D. Stokoe, H. Erdjument-Bromage, G. F. Painter, A. B. Holmes, P. R. Gaffney, C. B. Reese, F. McCormick, P. Tempst, J. Coadwell, and P. T. Hawkins, "Protein kinase B kinases that mediate phosphatidylinositol 3,4,5-trisphosphate-dependent activation of protein kinase B," *Science*, Vol. 279, no. 5351, pp. 710–714, 1998.

130. Meier, R., D. R. Alessi, P. Cron, M. Andjelkovic, and B. A. Hemmings, "Mitogenic activation, phosphorylation, and nuclear translocation of protein kinase B β," *J Biol Chem*, Vol. 272, no. 48, pp. 30491–30497, 1997.

131. Andjelkovic, M., D. R. Alessi, R. Meier, A. Fernandez, N. J. Lamb, M. Frech, P. Cron, P. Cohen, J. M. Lucocq, and B. A. Hemmings, "Role of translocation in the activation and function of protein kinase b," *J Biol Chem*, Vol. 272, no. 50, pp. 31515–31524, 1997.

132. Tao, J., J. S. Sanghera, S. L. Pelech, G. Wong, and J. G. Levy, "Stimulation of stress-activated protein kinase and p38 HOG1 kinase in murine keratinocytes following photodynamic therapy with benzoporphyrin derivative," *J Biol Chem*, Vol. 271, pp. 27107–27115, 1996.

133. Xue, L., J. He, and N. L. Oleinick, "Promotion of photodynamic therapy-induced apoptosis by stress kinases," *Cell Death Differ*, Vol. 6, pp. 855–864, 1999.

134. Hendrickx, N., C. Volanti, U. Moens, O. M. Seternes, P. de Witte, J. R. Vandenheede, J. Piette, and P. Agostinis, "Up-regulation of cyclooxygenase-2 and apoptosis resistance by p38 MAPK in hypericin-mediated photodynamic therapy of human cancer cells," *J Biol Chem*, Vol. 278, no. 52, pp. 52231–52239, 2003.

135. Tong, Z., G. Singh, and A. J. Rainbow, "Sustained activation of the extracellular signal-regulated kinase pathway protects cells from photofrin-mediated photodynamic therapy," *Cancer Res*, Vol. 62, pp. 5528–5535, 2002.

136. Klotz, L. O., C. Fritsch, K. Briviba, N. Tsacmacidis, F. Schliess, and H. Sies, "Activation of JNK and p38 but not ERK MAP kinases in human skin cells by 5-aminolevulinate-photodynamic therapy," *Cancer Res*, Vol. 58, pp. 4297–4300, 1998.

137. Ahmad, N., K. Kalka, and H. Mukhtar, "In vitro and in vivo inhibition of epidermal growth factor receptor-tyrosine kinase pathway by photodynamic therapy," *Oncogene*, Vol. 20, pp. 2314–2317, 2001.

138. Piret, B., S. Legrand-Poels, C. Sappey, and J. Piette, "NF-kappa B transcription factor and human immunodeficiency virus type 1 (HIV-1) activation by methylene blue photosensitization," *Eur J Biochem*, Vol. 228, pp. 447–455, 1995.

139. Legrand-Poels, S., V. Bours, B. Piret, M. Pflaum, B. Epe, B. Rentier, and J. Piette, "Transcription factor NF-kappa B is activated by photosensitization generating oxidative DNA damages," *J Biol Chem*, Vol. 270, pp. 6925–6934, 1995.

140. Matroule, J. Y., G. Bonizzi, P. Morlière, N. Paillous, R. Santus, V. Bours, and J. Piette, "Pyropheophorbide-a methyl ester-mediated photosensitization activates transcription factor NF-kappaB through the interleukin-1 receptor-dependent signaling pathway," *J Biol Chem*, Vol. 274, pp. 2988–3000, 1999.

141. Volanti, C., J. Y. Matroule, and J. Piette, "Involvement of oxidative stress in NF-kappaB activation in endothelial cells treated by photodynamic therapy," *Photochem Photobiol*, Vol. 75, pp. 36–45, 2002.

142. Yao, R., and G. M. Cooper, "Requirement for phosphatidylinositol-3 kinase in the prevention of apoptosis by nerve growth factor," *Science*, Vol. 267, no. 5206, pp. 2003–2006, 1995.

143. Datta, S. R., A. Brunet, and M. E. Greenberg, "Cellular survival: a play in three Akts," *Genes Dev*, Vol. 13, no. 22, pp. 2905–2927, 1999.

144. Vanhaesebroeck, B., and D. R. Alessi, "The PI3K-PDK1 connection: more than just a road to PKB," *Biochem J*, Vol. 346, no. 3, pp. 561–576, 2000.

145. Lawlor, M. A., and D. R. Alessi, "PKB/Akt: a key mediator of cell proliferation, survival and insulin responses?," *J Cell Sci*, Vol. 114, no. 16, pp. 2903–2910, 2001.

146. Brunet, A., A. Bonni, M. J. Zigmond, M. Z. Lin, P. Juo, L. S. Hu, M. J. Anderson, K. C. Arden, J. Blenis, and M. E. Greenberg, "AKT promotes cell survival by phosphorylating and inhibiting a Forkhead transcription factor," *Cell*, Vol. 96, no. 6, pp. 857–868, 1999.

147. Pap, M., and G. M. Cooper, "Role of glycogen synthase kinase-3 in the phosphatidylinositol 3-Kinase/Akt cell survival pathway," *J Biol Chem*, Vol. 273, no. 32, pp. 19929–19932, 1998.

148. Zhou, B. P., Y. Liao, W. Xia, Y. Zou, B. Spohn, and M. C. Hung, "HER-2/neu induces p53 ubiquitination via Akt-mediated MDM2 phosphorylation," *Nat Cell Biol*, Vol. 3, no. 11, pp. 973–982, 2001.

149. Mayo, L. D., and D. B. Donner, "A phosphatidylinositol 3-kinase/Akt pathway promotes translocation of Mdm2 from the cytoplasm to the nucleus," *Proc Natl Acad Sci USA*, Vol. 98, no. 20, pp. 11598–11603, 2001.

150. Ashcroft, M., R. L. Ludwig, D. B. Woods, T. D. Copeland, H. O. Weber, E. J. MacRae, and K. H. Vousden, "Phosphorylation of HDM2 by Akt," *Oncogene*, Vol. 21, no. 13, pp. 1955–1962, 2002.

151. Datta, S. R., H. Dudek, X. Tao, S. Masters, H. Fu, Y. Gotoh, and M. E. Greenberg, "Akt phosphorylation of BAD couples survival signals to the cell-intrinsic death machinery," *Cell*, Vol. 91, no. 2, pp. 231–241, 1997.

152. Ozes, O. N., L. D. Mayo, J. A. Gustin, S. R. Pfeffer, L. M. Pfeffer, and D. B. Donner, "NF-kappaB activation by tumour necrosis factor requires the Akt serine-threonine kinase," *Nature*, Vol. 401, no. 6748, pp. 82–85, 1999.

153. Cardone, M. H., N. Roy, H. R. Stennicke, G. S. Salvesen, T. F. Franke, E. Stanbridge, S. Frisch, and J. C. Reed, "Regulation of cell death protease caspase-9 by phosphorylation," *Science*, Vol. 282, no. 5392, pp. 1318–1321, 1998.

154. Kohn, A. D., S. A. Summers, M. J. Birnbaum, and R. A. Roth, "Expression of a constitutively active Akt Ser/Thr kinase in 3T3-L1 adipocytes stimulates glucose uptake and glucose transporter 4 translocation," *J Biol Chem*, Vol. 271, no. 49, pp. 31372–31378, 1996.

155. Gottlob, K., N. Majewski, S. Kennedy, E. Kandel, R. B. Robey, and N. Hay, "Inhibition of early apoptotic events by Akt/PKB is dependent on the first committed step of glycolysis and mitochondrial hexokinase," *Genes Dev*, Vol. 15, no. 11, pp. 1406–1418, 2001.

156. Sabatini, D. M., "mTOR and cancer: insights into a complex relationship," *Nat Rev Cancer*, Vol. 6, no. 9, pp. 729–734, 2006.

157. Hay, N., and N. Sonenberg, "Upstream and downstream of mTOR," *Genes Dev*, Vol. 18, pp. 1926–1945, 2004.

158. Sarbassov, D. D., D. A. Guertina, S. M. Ali, and D. M. Sabatini, "Phosphorylation and regulation of Akt/PKB by the rictor-mTOR complex," *Science*, Vol. 307, no. 5712, pp. 1098–1101, 2005.

159. Hresko, R. C., and M. Mueckler, "mTOR/RICTOR is the Ser473 kinase for Akt/PKB in 3T3-L1 adipocytes," *J Biol Chem*, Vol. 280, pp. 40406–40416, 2005.

160. Vivanco, I., and C. L. Sawyers, "The phosphatidylinositol 3-Kinase AKT pathway in human cancer," *Nat Rev Cancer*, Vol. 2, no. 7, pp. 489–501, 2002.

161. Kandel, E. S., and N. Hay, "The regulation and activities of the multifunctional serine/threonine kinase Akt/PKB," *Exp Cell Res*, Vol. 253, no. 1, pp. 210–229, 1999.

162. Roy, H. K., B. F. Olusola, D. L. Clemens, W. J. Karolski, A. Ratashak, H. T. Lynch, and T. C. Smyrk, "AKT proto-oncogene overexpression is an early event during sporadic colon carcinogenesis," *Carcinogenesis*, Vol. 23, no. 1, pp. 201–205, 2002.

163. Altomare, D. A., S. Tanno, A. D. Rienzo, A. J. Klein-Szanto, S. Tanno, K. L. Skele, J. P. Hoffman, and J. R. Testa, "Frequent activation of AKT2 kinase in human pancreatic carcinomas," *J Cell Biochem*, Vol. 87, no. 4, pp. 470–476, 2002.

164. Tanno, S., N. Yanagawa, A. Habiro, K. Koizumi, Y. Nakano, M. Osanai, Y. Mizukami, T. Okumura, J. R. Testa, and Y. Kohgo, "Serine/threonine kinase AKT is frequently activated in human bile duct cancer and is associated with increased radioresistance," *Cancer Res*, Vol. 64, no. 10, pp. 3486–3490., 2004.

165. Gupta, A. K., W. G. M. abd C N Weber, M. D. Feldman, J. D. Goldsmith, R. Mick, M. Machtay, D. I. Rosenthal, V. J. Bakanauskas, G. J. Cerniglia, E. J. Bernhard, R. S. Weber, and R. J. Muschel, "Local recurrence in head and neck cancer: relationship to radiation resistance and signal transduction," *Clin Cancer Res*, Vol. 8, no. 3, pp. 885–892, 2002.

166. Pérez-Tenorio, G., and O. Stål, "Activation of AKT/PKB in breast cancer predicts a worse outcome among endocrine treated patients," *Br J Cancer*, Vol. 86, no. 4, pp. 540–545, 2002.

167. Clark, A. S., K. West, S. Streicher, and P. A. Dennis, "Constitutive and inducible Akt activity promotes resistance to chemotherapy, trastuzumab, or tamoxifen in breast cancer cells," *Mol Cancer Ther*, Vol. 1, no. 9, pp. 707–717, 2002.

168. Brognard, J., A. S. Clark, Y. Ni, and P. A. Dennis, "Akt/protein kinase B is constitutively active in non-small cell lung cancer cells and promotes cellular survival and resistance to chemotherapy and radiation," *Cancer Res*, 2001.

169. Wymann, M. P., M. Zvelebil, and M. Laffargue, "Phosphoinositide 3-kinase signalling–which way to target?," *Trends Pharmacol Sci*, Vol. 24, no. 7, pp. 366–376, 2003.

170. Bachman, K. E., P. Argani, Y. Samuels, N. Silliman, J. Ptak, S. Szabo, H. Konishi, B. Karakas, B. G. Blair, C. Lin, B. A. Peters, V. E. Velculescu, and B. H. Park, "The PIK3CA gene is mutated with high frequency in human breast cancers," *Cancer Biol Ther*, Vol. 3, pp. 772–775, 2004.

171. Broderick, D. K., C. Di, T. J. Parrett, Y. R. Samuels, J. M. Cummins, R. E. McLendon, D. W. Fults, V. E. Velculescu, D. D. Bigner, and H. Yan, "Mutations of PIK3CA in anaplastic oligodendrogliomas, high-grade astrocytomas, and medulloblastomas," *Cancer Res*, Vol. 64, pp. 5048–5050, 2004.

172. Fan, Q. W., Z. A. Knight, D. D. Goldenberg, W. Yu, K. E. Mostov, D. Stokoe, K. M. Shokat, and W. A. Weiss, "A dual PI3 kinase/mTOR inhibitor reveals emergent efficacy in glioma," *Cancer Cell*, Vol. 9, no. 5, pp. 341–349, 2006.

173. Workman, P., P. A. Clarke, S. Guillard, and F. I. Raynaud, "Drugging the PI3 kinome," *Nat Biotechnol*, Vol. 24, no. 7, pp. 794–796, 2006.

174. Geldi, C., O. Bozkulak, H. O. Tabakoglu, S. Isci, A. Kurt, and M. Gulsoy, "Development of a surgical diode-laser system: controlling the mode of operation," *Photomed Laser Surg*, Vol. 24, no. 6, pp. 723–729, 2006.

175. Song, G., G. Ouyang, and S. Bao, "The activation of Akt/PKB signaling pathway and cell survival," *J Cell Mol Med*, Vol. 9, no. 1, pp. 59–71, 2005.

176. Bozkulak, O., S. Wong, M. Luna, A. Ferrario, N. Rucker, M. Gulsoy, and C. J. Gomer, "Multiple components of photodynamic therapy can phosphorylate Akt," *Photochem Photobiol*, Vol. 83, no. 5, pp. 1029–1033, 2007.

177. Alvarez-Tejado, M., S. Naranjo-Suarez, C. Jimenez, A. C. Carrera, M. O. Landazuri, and L. del Peso, "Hypoxia induces the activation of the phosphatidylinositol 3 kinase? AKT cell survival pathway in PC12 cells," *J Biol Chem*, Vol. 276, pp. 22368–22374, 2001.

178. Wang, X., K. D. McCullough, T. F. Franke, and N. J. Holbrook, "Epidermal growth factor receptor-dependent Akt activation by oxidative stress enhances cell survival," *J Biol Chem*, Vol. 275, no. 19, pp. 14624–14631, 2000.

179. Ramos, J., M. Sirisawad, R. Miller, and L. Naumovski, "Motexafin gadolinium modulates levels of phosphorylated Akt and synergizes with inhibitors of Akt phosphorylation," *Mol Cancer Ther*, Vol. 5, pp. 1176–1182, 2006.

180. Arruda, M. A., A. G. Rossi, M. S. de Freitas, C. Barja-Fidalgo, and A. V. Graca-Souza, "Heme inhibits human neutrophil apoptosis: involvement of phosphoinositide 3-kinase, MAPK, and NF-kB," *J Immunol*, Vol. 173, pp. 2023–2030, 2004.

181. Parkin, D. M., P. Pisani, and J. Ferlay, "Estimates of the worldwide incidence of 25 major cancers in 1990," *Int J Cancer*, Vol. 80, pp. 827–841, 1999.

182. Bozkulak, O., R. F. Yamaci, H. O. Tabakoglu, and M. Gulsoy, "Photo-toxic effects of 809-nm diode laser and indocyanine green on MDA-MB231 breast cancer cells," *Photodiag Photodyn Ther*, Vol. 6, no. 2, pp. 117–121, 2009.

183. Bozkulak, O., R. F. Yamaci, and M. Gulsoy, "Indocyanine Green (ICG)-Photodynamic Therapy (PDT) with 809-nm Diode Laser," *Natl Meeting Biomedical Engineering*, 2006.